Nicotine regulates the firing rate and the oscillatory behavior of O-LM interneurons

Thesis submitted for the degree of "Doctor Philosophiae"

International School for Advanced Studies (SISSA)

Neurobiology Sector

Candidate:

Marilena Griguoli

Supervisor:

Prof. Enrico Cherubini

Declaration

The work described in this dissertation was conceived and carried out at the International School for Advanced Studies (SISSA) in Trieste, between October 2006 and November 2010.
All works reported here arise from my own experiments and data analysis.
In the first paper the calcium imaging experiments were carried out in the lab of Prof. Ragozzino in Rome (Italy). In the second paper the molecular dynamic studies were carried out by the group of Prof. Carloni in Trieste (Italy).

N1.

GRIGUOLI M, SCURI R, RAGOZZINO D, CHERUBINI E (2009). Activation of nicotinic acetylcholine receptors enhances a slow calcium-dependent potassium conductance and reduces the firing of stratum oriens interneurons. *European Journal of Neuroscience* Sep;30 (6):1011-22.

N2.

GRIGUOLI M, MAUL A, NGUYEN C, GIORGETTI A, CARLONI P, CHERUBINI E (2010). Nicotine blocks the hyperpolarization-activated current I_h and severely impairs the oscillatory behaviour of O-LM interneurons. *Journal of Neuroscience* Aug 11; 30 (32):10773-10783.

The following study arises from a collaborative project not included in the present thesis:

CHERUBINI E, **GRIGUOLI M**, SAFIULINA V, LAGOSTENA L. The depolarizing action of GABA in the hippocampus controls early network activity and contributes to reshape neuronal circuits in an adult animal model of neurodegeneration. (Submitted)

CONTENTS

Abbreviations 5

Abstract 7

Introduction 10

Hippocampus: structure and circuitry 10

Hippocampal GABAergic interneurons 14

Classification of GABAergic interneurons 15

Morphological characteristics 17

Neurochemical markers 18

O-LM interneurons 20

Short- and long-term plasticity processes 21

Short-term plasticity 22

Long-term plasticity 22

Control of cell excitability and rhythmogenesis 23

Cholinergic innervation of the hippocampus 26

Neuronal nACh receptors 27

nAChR distribution in the hippocampus 31

nAChRs in O-LM interneurons 32

Physiological relevance 32

Aim of the work 34

Methods 37

Results

N1. *Activation of nicotinic acetylcholine receptors enhances a slow calcium-dependent potassium conductance and reduces the firing of stratum oriens interneurons.* 45

N2. *Nicotine blocks the hyperpolarization-activated current I_h and severely impairs the oscillatory activity of O-LM interneurons in the hippocampus.* 58

Conclusions and future perspectives 70

Bibliography 87

Acknowledgements 115

Abbreviations

ACh	Acetylcholine
AChE	Acetylcholinesterase
AHP	After-Hyperpolarization
AMPA	α-Amino-3-hydroxyl-5-Methyl-4-isoxazole-Propionate
α-BgTx	α-Bungarotoxin
BK	Large conductance calcium-activated potassium channels
CA	*Cornu Ammonis* area
ChAT	Choline Acetyltransferase
CNS	Central Nervous System
DCG-IV	(2S,2'R,3'R)-2-(2',3'dicarboxycyclopropyl) glycine
EPSP	Excitatory Postsynaptic Potential
GABA	γ-aminobutyric acid
GAD	Glutamic Acid Decarboxylase
EGFP	Enhanced Green Fluorescent Protein
GIN	GFP-expressing Inhibitory Neurons
GluR-5/6	Glutamate kainate Receptor subunits
GluR-B/D	Glutamate AMPA Receptor subunits
HCN	Hyperpolarization-activated Cyclic Nucleotide-gated channels
I_{AHP}	After-hyperpolarization underling current
I_h	Hyperpolarization-activated current
IPSC	Inhibitory Postsynaptic Current
KCNK	Two pore domain potassium channel
K_v	Voltage-gated potassium channel
L-AP4	L(+)-2-amino-4-phosponobutyric acid
LTD	Long Term Depression
LTP	Long Term Potentiation
mAChR	muscarinic Acetylcholine Receptor
mGluR	metabotropic Glutamate Receptor
mRNA	messenger Ribonucleic Acid
MS-DBB	medial septal-diagonal band of Broca

nAChR	nicotinic Acetylcholine Receptor
NMDA	N-Methyl-D-Aspartate
O-LM	*Oriens Lacunosum-Moleculare*
P	Permeability
SK	Small conductance calcium-activated potassium channel
TASK	TWIK-related acid-sensitive K^+ channel
ZAP	Impedance Amplitude Profile
ZD 7288	4-ethylphenylamino-1,2-dimethyl-6-methylaminopyrimidinium chloride

Abstract

γ-aminobutyric acid (GABA) is the principal inhibitory neurotransmitter released by interneurons in the adult brain. By releasing GABA onto principal cells, interneurons exert a powerful control on neuronal excitability and are responsible for network oscillations crucial for information processing. In contrast to the more homogeneous excitatory principal cell population, interneurons are characterized by their large diversity in terms of morphological appearance and functional properties. Among different subtypes of GABAergic cells present in the hippocampus, *oriens-lacunosum moleculare* (O-LM) interneurons, innervating the distal dendrites of pyramidal cells, are thought to play a crucial role in generating the theta rhythm, known to be associated with different behavioral states of the animal.

The hippocampus receives a strong cholinergic innervation from the basal forebrain and O-LM cells are endowed with nicotinic acetylcholine receptors (nAChRs). How these receptors regulate the signaling properties of O-LM cells is virtually unknown. Taking advantage of transgenic mice expressing EGFP in a subpopulation of somatostatin-positive interneurons (GIN mice), during my PhD I studied the mechanisms by which nicotine affects two important conductances controlling the firing and the oscillatory behavior of O-LM cells. I found that nicotine, *via* activation of calcium-permeable nAChRs, potentiates the calcium-activated potassium current carried by SK channels and independently of nAChRs activation reduces the pacemaker current I_h carried by HCN channels.

These effects lead to a reduction of O-LM cells firing and an altered rhythmogenesis.

In the first study combined electrophysiological and imaging techniques were used to investigate the effects of nicotine on the firing properties of O-LM cells.

I found that a low concentration of the alkaloid (applied in the presence of blockers of fast synaptic transmission), through the activation of α7 and non-α7 nAChRs, induces spike frequency adaptation. This was often preceded by a brief

increase in firing. Spike frequency adaptation was blocked by the bee venom toxin apamin, a selective antagonist of small conductance calcium-activated potassium (SK) channels, suggesting the involvement of SK channels in the observed effect. In voltage clamp experiments, nicotine enhanced the slow tail current following robust and unclamped calcium action currents, an effect associated with a reduction in the numbers of unclamped spikes. In addition, when nicotine was applied in the presence of apamin, it failed to produce any effect, indicating that both nicotine and apamin exert their effect on the same target, namely the slow I_{AHP} carried by SK channels. The effects of nicotine on I_{AHP} were dependent on calcium rise *via* calcium-permeable nAChRs and voltage-activated calcium channels. Thus, the effects of nicotine on O-LM firing were prevented when the patch pipette was loaded with BAPTA or when the extracellular solution was deprived of calcium or contained cadmium. The enhancement in cytosolic calcium by nicotine was directly assessed by calcium imaging experiments which confirmed the electrophysiological evidence. Furthermore, nicotine effects on the firing rate of O-LM cells required mobilization of calcium from intracellular stores since nicotine-induced spike accommodation was prevented by blocking ryanodine receptors with ryanodine or the sarcoplasmatic-endoplasmic reticulum calcium ATPase with thapsigargin and cyclopiazonic acid. Finally, activation of nAChRs by endogenously released acetylcholine from cholinergic fibers mimicked the effects of nicotine on O-LM firing. These results suggest that nAChR signaling is instrumental in regulating the integrative asset and the output of O-LM interneurons which could have a strong impact on network activity.

In the second study, I found that a low concentration of nicotine severely affected the pacemaker current $I_{h,}$ independently of nAChR activation. Nicotine suppressed the theta resonance of O-LM interneurons at hyperpolarized potentials. Resonance is the property by which neurons oscillate with maximal amplitude at certain input frequencies and O-LM cells are known to exhibit intrinsic resonance and spike transfer frequency preferences in the theta range. The effect of nicotine was mimicked by ZD 7288, a selective blocker of I_h,

suggesting that this current was indeed the target of nicotine. In voltage clamp experiments I found that similarly to ZD 7288 nicotine blocked I_h by directly interfering with the HCN channels which carry the pacemaker current. A dose response curve for nicotine effects on I_h gave an EC_{50} value of 62 nM. The majority of native HCN channels present on O-LM cells were insensitive to cAMP as demonstrated by the relative low percentage of cells in which forskolin or Br-cAMP were able to enhance I_h. This suggests that in O-LM interneurons cAMP-dependent HCN subunits are relatively rare. The effects of nicotine on I_h were similar to those of the nicotine analogue epibatidine. Furthermore, nicotine slowed down the firing rate and the interspike depolarizing slope, thus severely disrupting the oscillatory behavior of O-LM cells. This effect probably occurred through the direct interaction of nicotine with HCN channels, carrying I_h. Molecular dynamic studies proposed that the putative binding site of the alkaloid could be in a position similar to that of ZD 7288. This effect could compromise the ability of O-LM cells to optimally respond to theta frequency inputs. This finding could be relevant for rhythmogenesis and high cognitive functions in smokers.

Introduction

The Hippocampus

The hippocampus is a paired structure with mirror-image halves in either hemisphere of the brain, located inside the medial temporal lobe. Along with other limbic structures, the hippocampus is involved in learning and memory processes (Kandel, 2001), and plays an important role in storage long-term memory traces in humans and other mammalian species (Milner et al., 1998; Kim & Baxter, 2001; Burgess, 2002). In rodents, the hippocampus plays a crucial role in spatial information processing, where specific cells called "place cells" exhibit an increased firing frequency when the animal moves through a specific location of the environment referred to as the cell's place field (O'Keefe, 1983). Place cells are part of a broad circuit for dynamic representation of self-location. They interact with the grid cells of enthorinal cortex, characterized by their periodic firing fields which tile the entire environment explored by the animal (Fyhn et al. 2004; Hafting et al. 2005).

Structure and circuitry

The hippocampus which originates from the allocortex, is an elongated structure located on the medial wall of the lateral ventricle. The longitudinal axis of the hippocampus forms a semicircle around the thalamus. This gives it a shape resembling a seahorse after which the hippocampus (hippo= horse, kampos= sea monster) was named by Giulio Cesare Aranzi (1529-1589) according to the sea horse monster of Greek mythology. The resemblance of the hippocampus to the horns of a ram prompted another name: "cornu arietis", later changed by Rene Croissant de Garengeot (1688 – 1759) to "cornu ammonis" because of the ancient Egyptian God of Theba Amun, who was presented as a ram headed man, or a ram headed sphinx. The hippocampus proper and the surrounding regions, the dentate gyrus, subiculum and entorhinal cortex, together comprise the "hippocampal formation". Figure 1 shows the organization of the hippocampal

formation in the rat brain. The shape of the hippocampus is conserved across a wide range of mammalian species.

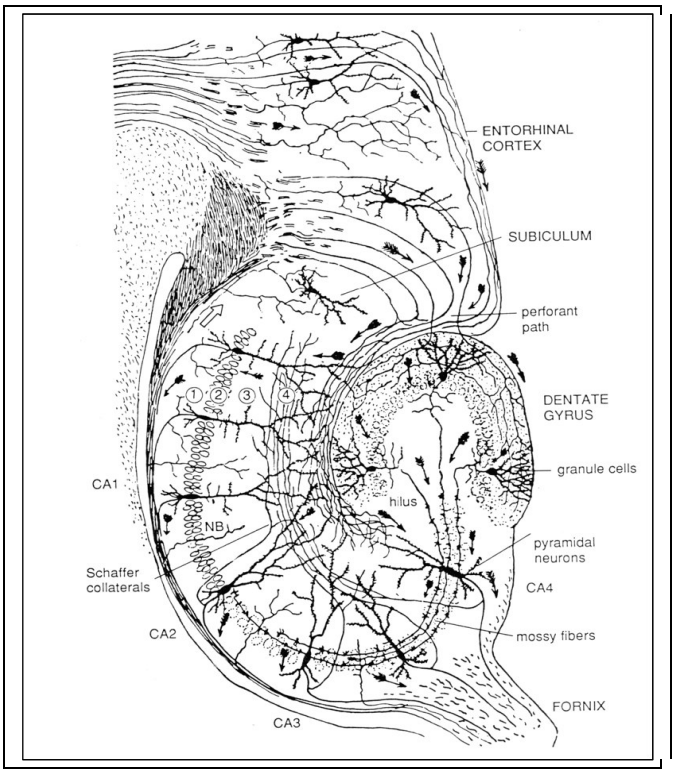


Figure 1: Structural organization of the hippocampal formation which consists of the subiculum, the entorhinal cortex, the dentate gyrus and the hippocampus proper (subdivided into regions CA1 to CA4). The four layers of the hippocampus are called *stratum oriens* (1), *stratum pyramidale* (2), *stratum radiatum* (3) and *stratum lacunosum-moleculare* (4). (Modified from Ramón y Cajal, 1911).

The hippocampus is divided into four areas according to the size and appearance of their neurons (CA1-CA4). CA1 and CA3 are the largest areas; the CA4 region (called also hilus) corresponds to the initial part of the CA3. The CA2 area is small and often included in the CA1.

The hippocampus is a four-layered structure comprising: the *stratum oriens, the stratum pyramidale,* the *stratum radiatum* and the *stratum lacunosum-moleculare*. The somata of excitatory neurons (pyramidal cells) are arranged in a layer that forms the *stratum pyramidale*. All pyramidal neurones bear basal dendrites that arborise in the *stratum oriens* and apical dendrites that are radially oriented in the *stratum radiatum* and *lacunosum-moleculare*. In contrast to pyramidal neurons inhibitory GABAergic interneurons are widely distributed in all hippocampal layers.

The information processing follows a well-defined tri-synaptic pathway which is glutamatergic and uni-directional. The main inputs to the hippocampus come from the entorhinal cortex, the septum and the controlateral hippocampus. From the entorhinal cortex, a region which receives and integrates multisensory inputs (including those coming from touch, auditory, olfactory and visual pathways), output fibers (constituting the perforant path) cross the surrounding cortex and terminate into the dentate gyrus and the CA3 region establishing glutamatergic connections. Then, the distinctive unmyelinated axons of the granule cells, called mossy fibers project to the *hilus* and to *stratum lucidum* of the CA3 region. Here they make synapses *en passant* on CA3 pyramidal neurons showing the large, presynaptic varicosities typical of mossy fibers-CA3 contacts. These presynaptic expansions form a unique synaptic complex with equally intricate postsynaptic processes called *thorny excrescences* and they may contain tens of release sites (Jonas *et al.*, 1993). Information is therefore transferred, through Schaffer collaterals, from CA3 to CA1 pyramidal neurons, which send their axons to the subiculum and the deep layers of the entorhinal cortex. It is worth noting that the vast majority of mossy fibers terminals make synaptic contacts with GABAergic interneurons localized in the *stratum radiatum* or *pyramidale* (Acsady et al., 1998). Therefore, signaling entering the entorhinal cortex from a particular cortical area can traverse the entire hippocampus and return to the cortical area from which it has originated. The transformations taking place during this process are presumably essential for information storage (Johnston & Amaral, 1998). Furthermore, commissural associative fibers provide synaptic contacts

between CA3 pyramidal neurons and between the two hippocampi, *via* the fornix. Mossy fibers-elicited excitatory postsynaptic currents or potentials can be distinguished from those evoked by commissural fibers on the basis of their faster kinetics (Yeckel *et al.*, 1999) and their sensitivity to selective type II/III metabotropic glutamate receptors (mGluRs) agonists, (2S,2'R,3'R)-2-(2',3'dicarboxycyclopropyl) glycine (DCG-IV; Kamiya *et al.*, 1996) and L(+)- 2-amino-4-phosphonobutyric acid (L-AP4; Tan *et al.*, 2006), respectively. Recurrent excitatory connections between pyramidal neurons are particularly abundant in the CA3 region and they are responsible for making this region quite unstable and more prone to seizures (Ben Ari & Cossart, 2000). The simultaneous activation of a certain percentage of these connections is sufficient for generating epileptiform activity, characterized by spontaneous, synchronized and rhythmic firing in a large number of neurons (Miles & Wong, 1986; Traub & Miles, 1991).

In addition to pyramidal cells, the hippocampus is endowed by a large variety of inhibitory GABAergic interneurons (Ramón y Cajal, 1911; Freund & Buzsáki, 1996) which, by releasing GABA onto principal cells and other interneurons, exert a powerful control on network excitability and are responsible for the oscillatory behavior crucial for information processing in the brain. Due to their extensive dendritic and axonal arborization, GABAergic interneurons can phase the output of principal cells giving rise to a coherent oscillatory activity (Klausberger *et al.*, 2003; Klausberger *et al.*, 2004; Somogyi & Klausberger, 2005) occurring at different frequencies (within the theta and gamma range). Correlated network activity, which is associated with different behavioral states of the animal (Buzsáki et al., 1983; Steriade et al., 1993), is thought to be involved in higher cognitive functions (Buzsáki, 2002; Whittington & Traub, 2003). Membrane oscillations are facilitated by the intrinsic properties of GABA releasing cells (Maccaferri & McBain, 1996) and by their electrical coupling *via* gap junctions (Hestrin & Galarreta, 2005).

Hippocampal GABAergic interneurons

Inhibitory interneurons, which form about 10% of the total hippocampal neuronal population, constitute a heterogeneous group of cells scattered throughout the hippocampus which contain GABA as a neurotransmitter (Storm-Mathisen et al., 1983) as well as the GABA-synthesizing enzynes GAD65 and GAD67 (Ribak et al., 1978).

They differ from pyramidal cells in their active and passive membrane properties. For instance, pyramidal cells accommodate (during a steady current pulse the firing is not maintained but declines with time) while interneurons usually do not accommodate and can fire at frequencies up to 400 Hz (Lacaille et al., 1987). The ability of interneurons to generate short-duration action potentials at high frequencies depends on the expression of specific voltage-gated K^+ channels (Maccaferri & McBain, 1996; Lupica et al., 2001; Gorelova et al., 2002). Interneurons are usually more depolarized than principal cells. The more depolarized resting membrane potential may depend on the different expression of distinct α-subunits of the Na^+/K^+-ATPase (Richards et al., 2007). The Na^+/K^+-ATPase is known to contribute to regulate the neuronal membrane potential, since the transmembrane Na^+ and K^+ exchange is electrogenic. Moreover, in comparison with principal cells, interneurons exhibit a higher input resistance (Morin et al., 1996; Cauli et al., 1997; Savic et al., 2001). These differences seem to depend on the differential expression of pH-sensitive leak potassium channel TASK, a subtype of KCNK channel that regulates resting membrane potential and input resistance (Taverna et al., 2005).

In addition, respect to principal cell which exhibit long axons projecting information to distant brain regions, interneurons (a part few exceptions) are short axon inhibitory cells which play an essential role in regulating local circuit excitability (Seress & Ribak; Toth & Freund, 1992; Toth et al., 1993). GABAergic interneurons control pyramidal cell excitability *via* feed-back and feed-forward

inhibition (Cobb et al., 1995; Pouille & Scanziani, 2001). While feed-forward inhibition is mediated by GABAergic interneurons activated by extra- or intra hippocampal inputs (Buzsáki, 1984; Lacaille et al., 1987), feed-back inhibition is mediated by local interneurons excited by pyramidal cells *via* recurrent collaterals (Andersen et al., 1964).

Axons of different inhibitory cells target precise and different zones of pyramidal cell membrane. Some of them contact pyramidal cells perisomatically, while others terminate exclusively on dendrites (Buhl et al., 1994; Miles et al., 1996). While perisomatic inhibition regulates the output of principal cells by limiting the repetitive discharge of sodium-dependent spikes (Miles et al., 1996), dendritic inhibition controls the efficacy of afferent inputs by suppressing the generation of dendritic calcium spikes and by limiting the depolarization due to excitatory synaptic events (Wingstrom & Gustaffson, 1983; Kullman et al., 1992). These inhibitory mechanisms play a key role in synchronizing the activity of widely distributed neurons (Cobb et al., 1995), thus controlling the generation of oscillatory activity in neural networks (Murthy & Fetz, 1992; Buzsaki & Chrobak, 1995).

Classification of GABAergic interneurons

Since the early studies of Ramón y Cajal (1893) and Lorente de No (1934) describing the different neuronal types that make up the hippocampal circuitry, it has become clear that a high level of heterogeneity is present in the morphology and connectivity of local circuit neurons, as opposed to principal cells, which are much more uniform in their appearance.

Interneurons differ from each other in their intrinsic biophysical properties and in their morphological and molecular biological features, as well as in their connectivity (Freund and Buzsaki; 1996). This heterogeneity (only in the CA1 region, 20 different subtypes have been described, see Figure 2), makes it difficult to classify them in a single scheme. Although several attempts have been made to classify GABAergic interneurons on the basis of their specific features

(i.e. morphology, neurochemical markers) a unifying scheme is far from be achieved (Freund & Buzsaki 1996; McBain & Fisahn 2001; Maccaferri & Lacaille 2003; Somogyi & Klausberger 2005).

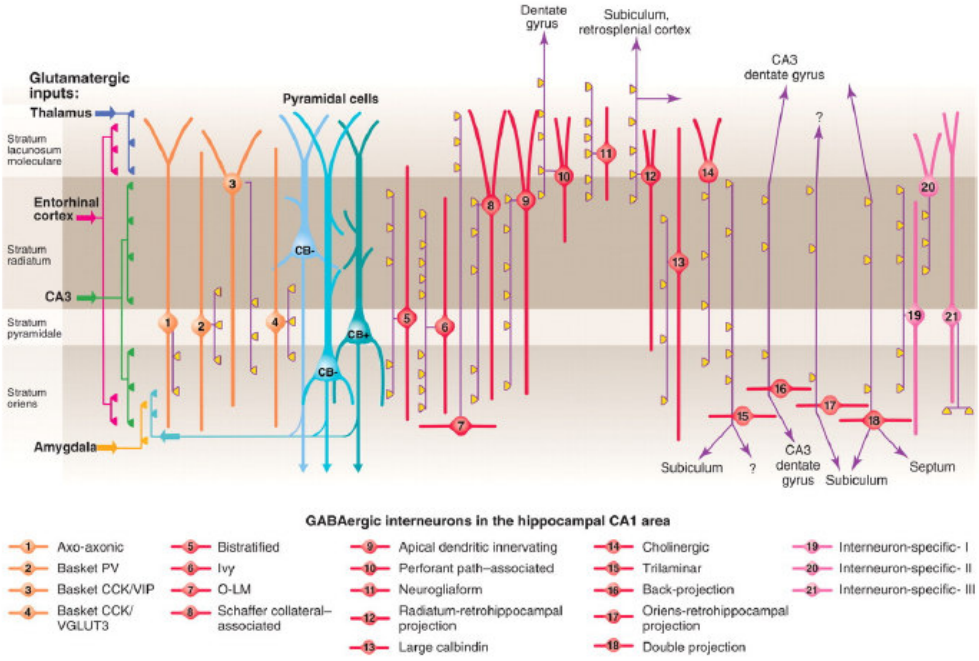


Figure 2: Different classes of interneurons in CA1 region of the hippocampus (Klausberger & Somogyi, 2008)

There is a strong need for an accepted interneuron nomenclature. The Petilla Interneuron Nomenclature Group (PING) constitutes a representative group of researchers that has provided a set of terms to describe the anatomical, physiological and molecular features of GABAergic interneurons of the cerebral cortex (Ascoli et al. 2008).

Morphological characteristics

The morphological appearance of interneurons is a source of important information regarding their specific role in neuronal circuits. In early studies (Cajal, 1893; Lorente de No, 1934) 20 different types of interneurons have been characterised on the basis of Golgi staining. Using this method, specific cell types have been described according to the particular feature of their axonal or dendritic processes (e.g. basket cells, horizontal cells and stellate cells).

Intracellular labelling with horseradish peroxidase allowed revealing in more detail the axonal arborization leading to new classification efforts (Somogyi, et al., 1998; Douglas & Martin, 1998). Mapping axonal arbours to specific domains of targeted dendritic trees has provided important clues on the functional role of various interneuron subtypes (Buhl et al., 1994, Miles et al., 1996, Halasy et al., 1996, Maccaferri et al., 2000). To match the large number of interneuron types, an equally reach terminology was adopted. Specific cellular types were defined by a combination of classical terms (e.g. basket cells, interneurons with heterogeneous afferent connection innervating the perisomatic region of principal cells) and new descriptive terms that emphasized different aspect of interneuron anatomy (Gulyas et al., 1933). In some cases the postsynaptic targeted domain was highlighted like axo-axonic cells in the dentate gyrus, (called also chandelier cells), which innervate the axon initial segment of the postsynaptic cell (Buhl et al., 1994). In other studies, specific groups of interneurons were defined on the basis of the localization of their soma and axonal processes: *oriens-lacunosum moleculare* (O-LM) cells (Freund and Buzsáki 1996), *pyramidale-lacunosum moleculare* (P-LM) cells (Oliva et al., 2000) and *oriens-oriens* and *oriens-radiatum* (O-bistratified) cells (Maccaferri et al., 2000). In other cases, the orientation of dendrites (see stellate cells), the vertical or horizontal cells of *stratum oriens*, as well as the nearby excitatory synapses on post-synaptic sites such as the Schaffer-collateral associated interneurons or hilar perforant path associated cells (HIPP cells in the dentate gyrus, Han et al., 1993) have been emphasized. However in the absence of a universal nomenclature the same type of interneuron has been named differently

by different investigators (e.g. horizontal and vertical cells in McBain et al. 1994, O–LM cells in Maccaferri et al. 2000 and basket or bistratified cells in Buhl et al. 1994).

Neurochemical markers

Specific interneuron populations have been found to contain different Ca^{2+}-binding proteins, neuropeptides, neurotrasmitters receptors, ion channels and membrane transporters. On the basis of Ca^{2+}-binding proteins, GABAergic interneurons have been classified as parvalbumin- calbindin- and calretinin-positive. This has allowed discriminating between interneurons with different dendritic geometry, postsynaptic target selection and synaptic input density (Gulyas et al. 1999). In addition they have been classified on the basis of the different expressed peptides including somatostatin, cholecystokinin, VIP, enkephalins, NPY and substance P. These neuropeptides act as possible co-transmitters or modulators (Hökfelt et al., 1980). However different types of morphological defined interneurons could coexist and overlap in a single neurochemically identified subgroup. For example, O–LM, O–bistratified, P–LM and *radiatum–lacunosum moleculare* interneurons of the CA1 hippocampal subfield are all immunoreactive for somatostatin (Katona et al. 1999; Maccaferri et al. 2000; Oliva et al. 2000; Losonczy et al. 2002). Similarly, parvalbumin is expressed by basket and axo–axonic cells (Kosaka et al. 1987; Klausberger et al. 2003) as well as at lower levels in the soma and dendrites but not terminals of O–LM cells (Maccaferri et al. 2000; Losonczy et al. 2002). This difference in compartmentalization is important because expression in the terminals can affect the dynamics of GABA release (Vreugdenhil et al., 2003). Furthermore distinct markers may be expressed in interneurons bearing similar morphological features but different functional properties. Basket cells for instance express parvalbumin or cholecystokinin (Freund, 2003).

Many interneuron functions critically depend on the fast and temporally precise conversion of an excitatory input into an inhibitory synaptic output. Synapses that excite interneurons generate fast currents, owing to the expression of

glutamate receptors of specific subunit composition. Combining single cell RT-PCR with electrophysiological approaches has been successfully used to elucidate how different AMPA receptor subunits (GluR) regulate their functional properties (Bochet et al., 1994; Jonas et al., 1994). In general, GABAergic interneurons express higher levels of GluR-D respect to GluR-B subunits which confer to AMPARs fast deactivation and desensitization kinetics (Catania et al., 1995; Leranth et al., 1996). While fast spiking parvalbumin-positive cells express high levels of calcium-permeable AMPA receptors (Hestrin, 1993; Jonas et al., 1994) other GABAergic interneurons express mainly calcium-impermeable AMPA receptors (Geiger et al., 1995). In parvalbumin-positive cells, the high density of synaptic AMPA receptors (particularly on dendrites, Baude et al., 1995), appears to be inversely related to synaptic NMDA-receptors content (Gulyás et al., 1999). High level on GluR5- associated with low level of GluR6-containing kainate receptors have also been detected in O-LM cells and *stratum radiatum* interneurons (Bureau et al., 1999; Mulle et al., 2000; Cossart et al., 1998). Concerning metabotropic glutamate receptors, horizontal dendrites of O-LM cells are particularly enriched in mGluR1a subunits (Martin et al., 1992).

Hippocampal interneurons express high levels of GABA-A receptors (Richards et al., 1987; Houser et al., 1988; Zimprich et al., 1991; Nusser et al., 1995) including those comprising α1 and ß2-3 subunits (Gao & Fritschy, 1994; Nusser et al., 1995). α1 subunits are not equally expressed in all GABAergic interneurons. While they are present in all parvalbumin-positive cells they are expressed in about 50% of calretinin- and in a subset of somatostatin-positive cells. These subunits have not been found in VIP- and cholecystokinin-containing cells. No difference between diverse interneuron subpopulations has been detected in the expression of ß2-3 GABA-A containing receptors (Nusser et al., 1995).
Selective GABA-A receptors ensure a rapid synaptic output leading, in comparison to principal cells, to a faster GABA-A mediated inhibition (Bartos et al., 2001; Hormuzdi et al., 2001).

Thus, the expression of distinct transmitter receptors and voltage-gated ion channels allow interneurons to operate with high speed and high temporal resolution.

O-LM interneurons

O-LM cells constitute a well defined interneurons population with soma and horizontal dendrites in *stratum oriens* and dense axonal projections to *stratum lacunosum-moleculare* (Figure 3) (Maccaferri et al., 2000; McBain et al., 1994). Occasional branches are also directed toward *stratum oriens*.

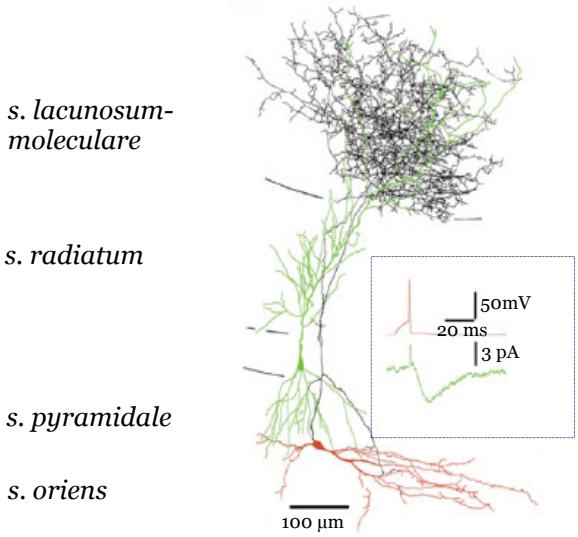


Figure 3: O-LM cell (soma and dendrites in red and axon in black) and pyramidal cell (green) filled with biocytin; in the inset an O-LM action potential evokes an IPSC in the post synaptic pyramidal cell (Maccaferri & Lacaille, 2003)

They express the Ca^{2+}-binding protein parvalbumin and the peptide somatostatin (Maccaferri et al., 2000; Katona, 1999; Lozonczy et al., 2002). O-LM interneurons exhibit fast spiking firing patterns caused by the expression of specific voltage-dependent K^+ channels (Kv 3.2 and Kv7/KCNQ/M) (Atzori et al., 2000; Lien & Jonas, 2003; Lien et al., 2002; Lawrence et al., 2006) and are endowed with hyperpolarization activated (HCN) channels carrying I_h, which

underlies their pacemaker properties (Maccaferri & McBain, 1996; Ali & Thomson, 1998; Svoboda & Lupica, 1998). They express also calcium-dependent potassium channels, which contribute to action potential repolarization and trigger the prominent afterhyperpolarization (AHP) following action potential firing. In particular, large conductance potassium (BK) channels mediate the action potential repolarization and the fast component of the AHP, while small conductance potassium (SK) channels underlie the slow AHP (Zhang & McBain, 1995a, b). Moreover, O-LM cells express a high density of dendritic Na^+ channels, which allow them generating action potentials (Martina et al., 2000). These intrinsic properties (Pike et al., 2000; Schreiber et al., 2004; Lawrence et al., 2006) together with their reciprocal connectivity (including gap junctions) and incoming synaptic inputs contribute to the generation of output signals.

Short- and long-term plasticity processes

Calcium plays a crucial role in many forms of synaptic plasticity. Using two-photon calcium imaging and whole cell recordings to study the properties of dendritic calcium signals mediated by different glutamate receptors and their regulation by synaptic activity, Topolnik et al. (2005) have found that O-LM interneurons express both calcium permeable and calcium impermeable AMPA receptors. The first ones provides fast calcium signals whereas the second one, which is often associated with metabotropic glutamate receptors of group I-II, gives rise to slower calcium signals. A weak synaptic stimulation activates calcium signals mediated by calcium-permeable AMPA receptors. A stronger stimulation or a weak stimulation coupled with a postsynaptic depolarization recruits calcium signals mediated by mGluR. Therefore, it is likely that the differential activation of specific glutamate receptor-mediated calcium signals within spatially restricted dendritic microdomains may serve distinct signaling functions and allow O-LM interneurons exhibiting multiple forms of calcium-dependent synaptic plasticity processes. O-LM cells are driven by excitatory collaterals of CA1 principal cells (Lacaille *et al.* 1987; Blasco-Ibanez & Freund,

1995; Maccaferri & McBain, 1995; Ali & Thomson, 1998; Losonczy *et al.* 2002; Pouille & Scanziani, 2004). These synapses can undergo short and long-term synaptic plasticity processes.

Short-term plasticity

O-LM interneurons exhibit paired-pulse facilitation (Lozonczy et al., 2002, Ali & Thomson, 1998) and short-term facilitation. The use- and voltage-dependent relief of the polyamine block from calcium-permeable AMPA receptors would be responsible for this type of potentiation (Toth & McBain, 1998). In pair recordings from interconnected CA1 principal cells and O-LM interneurons EPSCs evoked by presynaptic spikes are highly reliable and follow a wide range of frequencies (between 20 and 100 Hz) (Minneci et al., 2007).

Long-term plasticity

Like other interneurons, O-LM cells undergo long-lasting activity-dependent changes in synaptic efficacy. According to the Hebb postulate, long-term synaptic potentiation (LTP) is an associative form of learning which can be induced by pairing presynaptic stimulation with postsynaptic depolarization. However, in some cells, other non-Hebbian forms of LTP, including anti-Hebbian, may coesist. O-LM interneurons exhibit both Hebbian and anti-Hebbian forms of LTP. The term "anti-Hebbian" has been used to describe a non-associative type of learning, occurring when the presynaptic firing does not coincide with the postsynaptic depolarization. This form of LTP which is typical of synapses that express Ca^{2+}-permeable AMPA receptors (Lamsa et al., 2007; Oren et al., 2009) is induced by presynaptic activity when the cell is maintained at a relatively negative potential (a condition that allow maximal calcium influx) but is prevented by postsynaptic depolarization. In fact, the strong rectification of calcium permeable AMPA receptors mediated by polyamine block does not allow calcium entry at depolarizing membrane potentials.

At CA1-O-LM synapses, a Hebbian form of LTP can be induced by pairing postsynaptic depolarization with theta bursts stimulation. This form of LTP is independent of NMDA receptor activation but is dependent on metabotropic glutamate receptor subtype 1a (Perez et al. 2001).

GluR1a-containing metabotropic glutamate receptors and GluK1-containing kainate receptors would play a permissive role in this form of LTP probably reducing the threshold for LTP induction (Oren et al., 2009; Perez et al., 2001). Interestingly LTP (as well as LTD) can be also passively propagated from pyramidal cells to O-LM interneurons (Maccaferri & McBain, 1995; 1996) indicating that synaptic efficacy in the CA1 pyramidal neurons contributes to modulate the output activity of O-LM cells and, consequently, the level of feedback inhibition to the *stratum lacunosum moleculare*.

Control of cell excitability and rhythmogenesis

O-LM interneurons regulate the gain of EPSPs on pyramidal cell distal dendrites through a feedback inhibitory mechanism (Maccaferri & McBain, 1995; Maccaferri et al., 2000). The IPSCs evoked in pyramidal cells by O-LM stimulation do not show paired-pulse inhibition. This suggests a non-decremental charge transfer generated in the distal pyramidal dendrites during recurrent activation of O-LM cells (Maccaferri et al., 2000). A non-decremental activation of GABA-A receptors by GABA released on the distal dendrites of pyramidal cells may shunt entorhinal or Schaffer collateral EPSPs or may reduce their effectiveness through dendritic hyperpolarization (Maccaferri & McBain, 1995; Katona et al. 1999). The shunting action may limit regenerative responses and/or action potentials in the distal dendrites (Miles et al. 1996; Tsubokawa & Ross, 1996; Kamondi et al. 1998). In a more cooperative mode of interaction with excitatory events, a local hyperpolarization of the membrane may also remove the inactivation of low threshold calcium channels (Magee et al. 1995) and/or sodium channels, facilitating the ability of dendrites to generate dendritic spikes. Distal dendrites have been shown to play an important role in calcium electrogenesis and action potential generation (Kamondi et al. 1998). At the network level, the strong facilitatory input of O-LM cells predicts their activation by repetitive firing of pyramidal cells (Lacaille et al. 1987; Ali & Thomson, 1998) particularly at the theta frequency. In behaving animals during the theta rhythm, pyramidal cells fire in phase with the population activity (Buzsáki & Eidelberg, 1983; O'Keefe &

Recce, 1993). O-LM cells fire rhythmically at the trough of theta cycles while axo-axonic and parvalbumin expressing basket cells fire preferentially just after the peak or during the descending phase of the theta wave, respectively. The O-LM firing is suppressed during ripple episodes (Klausberger et al. 2003, Figure 4).

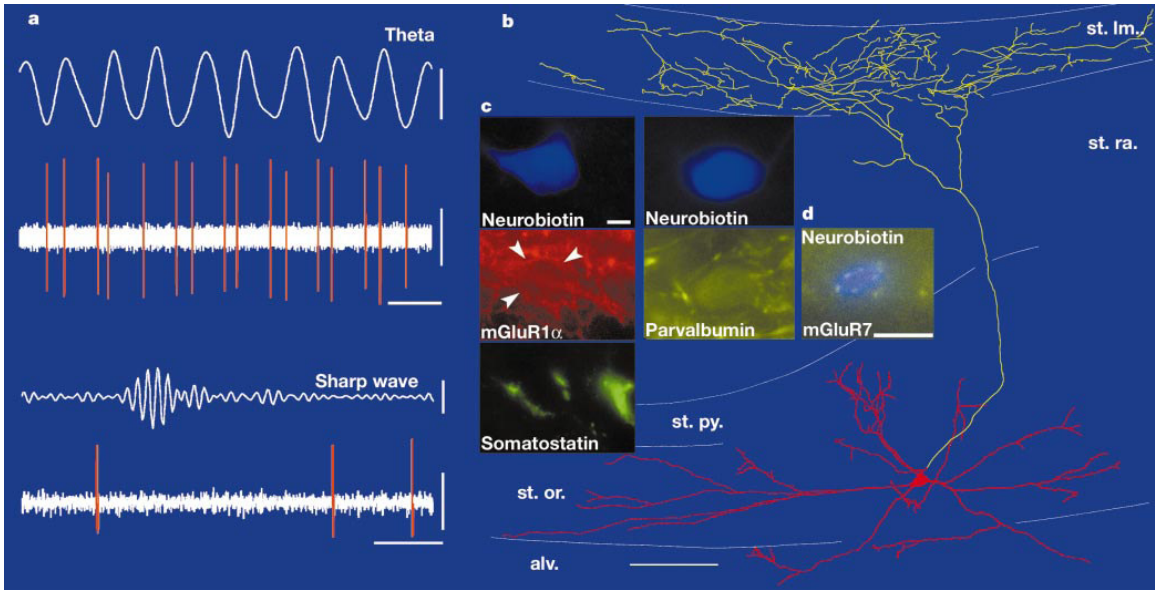


Figure 4: Firing pattern of an O-LM neuron *in vivo* related to theta cycles of field potential recording. **a**, The cell fired rithmically on the trough of theta oscillations, but was silent during sharp-wave-associated ripples. Scales: unit, 0.3 mV; theta, 0.2 mV, 300 ms; sharp wave, 0.05 mV, 50 ms. **b**, Reconstruction of the neurobiotin-filled O-LM cell. Soma and dendrites are in red; the axon restricted to *stratum lacunosum moleculare* is in yellow. **c**, The soma was cut into two sections; one shows somatostatin and metabotropic glutamate receptor mGluR1α immunoreactivity; the other shows parvalbumin immunoreactivity. **d**, The dendrite of another recorded O-LM cell is decorated with highly mGluR7a-immunopositive terminals (yellow). Scales: **b**, 100 μm; c, d, 5 μm (Klausberger et al., 2003).

In vitro studies have demonstrated that O-LM interneuron fire preferentially at theta frequency (Pike et al. 2000; Gillies et al. 2002; Hájos et al. 2004; Gloveli et

al. 2005), indicating that indeed O-LM interneurons contribute to theta oscillations in the hippocampus. Phase coding by place cells may be substantially assisted and enhanced by O-LM cells feedback circuits to pyramidal cells, which govern the timing of entorhinal and Schaffer collateral/commissural inputs, respectively as a function of pyramidal cell output.

Cholinergic innervation of the hippocampus

Acetylcholine (ACh), released from cholinergic fibers, modulates cell excitability and synaptic transmission within hippocampal circuits resulting in the emergence of a range of stable oscillatory network states.

Cholinergic neurons, located in the medial septal (MS) and the diagonal band of Broca (DBB), provide most of the cholinergic innervation to the hippocampus (Dutar et al., 2005). From the MS-DBB complex cholinergic fibers innervate the hippocampal formation *via* three main routes: the fimbria, the dorsal fornix and the supracallosal striae (Gage et al., 1984, Milner & Amaral, 1984). Within the hippocampal formation cholinergic fibers terminate in a laminar pattern in both the hippocampus and the dentate gyrus. The cholinergic neurons are detectable using the choline acetyltransferase (ChAT) immunostaing and cholinergic axons are visualized using acetylcholinesterase (AChE) immunostaining. In rodents, ChAT-positive cells can be detected in the MS-DBB area since embryonic *day 17*. AChE-positive axons enter the hippocampus on postnatal *day 2* (Hohmann & Ebner, 1985). The neurons of MS-DBB show continuous growth until the end of the second or third postnatal week. Two types of septal fibers have been described: thick coarse axons with large terminal boutons present in the hippocampal stratum oriens, radiatum, moleculare, in the hilus and the infragranular zone of the dentate gyrus and thin fibers displaying varicosities in the hippocampal pyramidal cell layer, dentate molecular and granular layers (Gaykema et al., 1991; Nyakas et al., 1987). Hippocampal thin sections for electron microscopy and stereological extrapolation approaches have revealed that only a small portion (~ 7%) of cholinergic fibers is characterized by junctional specializations (Umbriaco et al., 1994, 1995; Contant et al., 1996). This suggests that ACh is mainly released in a non-conventional way to reach and modulate relatively distant targeted and vast cellular ensembles.

To enable effective transmission of patterned cholinergic inputs, the hippocampus is endowed with a variety of muscarinic and nicotinic acetylcholine receptors (mAChRs and nAChRs).

Neuronal nAChRs

nAChR belongs to the large cystein (cys)-loop of ligand-gated ion channels superfamily which includes the serotonin 5-HT3, GABA-A and and glycine receptors. The cys-loop (characterized by two cys residues separated by 13 amino acids at level of the first extracellular domain) is required for agonist binding (Karlin et al., 1986). nAChRs firstly identified at neuromuscular junction, are highly expressed in the CNS. They are composed of five subunits assembled around a central pore permeable to cations (Lukas et al., 1999). Different subunits may combine in various combinations to generate a large variety of nAChRs subtypes with different biophysical and pharmacological properties (Albuquerque et al., 2009).

Neuronal nAChRs subunits include α2–α6 and β2–β4 subunits (Figure 5).

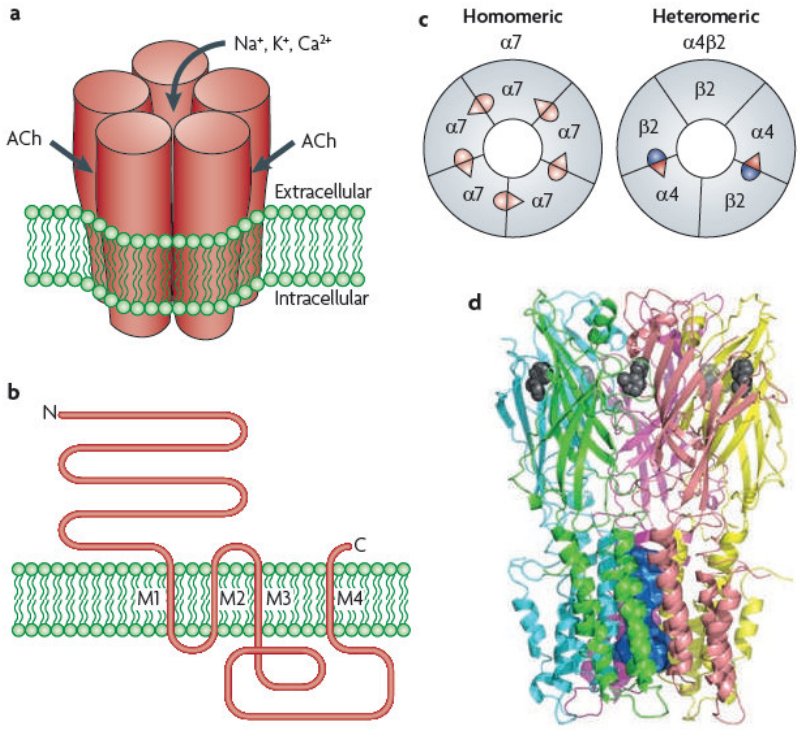


Figure 5: nAChR struc ture and agonist binding sites. **a**, nAChRs are transmembrane oligomers consisting of five subunits. **b**, Each subunit consists of a large amino-terminal extracellular domain with an immunoglobulin-like β-sandwich, a transmembrane domain and a variable

cytoplasmic domain. The extracellular domain carries the ACh-nicotine binding sites at the boundary between subunits. The number of binding sites per pentamer ranges, depending on its composition, from two (in the α4β2 nAChRs) to five (in the α7 homopentamer). Sites for allosteric modulators are located in the transmembrane domain. **c**, The two main types of neuronal nAChRs are the α7 homo-oligomer, characterized by a fast activation, a low affinity and a high Ca^{2+} permeability, and the α4β2 hetero-oligomer, typified by a high affinity and slow desensitization. **d**, Side view of an α7 nAChR pentamer model, showing five nicotine molecules (dark grey) in the binding sites and the volume of the ion channel (dark blue) (Changeux, 2010).

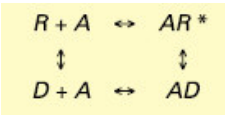
The α7–α9 subunits form homopentamers while α10 subunits form heteromers with α9. The α8 subunits have not been found in mammals (they are present in avian tissue). The α7–α10 subunits are sensitive to the snake venom α-bungarotoxin (α-Bgtx). Of the subunits capable of forming homomers, only the α7 are widely distributed in the mammalian brain. They are the most abundant nAChR subtypes present in the hippocampus (Seguela et al., 1993; Role & Berg, 1996). Homomeric α7 nAChRs are low affinity receptors characterized by fast activation kinetics and a high calcium permeability ($P_{Ca}/_{Na}$ ~ 7-20; Fucile, 2004), higher than NMDA receptors ($P_{Ca}/_{Na}$ ~ 5-10). This characteristic allows nAChRs to play an important role in cellular events such as neurotransmitter release, second messenger cascades, cell survival and apoptosis. Most of heteromeric receptors contain α4 and β2 nAChR subunits. They are high affinity receptors, insensitive to α-Bgtx, characterized by the low calcium permeability ($P_{Ca}/_{Na}$ ~ 1.5; Fucile, 2004). The final stoichiometry of heteromeric receptors can be: $(\alpha4)_2(\beta2)_3$, $(\alpha4)_3(\beta2)_2$, $(\alpha4)_2(\beta2)_2$ α5 (Nelson et al., 2003; Zhou et al., 2003).
In homomeric α7 receptors, the binding site of neuronal nAChRs lies at the interface between two identical subunits while in the case of heteromeric α-Bgtx-insensitive receptors between the α and the β subunit. The α5 and β3 subunits do not carry the primary or the complementary components of the ACh binding site, and it is generally assumed that they do not directly participate in its formation. Therefore, while homomeric receptors have five identical ACh-binding sites per

receptor molecule (one on each subunit interface), heteromeric receptors have two binding sites per receptor (Corringer et al., 2000) (Figure 5c-d).

The prolonged or repeated exposure of nAChRs to the agonist induces receptor desensitization, leading to a decrease in cell responsiveness to the agonist. This phenomenon has been well characterized by Katz & Thesleff (1957) at the motor end-plate. In a simple schematic model (Figure 6**a**) these authors propose that upon agonist (A) binding, the receptor (R) in the bound close state can either open the cation-selective pore (AR*) or desensitize (AD).

The AD state is characterized by high affinity for the agonist, whereas AR for low affinity, and AR* for an intermediate one (Corringer et al., 2000). According to this model, the desensitization onset would be agonist-dependent whereas the recovery from desensitization agonist-independent. Another kinetic model proposed for nAChR desensitization is the high-affinity desensitization (Figure 6**b**) which suggests binding of two agonist molecules and transition into the desensitized state from both the agonist-bound closed state (AR) and from the open receptor state (A_2R^*). These transitions can occur in the presence of low agonist concentrations (nanomolar) (Paradiso & Steinbach, 2003).

a



b

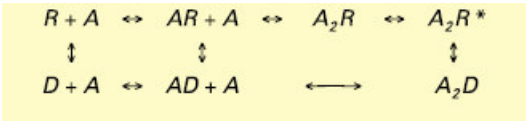


Figure 6: Scheme of the desensitization models. **a Classical desensitization:** A is the agonist, R, R* and D are the receptor in the resting, open and desensitized state respectively. According to Katz and Thesleff (1957), desensitization onset is agonist-dependent, recovery from desensitization is agonist-independent, desensitization corresponds to a high-affinity receptor state, and a fraction of receptors can exist in desensitized state. In this model, following agonist

(A) binding to the resting receptor (R) and subsequent receptor activation (AR*), desensitization arises as agonist-bound desensitized (AD) and agonist-free desensitized (D) states; **b**, **High affinity desensitization:** This model suggests binding of two agonist molecules and transition into the desensitized state from both the agonist-bound closed state (AR) and from the open receptor state (A2R*). The former has a high-affinity for agonist because it can be evoked by low (nanomolar) concentrations of agonist, and it could represent the receptor conformation responsible for generating high-affinity desensitization because no activation is involved (Giniatullin et al., 2005).

For α4β2 nAChRs, high-affinity desensitization can be induced by very low concentrations of nicotine (<10 nM), whereas for other nAChR subtypes, the high-affinity desensitization can overlap in different degrees with the classical desensitization (Giniatullin et al., 2003). Desensitization may cause additional long-term changes in receptor properties and an up-regulation of the number of high-affinity receptors in the brain (Fenster et al., 1999; Buisson & Bertrand, 2001).

For the purpose of this thesis, only the distribution and function of nAChRs in the hippocampus will be discussed in detail.

AChR distribution in the hippocampus

The main receptor subtypes present in the hippocampus of rodents are the homomeric $\alpha 7$ and the heteromeric $\alpha 4\beta 2$ (Alkondon & Albuquerque, 2004). The mRNAs for the $\alpha 7$ and $\beta 2$ subunits are present early during embryogenesis, but the expression patterns of $\alpha 7$ and $\beta 2$ subunits differ. The heteromeric nAChRs expression remains stable during postnatal development while, the expression of $\alpha 7$ mRNA and the density of [^{125}I]-α-bungarotoxin-binding sites are particularly high during the first postnatal week and decrease subsequently (Shacka & Robinson, 1998; Tribollet *et al.* 2004). These data suggest that in the hippocampus, the balance between $\alpha 7$- and $\beta 2$-containing subunit nAChRs changes during postnatal development. The localization of nAChRs is at presynaptic and somatodendritic level (Alkondon & Albuquerque, 1993; Zoli et al., 1998; Sudweeks & Yakel, 2000; Fabian-Fine et al., 2001). The activation of presynaptic nAChRs modulates the release of several neurotransmitters (Vizi & Lendvai, 1999). The α7 nAChR subunits are the main nAChR subtypes expressed on both glutamatergic (e.g. mossy fibers and Shaffer collateral) and GABAergic synaptic terminals. Their activation induces a Ca^{2+}-dependent increase in the probability of glutamate and GABA release (Gray et al., 1996; Alkondon & Albuquerque, 2001; Le Magueresse & Cherubini, 2007). The activation of postsynaptic nAChRs in hippocampal pyramidal cells and interneurons produces a fast and cell specific response. There has been some controversy about the presence of nAChRs on pyramidal neurons. Different electrophysiological studies have demonstrated that the local application of nAChR agonists generally produces either no or only a barely detectable current response in pyramidal cells (Frazier et al., 1998b; McQuiston & Madison, 1999; Khiroug et al., 2003; but see Ji et al., 2001). nAChRs are more abundant in interneurons than in pyramidal cells. Molecular studies have revealed the presence of different nAChR subunit mRNAs in hippocampal interneurons (Sudweeks and Yakel 2000; Son & Winzer-Serhan, 2008). The activation of these receptors (either synaptically or by direct agonist application) produces a brief membrane depolarization or an inward current whose kinetics and pharmacology vary between cell types (Frazier et al., 1998a).

nAChRs in O-LM interneurons

The predominant response of *stratum radiatum* interneurons to nicotine agonists consists in a fast depolarizing and rapidly desensitizing current mediated by α7 nAChRs subunits (Jones & Yakel, 1997; McQuiston & Madison, 1999). In contrast, interneurons with axons providing perisomatic inhibition are insensitive to nAChR agonists. *Stratum oriens* interneurons display a dual component response with an initial α7-dependent fast depolarizing phase followed by a slower non α7-dependent phase (McQuiston & Madison, 1999). Among the non-α7 nAChR subunits, α2 containing nAChR subunits seem to be expressed in O-LM interneurons (Wada et al., 1989) and a functional study has shown a sustained non-desensitizing excitatory response to nicotine mediated by α2 containing nAChR subunits (Jia et al. 2009). Moreover Jia et al. (2010) have recently demonstrated that Ca^{2+} entering through α2 containing nAChR subunits is responsible for nicotine-induced facilitation of LTP in O-LM cells indicating that Ca^{2+} entry through non-α7 nAChRs plays also a crucial role in synaptic plasticity processes.

Physiological relevance

The function of central cholinergic system is various. Evidence has been provided that an increase in cholinergic activity enhances cognitive functions (Everitt & Robbins, 1997). In particular, nicotinic stimulation has been shown to improve performance in certain cognitive tasks (Newhouse et al., 2004). The impact of the cholinergic activity is underlined by the fact that a deficit in the cholinergic system produces an impairment of cognitive functions that are particularly relevant during senescence and in aging-related neurodegenerative pathologies such as Alzheimer's disease. Alzheimer's disease is characterized by a selective loss of cholinergic neurons in the basal forebrain (Bartus et al., 1982) and nAChRs in particular regions controlling memory processes such as the cortex and the hippocampus (Paterson & Nordberg, 2000; Perry et al, 2000).

A large variety of studies have provided evidences regarding the involvement of nicotinic cholinergic system in neuronal processes such as synaptic plasticity and

network oscillations. I*n vitro* studies have revealed that the activation of presynaptic α7-nAChRs by nicotine or endogenously released acetylcholine enhances activity-dependent plasticity processes at glutamatergic and GABAergic synapses in the adult (Fujii et al., 1999; Mann & Geenfield, 2003) and in the immature hippocampus (Maggi et al., 2001; 2003; 2004; Le Magueresse et al., 2006; Le Magueresse & Cherubini, 2007). In *stratum radiatum* interneurons, the activation of somatodendritic α7-nAChRs decreases the amplitude of evoked IPSCs suggesting a role of α7-nAChRs in the modulation of inhibitory transmission among interneurons (Wanaverbecq et al., 2007; Zhang & Berg, 2007). This depression is mediated via Ca^{2+} entering through α7-nAChRs which activates an intracellular cascade involving the protein kinase C, known to negatively modulate $GABA_A$ receptors (Wanaverbecq et al., 2007).

At the network level cholinergic innervation is important for rhythmogenesis. Studies done mainly on anaesthetized animals suggest that the septal cholinergic input modulates the power of the theta rhythm while the septal GABAergic input determines its temporal pattern and frequency (Brazhnik & Fox, 1997; Stewart & Fox, 1990; Lee et al., 1994). Both mAChRs and nAChRs contribute to regulate network oscillations. While the activation of mAChRs by carbachol induces oscillatory activity (Fellous & Sejnowski, 2000; Traub et al., 2000) the activation of α7 nAChRs increases the power of the theta rhythm on hippocampal slices (Siok et al., 2006). Furthermore, a recent study has demonstrated that low concentrations of nicotine can induce theta frequency oscillations in hippocampal slices presumably through the activation of both the GABAergic and the glutamatergic circuitry (Lu & Henderson, 2010). Although hippocampal interneurons are the primary targets of septal cholinergic innervation the impact of cholinergic modulation on the oscillatory properties of interneurones has been virtually unexplored for a long time. A recent *in vitro* study has outlined the role of mAChRs in enhancing spike reliability and precision to theta frequency input in O-LM interneurons (Lawrence et al. 2006). Whether activation of nAChRs in O-LM cells by nicotine affects rhythmogenesis in the hippocampus is still unknown.

Aim of the work

Interneurons exert a powerful control of network excitability and participate to network oscillations associated with different behavioral states of the animal. In the hippocampus, O-LM interneurons, innervating the distal dendrites of pyramidal cells in *stratum lacunosum-moleculare*, are crucial for controlling the entorhinal and Schaffer collateral/commissural inputs. In addition these cells play a crucial role in generating the theta rhythm. O-LM cells receive a strong cholinergic innervation from the basal forebrain and are endowed with nAChRs.

During my PhD course I used combined electrophysiological and imaging approaches to understand whether activation of nAChRs by nicotine or endogenously released acetylcholine controls the firing properties of O-LM cells.

To target this particular subtype of interneurons I took advantage of a transgenic strain of mice expressing enhanced GFP in a subpopulation of somatostatin containing GABAergic interneurons (GIN mice, Oliva et al., 2000). Neurobiotin, injected routinely through the patch pipette allowed the late morphological identification of the recorded neurons.

I found that a low concentration of nicotine applied in the bath or by pressure to GFP-positive *stratum oriens* interneurons (in hippocampal slices from P14-21 mice), causes a slow down of the firing evoked by long depolarizing current pulses thus increasing spike accommodation. I followed the hypothesis that nicotine-induced reduction in firing rate can be due to the opening of calcium-dependent potassium channels following calcium entry through calcium permeable nAChRs and voltage dependent calcium channels. Indeed I found that this is the case. The increase in intracellular calcium concentration following nAChRs activation potentiates a calcium-dependent potassium conductance responsible for the slow AHP which, in turn reduces the firing rate of O-LM cells. In voltage clamp experiments I found that apamin-sensitive SK channels are involved in the observed effect. Ca^{2+} imaging experiments performed in the laboratory of Professor Davide Ragozzino in Rome further confirmed that O-LM firing is controlled by calcium entry *via* nAChRs. Interestingly, the effects of nicotine on I_{AHP} are facilitated by mobilization of calcium from intracellular

calcium stores. Finally, I tested whether acetylcholine, endogenously released from cholinergic fibers, can mimic the effect of nicotine. Similarly to nicotine, high frequency stimulation of cholinergic fibers in the alveus (in the presence of muscarinic receptor antagonists) produces spike frequency adaptation that can be prevented by nAChR antagonists suggesting that calcium signaling via nAChRs is crucial for regulating the output of O-LM cells.

This part of the work has been published in paper N.1

Subsequently, I focused on whether the activation of nAChRs by nicotine could affect intrinsic oscillatory properties of O-LM interneurons. Different *in vivo* and *in vitro* studies have demonstrated that O-LM cells fire preferentially at theta frequency suggesting a role in rhythmogenesis. It is assumed that hippocampal theta oscillations arise from the dynamic interplay between synaptic interactions and intrinsic electrical properties of the neurons. Intrinsic properties such as voltage dependent conductances underlie the resonance which is the tendency of the membrane potential to oscillate with maximal amplitude at a certain 'preferred' input frequency. In this study, in collaboration with Alena Maul, an undergraduate student in the lab, I focused on subthreshold resonance of O-LM cells. We used patch clamp in whole cell configuration (current clamp mode) to apply a ZAP protocol consisting in an oscillatory current with steady amplitude and increasing frequency (from 0.5 to 30 Hz) at two different membrane potentials (-70 mV and -90 mV). We found that the preferred frequency of O-LM cells is in the theta range (3-7 Hz). This resonance is known to depend on the activation of the hyperpolarization-activated current (I_h). The application of nicotine at low concentrations reduces O-LM theta resonance in the same way as ZD7288, a selective antagonist of I_h.
At this stage, I studied I_h in voltage clamp mode and surprisingly I found that nicotine significantly reduces I_h independently of nAChR activation presumably by directly interfering with HCN channels, which carry I_h. To better assess this point, molecular dynamics studies, performed in collaboration with the group of Prof. Carloni, an expert in this field, allowed to predict the possible binding site of

nicotine on a the HCN channel pore. Like ZD 7288, nicotine can bind a hydrophobic cavity in the inner pore of HCN channel.
In conclusions, it appears that by disrupting the theta rhythm, nicotine may contribute to alter information processing and high cognitive functions in smokers.

This part of the work is published in the paper N.2

Methods

All experimental procedures and materials used are described in detail in the original papers included in the next section (Results).

Hippocampal slices

Experiments were performed on hippocampal slices from P14-P21 transgenic mice expressing EGP in a subpopulation of somatostatin-containing GABAergic interneurons (GIN mice: Jackson Laboratories, ME; Oliva et al., 2000; Minneci et al. 2007). To confer EGFP expression to GABAergic interneurons, an upstream regulatory sequence from the murine *Gad1* gene was used for the transgene construction (Oliva et al., 2000).

All experiments were performed in accordance with the European Community Council Directive of 24 November 1986 (86/609EEC) and were approved by local authority veterinary service. Briefly, after being anaesthetized with an i.p. injection of urethane (2g/kg), the brain was quickly removed from the skull and placed in ice-cold artificial cerebrospinal fluid containing (in mM): 130 NaCl, 25 glucose, 3.5 KCl, 1.2 NaH_2PO_4, 25 $NaHCO_3$, 2 $CaCl_2$, 1.3 $MgCl_2$ (Sigma, Milan, Italy), saturated with 95% O_2 and 5% CO_2 (pH = 7.3-7.4). Transverse hippocampal slices (300 μm thick) were cut with a vibratome and stored at room temperature (22-24° C) in a holding chamber containing the same solution as above. After incubation for at least 1 h, an individual slice was transferred to a submerged recording chamber and continuously superfused at 33-34 °C with oxygenated artificial cerebrospinal fluid at a rate of 2–3 ml min^{-1}.

Patch clamp recordings

Electrophysiological experiments were performed from visually identified EGFP-positive cells localized in CA1 *stratum oriens* by using the whole-cell configuration of the patch-clamp technique in current- or voltage-clamp mode. Neurons were visualized using an upright fluorescent microscope (Nikon E600 FN) equipped with differential interference contrast (DIC) optics, and infrared video camera. Only those cells exhibiting round or fusiform cell bodies and

horizontal dendrites, often close to the alveus were used. All recordings were made with a Multiclamp 700A amplifier (Molecular Devices, Union City, CA) in the presence of DL-2-amino-5-phosphonopentaoic acid (DL-AP5; 50 μM), 6,7-dinitroquinoxaline- 2,3-dione (DNQX; 20 μM) and gabazine (SR 95531 hydrobromide; 10 μM) to block ionotropic glutamatergic and GABAergic synaptic currents, respectively. Patch electrodes were pulled from borosilicate glass capillaries (Hingelberg, Malsfeld, Germany). They had a resistance of 4–6 MΩ when filled with an intracellular solution containing (in mM): 135 $KMeSO_4$, 10 KCl, 10 HEPES, 0.5 EGTA, 2 Na_2ATP, and 0.4 Na_2GTP (osmolarity 280–300 mosM, pH 7.2–7.3, with KOH). In a set of experiments, recordings were performed with patch pipettes containing 20 mM BAPTA (Sigma–Aldrich, Milan, Italy). When 20 mM BAPTA was added to the pipette solution, $KMeSO_4$ was reduced from 135 to 115 mM. Membrane potential values were corrected for a liquid junction potential of 15.1 mV. Series resistance was assessed repetitively every five min throughout the experiment. Series resistance value varied between 20 and 25 MΩ; cells exhibiting more than 15-20% changes were excluded from the analysis. Data were sampled at 20 kHz and filtered with a cutoff frequency of 2 kHz. Data acquisition was done by using pClamp 9 (Axon Instruments). Values are given as mean ± SEM.

Significance of differences was assessed by Student's t test, Wilcoxon signed rank test, Mann-Whitney Rank Sum Test and ANOVA one way analysis of variance as indicated; $p<0.05$ was taken as significant.

Drugs

Drugs used were: DL-AP5, DNQX, SR 95531 hydrobromide, apamin, linopirdine dihydrocloride, ryanodine, thapsigargin, cyclopiazonic acid (CPA), ZD 7288, forskolin, bromo cyclic AMP (Br-cAMP), mecamylamine and epibatidine all purchased from Tocris Bioscience (Bristol, UK); nicotine, dihydro-β-eritroidine (DHβE), α-bungarotoxin (αBGT), methyllycaconitine (MLA), edrophonium atropine, choline and acetylcholine from Sigma (Milan, Italy); paxilline from

Alomone Labs (Jerusalem, Israel), tetrodotoxin (TTX) from Latoxan (Valence, France).

In the experiments with α-BGT, ryanodine, thapsigargin and CPA, slices were previously incubated with the drugs, for at least one hour, during the recovering time. Stock solutions were made in distilled water and then aliquoted and frozen at -20 °C. DNQX, thapsigargin and CPA were dissolved in dimethylsulphoxide (DMSO). The final concentration of DMSO in the bathing solution was 0.1%. At this concentration, DMSO alone did not modify the membrane potential, input resistance or the firing properties of O-LM interneurons. Ryanodine was dissolved in ethanol. The final concentration of ethanol was 1%. Drugs were applied in the bath *via* a three-way tap system, by changing the superfusion solution to one differing only in its content of drug(s). The ratio of flow rate to bath volume ensured complete exchange within 1-2 min. Nicotine was applied either in the bath (1-3 μM for 5-7 min) or by pressure ejection (only in the first study; 6-8 PSI for 50-100 ms) from a glass pipette (tip opening of ~ 1 μm; concentration of nicotine into the pipette 2 mM), localized close to the patched cell, using the Picospritzer II (General Valve, Fairfied, NJ).

Morphology

Slices were processed for *post hoc* identification of EGFP-positive stratum oriens interneurons filled with Neurobiotin (0.2%; Vector Laboratories) during patch recordings using a standard procedure (Goldin et al., 2007; Cossart et al., 2006). Briefly, slices were fixed overnight at 4°C in a solution containing 4% paraformaldehyde in 0.1 M phosphate buffer (PB), pH 7.4. After fixation, slices were rinsed in PB, cryoprotected in sucrose (30% in PBS), and quickly frozen on dry ice. To neutralize endogenous peroxidase, slices were pretreated for 30 min in 1%H_2O_2. After several rinses in 0.01 M PBS, pH7.4, slices were incubated for 24 h at room temperature, in 1:100 avidin– biotin peroxidase complex (Vector Laboratories) diluted in PBS containing 0.3% Triton X-100. After 30 min rinses in PBS, slices were processed with 0.04% 3–3-diaminobenzidine- HCl (Sigma) and 0.006% H_2O_2 diluted in PBS. All labeled neurons (n=30) except one that was excluded from this study showed complete axonal and dendritic labeling

characteristics of O-LM interneurons (McBain et al., 1994). Neurons were reconstructed using a *camera lucida*.

Detailed description of methods used in the first study

Patch clamp protocols and data analysis

Depolarizing current pulses of variable amplitude (lasting 400-800 ms) from a holding potential ranging from -65 to -75 mV were used to study different firing patterns of the recorded cells.

In some experiments, apamin-sensitive slow Ca^{2+}-dependent potassium currents (sI_{AHP}) mediated by SK channels (Sah, 1996) were recorded in the presence of tetrodotoxin (1 μM), linopirdine (10 μM) and paxilline (10 μM) to block fast sodium channels, KCQN/M and BK channels, respectively. I_{AHP} was elicited by depolarizing voltage steps (100 ms duration) from a holding potential of - 50 mV to + 10 mV, delivered every 20 s to elicit robust and unclamped Ca^{2+} action currents. In the experiments with cadmium NaH_2PO_4 was omitted from the bathing solution.

In some experiments to test the effects of endogenously released ACh on the firing properties of EGFP-positive stratum oriens interneurons, depolarizing currents steps were applied to the recorded neurons before and immediately after stimulation of cholinergic fibres with bipolar twisted NiCr-insulated electrodes positioned in *the alveus* (a 2 s train of pulses delivered at 25-50 Hz, 200 μs duration each, sometimes repeated after 10 s, Maggi et al. 2003). These experiments were performed in the presence of atropine (1 μM) to block muscarinic receptors.

In regular and irregular firing neurons, the sustained firing induced by steady depolarizing current pulses was not maintained through the pulse but underwent firing frequency adaptation. To measure this phenomenon we used the adaptation index (Avossa et al., 2003) which was calculated as:

$$A(t)=100[f\max - f(i)]/f\max$$

where *f*max is the firing frequency during the first 100 ms at the beginning of each pulse and *f*(i) is the firing frequency measured every 100 ms along the pulse The decaying phase of the slow AHP following a train of action potentials was fitted with exponential functions in the form:

$$y(t) = \sum_{i=1}^{n} A_i * \exp(- t / \tau_i)$$

where τ_i and A_i are the time constants and relative fractions of the respective components.

Ca^{2+} imaging

Fluorescence measurements were made using a conventional fluorescence microscopy system composed of an upright microscope (Axioskop; Zeiss, Jena, Germany), a digital 12-bit cooled camera (Imago; Till Photonics, Germany), and a monochromator (Till Germany). The system was driven by Till Vision software (Till Photonics). Images were acquired and stored on a Dell PC, then analyzed off line. Measurements of fluorescence over time had a resolution of 0.2-0.5 Hz.

Visually identified neurons were loaded with fura-2 (200 μM; Molecular Probes, Eugene, OR) for 45 min, dissolved in intracellular solution (containing 0.1 mM EGTA) through the recording pipette. After the establishment of the whole cell configuration, we waited 5-10 minutes, to allow the diffusion of the fluorescent dye into the cell. Fluorescence emission was monitored at 510 nm (optical filters and dichroic beam splitter were from Chroma, Brattleboro, VT) from the cell body. Changes in the level of intracellular free Ca^{2+} concentration were estimated from the ratio (R) between the digital images obtained with 340 and 380 nm excitation wavelengths. Fluorescence variations are expressed in arbitrary units (a.u.), where 1 a.u. is equal to 1/1000 R.

Detailed description of methods used in the second study

Patch clamp protocols and data analysis

In some experiments, the impedance (Z) amplitude profile (ZAP) was used to measure the electric resonance behaviour of O-LM cells (Puil et al. 1986; Hutcheon and Yarom, 2000). The voltage response upon injection through the patch pipette of a sinusoidal current (the ZAP current) with constant amplitude and linearly increasing frequency (0.5-30 Hz for 30 s; using Matlab) was recorded in current clamp conditions. Resonance was manifested as a distinct and reproducible peak in the voltage response corresponding to a certain frequency. The magnitude of the ratio of the Fast Fourier transform of the voltage response to the Fast Fourier transform of the ZAP stimulus formed the impedance amplitude profile. The frequency at which the impedance amplitude reached its maximum was the resonance frequency.

In current clamp experiments, the hyperpolarization-activated current I_h gives rise to a sag in the electrotonic potentials (obtained by injecting steady hyperpolarizing currents into the cell) followed by a rebound depolarization at the end of the pulses which often triggered action potentials. The sag was measured from the normalized steady state to peak voltage response of the cell to a hyperpolarizing current step of 250 pA (400 ms duration, from a holding potential of -70 mV) and was defined as:

$$100 \times (1-V_{ss}/V_{peak})$$

where, V_{ss} is the steady state voltage deflection from baseline and V_{peak} is the peak voltage deflection from baseline (Narayanan and Johnston, 2007).

Currents mediated by I_h were measured in voltage-clamp conditions by applying hyperpolarizing voltage steps (2 s duration) from a holding potential of -50 mV up to -120 mV (in 10 mV increment) in the presence of tetrodotoxin (TTX, 1 μM) and cadmium (200 μM) to block fast Na^+ channels and voltage-dependent Ca^{2+} channels, respectively.

In the experiments with cadmium NaH_2PO_4 was omitted from the bathing solution. The current-voltage relationship was obtained by measuring the steady state current values at the end of 2 s voltage steps after subtracting the instantaneous current at the beginning of the voltage steps. The activation curve was determined from tail current amplitudes (at the end of each hyperpolarized voltage step from -50 mV to -120 mV), measured after subtracting current

responses obtained in the presence of nicotine and ZD 7288 from their respective controls (Janigro et al., 1997). Current values at each voltage were normalized by current value obtained at -120 mV. The resulting values were plotted versus the hyperpolarization step voltages and were fitted with the Boltzmann equation:

$$I/I_{MAX} = 1/\{1+\exp[(V_{1/2}- V_m)/k]\}$$

where $V_{1/2}$ is the voltage for half maximum activation and deactivation, V_m is the pulse potential and k is the slope factor.

Time constants were determined by fitting currents using pCLAMP with a double-exponential function of the form:

$$I_h(t) = A_f \exp(-t/\tau_f) + A_s \exp(-t/\tau_s)$$

where $I_h(t)$ is the amplitude of the current at time t and A_f and A_s are the initial amplitudes of the fast (τ_f) and slow (τ_s) activation time constant components, respectively.

The dose-response curve for nicotine was constructed by applying hyperpolarizing voltage steps from -50 mV to -120 mV in the absence or in the presence of the alkaloid. The amplitudes of the steady state currents (measured at the end of the voltage steps) obtained in the presence of increasing concentrations of nicotine (from 10 nM to 10 μM) and normalized to those obtained in controls were plotted as "I_h block (%)" for different nicotine concentrations.

To investigate whether nicotine affected the intrinsic oscillatory properties of O-LM interneurons, sinusoidal currents were injected into the cells at the frequency of 3-5 Hz (in the presence of blockers of synaptic transmission) before and during application of nicotine and slopes ($mVms^{-1}$) of the voltage responses during the upswing of cycle were measured.

Homology model

A homology model of the pore region of HCN channels has been developed (Giorgetti et al. 2005) based on the following assumptions: i. in the closed state, the topology of the inner pore of HCN channels is similar to that of K^+ channels. In particular, the orientation of the S5 and S6 helices is very similar to that of the corresponding helices of the K^+ KcsA and K^+ KirBac1.1 channels. Thus, we have used as templates the x-ray structure of these K^+ channels. ii. In the open state, the S6 helix is supposed to bend further than it is in the closed state. For this reason, the template of the open conformation was the x-ray structure of the MthK channel (Jiang et al., 2002). The structural models of the closed and open states turned out to be consistent with all the available electrophysiological data. Our modelling suggests that the bending amplitude of the S6 helix upon gating is significantly smaller than that found in MthK channels (Jiang et al., 2002). The model has been further validated by a recent study (Cheng et al., 2007), in which the aminoacids involved in the interaction between ZD 7288 and cilobradine with HCN channels has been identified.

Molecular modeling

Nicotine and epibatidine were docked onto the modelled open structure of HCN channels, using the AUTODOCK 4.0 program. The parameters for the molecules were calculated using the AUTODOCK standard parameterization procedure (Morris et al., 1998). The Lamarckian Genetic Algorithm and 25 million energy evaluations per run were applied as a search method for the different docking results. The potential grid map for each atom type was calculated using a cubic box centred in the channel cavity, with a distance of 0.375 Å between grid points. For each complex, 100 docking runs were performed resulting in a total of 300 calculations. The lowest energy conformations within the most populated clusters were used to hypothesize the location of the ligands. The cluster analyses were based on the RMSD distance among the ligands on each run (RMSD cutoff of 2 Å).

Results

Paper N. 1.

Activation of nicotinic acetylcholine receptors enhances a slow calcium-dependent potassium conductance and reduces the firing of stratum oriens interneurons.

Marilena Griguoli, Rossana Scuri, Davide Ragozzino and Enrico Cherubini

European Journal of Neuroscience, Vol. 30, pp. 1011–1022, 2009

EJN fens EUROPEAN JOURNAL OF NEUROSCIENCE

European Journal of Neuroscience, Vol. 30, pp. 1011–1022, 2009 doi:10.1111/j.1460-9568.2009.06914.x

SYNAPTIC MECHANISMS

Activation of nicotinic acetylcholine receptors enhances a slow calcium-dependent potassium conductance and reduces the firing of stratum oriens interneurons

Marilena Griguoli,[1] Rossana Scuri,[1,*] Davide Ragozzino[2] and Enrico Cherubini[1]

[1]Neurobiology Department, International School for Advanced Studies (SISSA), Ed. Q1 Area Science Park, S.S.14 Km 163.5; 34012 Basovizza (Trieste), Italy

[2]Department of Physiology and Pharmacology, University Sapienza, Rome, Italy

Keywords: calcium-induced calcium release, GIN mice, O-LM interneurons, SK channels, spike frequency adaptation

Abstract

A large variety of distinct locally connected GABAergic cells are present in the hippocampus. By releasing GABA into principal cells and interneurons, they exert a powerful control on neuronal excitability and are responsible for network oscillations crucial for information processing in the brain. Here, whole-cell patch clamp recordings in current and voltage clamp mode were used to study the functional role of nicotinic acetylcholine receptors (nAChRs) on the firing properties of stratum oriens interneurons in hippocampal slices from transgenic mice expressing enhanced green fluorescent protein in a subpopulation of GABAergic cells containing somatostatin (GIN mice). Unexpectedly, activation of nAChRs by nicotine or endogenously released acetylcholine strongly enhanced spike frequency adaptation. This effect was blocked by apamin, suggesting the involvement of small calcium-dependent potassium channels (SK channels). Nicotine-induced reduction in firing frequency was dependent on intracellular calcium rise through calcium-permeable nAChRs and voltage-dependent calcium channels activated by the depolarizing action of nicotine. Calcium imaging experiments directly showed that nicotine effects on firing rate were correlated with large increases in intracellular calcium. Furthermore, blocking ryanodine receptors with ryanodine or sarcoplasmic–endoplasmic reticulum calcium ATPase with thapsygargin or cyclopiazonic acid fully prevented the effects of nicotine, suggesting that mobilization of calcium from the internal stores contributed to the observed effects. By regulating cell firing, cholinergic signalling through nAChRs would be instrumental for fine-tuning the output of stratum oriens interneurons and correlated activity at the network level.

Introduction

In the CA1 area of the hippocampus, more than 20 different interneuron subtypes have been characterized on the basis of their firing patterns, molecular expression profiles and innervation of different subcellular domains of principal cells (Klausberger & Somogyi, 2008). The spatio-temporal dynamic between the activity of interneurons and pyramidal cells leads to coherent oscillations (Klausberger *et al.*, 2003, 2004; Somogyi & Klausberger, 2005), which support different behavioural states and high cognitive tasks (Klausberger & Somogyi, 2008). Among different subpopulations of interneurons, those of the oriens-lacunosum moleculare (O-LM), which contains somatostatin, contribute to the theta rhythm *in vivo* (Buzsáki, 2002; Klausberger *et al.*, 2003; Klausberger & Somogyi, 2008). These cells, the soma of which lies in stratum oriens, target distal CA1 pyramidal cell dendrites in stratum lacunosum-moleculare (Lacaille *et al.*, 1987; Ali & Thomson, 1998; Maccaferri *et al.*, 2000; Maccaferri, 2005).

Hippocampal neurons receive an important cholinergic innervation from the medial septum-diagonal band complex of the basal forebrain (Frotscher & Léránth, 1985) and are endowed with a variety of muscarinic and nicotinic acetylcholine receptors (mAChRs and nAChRs; Levey *et al.*, 1995; Tribollet *et al.*, 2004). The majority of cholinergic nerve endings lack junctional membrane specializations (Umbriaco *et al.*, 1995; Descarries *et al.*, 1997). Therefore, it is assumed that acetylcholine (ACh) carries mainly a diffuse signal which might reach relatively distant targets (Wanaverbecq *et al.*, 2007; Rózsa *et al.*, 2008). Although previous studies from stratum oriens interneurons (the vast majority comprising O-LM interneurons) have demonstrated that cholinergic signalling via muscarinic receptors is crucial for tuning active conductances and enhancing firing reliability (Lawrence *et al.*, 2006a,b), no information is available on the effects of nAChRs.

nAChRs, which belong to the large family of ligand-gated ion channels, comprise five subunits organized in a variety of allosteric oligomers (Changeux & Edelstein, 2005). Using electrophysiological and molecular biology approaches, at least four different classes of nAChRs seem to be expressed in GABAergic interneurons of the CA1 hippocampal region: these include the α7 and the non-α7 nAChR containing the α2, α3 and α4 subunits (Alkondon *et al.*, 1998, 1999; Frazier *et al.*, 1998; Alkondon & Albuquerque, 2001, 2004;

Correspondence: Dr E. Cherubini, as above.
E-mail: cher@sissa.it

**Present address*: Department of Biology, General Physiology, University of Pisa, Italy

Received 14 May 2009, revised 21 July 2009, accepted 22 July 2009

© The Authors (2009). Journal Compilation © Federation of European Neuroscience Societies and Blackwell Publishing Ltd

McQuiston & Madison, 1999; Sudweeks & Yakel, 2000; Ishii *et al.* 2005). In particular, in O-LM interenurons, two distinct excitatory responses to ACh or nicotine, a fast and a slow one, mediated by α7 and non-α7 nAChRs, respectively have been reported (McQuiston & Madison, 1999). More recently, a sustained excitatory response to nicotine has been also characterized, mediated by α2-containing nAChR subunits (Jia *et al.*, 2009). It has been proposed that by altering local GABAergic inhibition, activation of non-desensitizing α2-containing nAChRs would serve as a molecular switch for gating information flow and synaptic plasticity (Jia *et al.*, 2009).

The aim of the present study was to assess the functional role of nAChRs on the firing properties of GABAergic interneurons. We focused on CA1 stratum oriens interneurons with horizontally orientated dendrites that largely comprise O-LM cells (Lacaille *et al.*, 1987; Ali & Thomson, 1998; Maccaferri *et al.*, 2000; Maccaferri, 2005). To target these cells, we used transgenic mice expressing enhanced green fluorescent protein (EGFP) in a subpopulation of GABAergic interneurons containing somatostatin (GIN mice; Oliva *et al.*, 2000; Minneci *et al.*, 2007). We found that activation of nAChRs by nicotine or endogenously released ACh strongly enhanced spike frequency adaptation of EGFP-positive cells. This effect was dependent on the activation of an apamin-sensitive calcium-dependent potassium conductance following intracellular calcium rise via nAChRs and voltage-dependent calcium channels and involved calcium-induced calcium release mechanisms.

Materials and methods

Hippocampal slice preparation

All experiments were carried out in accordance with the European Community Council Directive of 24 November 1986 (86/609EEC) and were approved by the local authority veterinary service. Hippocampal slices were obtained from juvenile (postnatal day P14–P21) transgenic mice expressing EGFP in a subpopulation of somatostatin-containing GABAergic interneurons (GIN mice: Jackson Laboratories, Bar Harbor, ME, USA; Oliva *et al.*, 2000; Minneci *et al.*, 2007) using a standard protocol (Rosato-Siri *et al.*, 2006). Briefly, after being anaesthetized with an i.p. injection of urethane (2 g/kg), the brain was quickly removed from the skull and placed in ice-cold artificial cerebrospinal fluid (ACSF) containing (in mM): 130 NaCl, 25 glucose, 3.5 KCl, 1.2 NaH_2PO_4, 25 $NaHCO_3$, 2 $CaCl_2$, 1.3 $MgCl_2$ (Sigma, Milan, Italy), saturated with 95% O_2 and 5% CO_2 (pH 7.3–7.4). Transverse hippocampal slices (300 μm thick) were cut with a vibratome and stored at room temperature (22–24°C) in a holding bath containing the same solution as above. After incubation for at least 1 h, an individual slice was transferred to a submerged recording chamber and continuously superfused at 33–34°C with oxygenated ACSF at a rate of 2–3 mL/min.

Electrophysiological recordings

Whole-cell patch clamp recordings (in current and voltage clamp mode) were obtained from visually identified EGFP-positive cells localized in stratum oriens of the CA1 hippocampal region. According to Goldin *et al.* (2007) about 50% of these cells are O-LM interneurons. We patched only those cells exhibiting round or fusiform cell bodies and horizontal dendrites, often close to the alveus border. Neurons were visualized using an upright fluorescent microscope (Nikon E600 FN) equipped with differential interference contrast (DIC) optics, and infrared video camera. In some experiments (n = 10) neurobiotin (0.2%; Vector Laboratories, Burlingame, CA, USA) was added to the intracellular solution for *post hoc* morphological identification (Fig. 1A). Recordings were made from 139 stratum oriens EGFP-positive cells with a Multiclamp 700A amplifier (Molecular Devices, Union City, CA, USA) in the presence of DL-2-amino-5-phosphonopentaoic acid (DL-AP5; 50 μM), 6,7-dinitroquinoxaline-2,3-dione (DNQX; 20 μM) and gabazine (SR 95531 hydrobromide; 10 μM) to block ionotropic glutamatergic and GABAergic synaptic currents, respectively. Patch electrodes were pulled from borosilicate glass capillaries (Hingelberg, Malsfeld, Germany). They had a resistance of 4–6 MΩ when filled with an intracellular solution containing (in mM): 135 $KMeSO_4$, 10 KCl, 10 HEPES, 0.5 EGTA, 2 Na_2ATP and 0.4 Na_2GTP (osmolarity 280–300 mOsm, pH 7.2–7.3, with KOH). In some experiments recordings were performed with patch pipettes containing the calcium chelator 1,2-bis (2-aminophenoxy) ethane-N,N,N′,N′-tetraacetic acid (BAPTA 10 mM, purchased from Sigma, Milan, Italy). In these cases, to maintain the same osmolarity (∼290 mOsm), the intrapipette concentration of $KMeSO_4$ was reduced from 135 to 125 mM and EGTA was omitted from the intracellular solution. Series resistance was assessed repetitively every 5 min and in current-clamp recordings compensated at 75% throughout the experiment (the series resistance value varied between 20 and 25 MΩ). Cells exhibiting more than 15–20% changes in series resistance were excluded from the analysis. Membrane potential values were corrected for a liquid junction potential of 15.1 mV.

Depolarizing current pulses of variable amplitude (lasting 400–800 ms) from a holding potential ranging from −65 to −75 mV were used to study different firing patterns of the recorded cells.

In some experiments, apamin-sensitive slow Ca^{2+}-dependent potassium currents (sI_{AHP}) mediated by SK channels (Sah, 1996) were recorded in the presence of tetrodotoxin (1 μM), linopirdine (10 μM) and paxilline (10 μM) to block fast sodium channels, KCQN/M and BK channels, respectively. I_{AHP} was elicited by depolarizing voltage steps (100-ms duration) from a holding potential of −50 to +10 mV, delivered every 20 s to elicit robust and unclamped Ca^{2+} action currents. In the experiments with cadmium, NaH_2PO_4 was omitted from the bathing solution.

In some experiments to test the effects of endogenously released ACh on the firing properties of EGFP-positive stratum oriens interneurons, depolarizing currents steps were applied to the recorded neurons before and immediately after stimulation of cholinergic fibres with bipolar twisted NiCr-insulated electrodes positioned in the alveus (a 2-s train of pulses delivered at 25–50 Hz, 200-μs duration each, sometimes repeated after 10 s, Maggi *et al.*, 2003). These experiments were performed in the presence of atropine (1 μM) to block muscarinic receptors.

Ca^{2+} imaging

Fluorescence measurements were made using a conventional fluorescence microscopy system consisting of an upright microscope (Axioskop; Zeiss, Jena, Germany), a digital 12-bit cooled camera (Imago; Till Photonics, Munich, Germany) and a monochromator (Till Photonics). The system was driven by Till Vision software (Till Photonics). Images were acquired and stored on a Dell PC, then analysed off line. Measurements of fluorescence over time had a resolution of 0.2-0.5 Hz.

Visually identified neurons were loaded with Fura-2 (200 μM; Molecular Probes, Eugene, OR, USA) for 45 min, dissolved in intracellular solution (containing 0.1 mM EGTA) through the recording pipette. After establishment of the whole-cell configuration, 5–10 min was permitted to allow the diffusion of the fluorescent dye

© The Authors (2009). Journal Compilation © Federation of European Neuroscience Societies and Blackwell Publishing Ltd

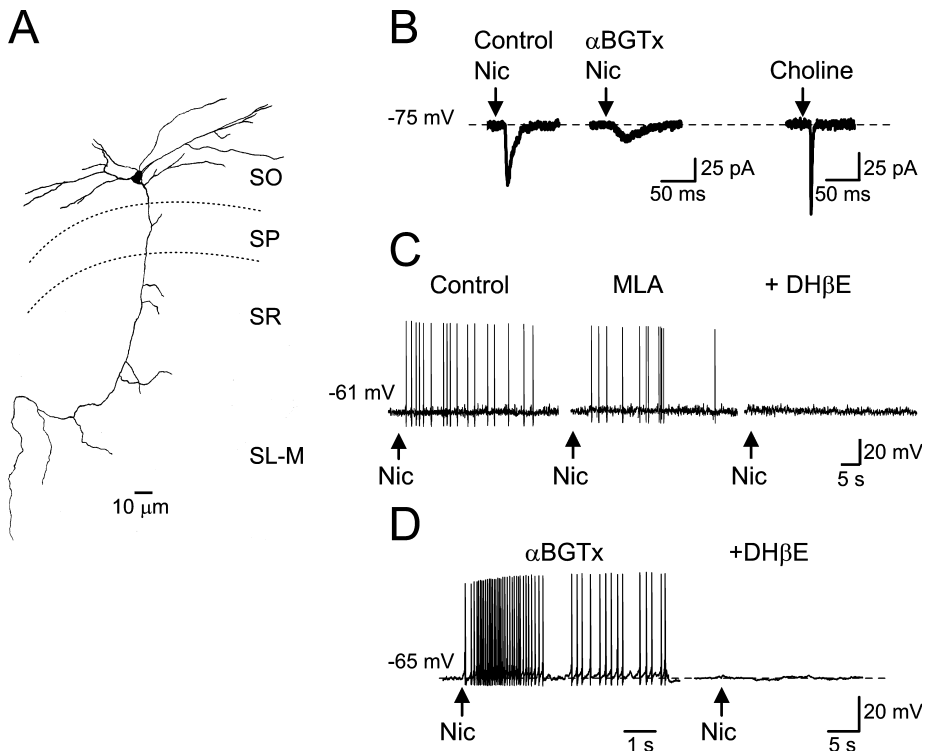


FIG. 1. Pressure application of nicotine to stratum oriens interneurons induces fast and slow α7- and non-α7 nAChR-mediated responses. (A) *Post-hoc* camera lucida reconstruction of a cell recorded with a patch pipette containing neurobiotin, showing characteristic horizontal dendrites and long axon projecting to stratum lacunosum-moleculare. (B) Puff application of nicotine (left, arrow) to an EGFP-positive cell localized in stratum oriens, voltage-clamped at −75 mV (in the presence of 50 μM DL-AP5, 20 μM DNQX and 10 μM gabazine), induced a fast inward current followed by a slow one. In the presence of αBGTx (100 nM, middle) a slow component was unveiled. Pressure application of choline to another cell (right, arrow) voltage clamped at the same potential induced only a fast inward current. (C) Application of nicotine (arrows) in current clamp conditions induced repetitive firing which was partially antagonized by MLA (10 nM) and completely blocked by concomitant application of MLA and DHβE (500 nM). (D) In another cell, puff application of nicotine (arrow) in the presence of αBGTx slightly depolarized the membrane and triggered a sustained firing which was abolished by adding DHβE to the bathing solution.

into the cell. Fluorescence emission was monitored at 510 nm (optical filters and dichroic beam splitter were from Chroma, Brattleboro, VT, USA) from the cell body. Changes in the level of intracellular free Ca^{2+} concentration were estimated from the ratio (R) between the digital images obtained with 340- and 380-nm excitation wavelengths. Fluorescence variations are expressed in arbitrary units (a.u.), where 1 a.u. is equal to 1/1000 R.

Drugs

Drugs used were: DL-AP5, DNQX, SR 95531 hydrobromide, apamin, linopirdine dihydrocloride, ryanodine, thapsigargin and cyclopiazonic acid (CPA), all purchased from Tocris Bioscience (Bristol, UK); nicotine, dihydro-β-eritroidine (DHβE), α-bungarotoxin (αBGT), methyllycaconitine (MLA), atropine and choline from Sigma; paxilline from Alomone Labs (Jerusalem, Israel); and tetrodotoxin (TTX) from Latoxan (Valence, France).

In the experiments with αBGT, ryanodine, thapsigargin and CPA, slices were previously incubated with the drugs, for at least 1 h, during the recovering time. Stock solutions were made in distilled water and then aliquoted and frozen at −20°C. DNQX, thapsigargin and CPA were dissolved in dimethylsulphoxide (DMSO). The final concentration of DMSO in the bathing solution was 0.1%. At this concentration, DMSO alone did not modify the membrane potential, input resistance or the firing properties of O-LM interneurons. Ryanodine was dissolved in ethanol. The final concentration of ethanol was 1%. Drugs were applied in the bath via a three-way tap system, by changing the superfusion solution to one differing only in its content of drug(s). The ratio of flow rate to bath volume ensured complete exchange within 1–2 min. Nicotine was applied either in the bath (1–3 μM for 5 min) or by pressure ejection ($41–55*10^3$ Pa for 50–100 ms) from a glass pipette (tip opening of ∼1 μm; concentration of nicotine into the pipette 2 mM), localized close to the patched cell, using the Picospritzer II (General Valve, Fairfied, NJ, USA).

Data analysis

Data were transferred to computer hard disk after digitization with an A/D converter (Digidata 1322, Molecular Devices). Data acquisition (digitized at 20 kHz and filtered at 2 kHz) was performed with pClamp 9.2 software (Molecular Devices). Input resistance and capacitance of the cells were measured online with the membrane test feature of the pClamp software. Data were analysed with Clampfit 9.2 (Molecular Devices). In regular and irregular firing neurons, the sustained firing induced by steady depolarizing current pulses was not maintained through the pulse but underwent firing frequency adaptation. To measure this phenomenon we used the adaptation index (Avossa *et al.*, 2003), which was calculated as:

© The Authors (2009). Journal Compilation © Federation of European Neuroscience Societies and Blackwell Publishing Ltd

$$A(t) = 100\,[f_{max} - f(i)]/f_{max}$$

where f_{max} is the firing frequency during the first 100 ms at the beginning of each pulse and $f(i)$ is the firing frequency measured every 100 ms along the pulse The decaying phase of the slow AHP following a train of action potentials was fitted with exponential functions in the form:

$$y(t) = \sum_{i=1}^{n} A_i \times \exp(-t/\tau_i)$$

where τ_i and A_i are the time constants and relative fractions of the respective components.

Values are given as mean ± SEM. Significance of differences was assessed by Student's paired *t*-test, Wilcoxon signed rank test and Mann–Whitney rank sum test as indicated. $P < 0.05$ was taken as significant.

Results

Different firing patterns of stratum oriens interneurons

In agreement with previous reports (Oliva *et al.*, 2000; Minneci *et al.*, 2007), EGFP-expressing interneurons in stratum oriens were immunopositive for somatostatin, for metabotropic glutamate receptors 1α and for neuropeptide Y, but not for parvalbumin. On average, these cells exhibited a resting membrane potential of −66 ± 0.3 mV and an input resistance of 285 ± 19 MΩ ($n = 139$). The majority of them (96/139; 69%) fired spontaneously at resting membrane potential. The firing frequency ranged between 1.7 and 7.7 Hz. In addition, injection of hyperpolarizing current pulses (400-ms duration) of different amplitudes from the resting membrane potential revealed, in all cells examined, a sag in the electrotonic potentials that was abolished by ZD7288 (100 μM; data not shown), indicating that it was due to the activation of the time-dependent inwardly rectifying cationic current I_h (see also Maccaferri & McBain, 1996; Minneci *et al.*, 2007).

Long depolarizing current pulses applied from similar holding potentials (between −65 and −75 mV) to EGFP-positive stratum oriens interneurons revealed different firing patterns. These were classified into regular, irregular and clustered (see Fig. 3 in Minneci *et al.*, 2007). In regular firing cells, the interspike interval was constant for the entire duration of the pulse and the repolarization following each action potential directly initiated the next spike. In irregular firing neurons, the interspike interval was variable and spike repolarization was often followed by a variable delay before the occurrence of the next spike. In clustered cells, brief trains of spikes occurring at regular intervals were separated by silent periods of variable duration, usually exhibiting voltage-dependent oscillations (Parra *et al.*, 1998; Minneci *et al.*, 2007). Regular firing occurred in 108/139 neurons (77%), irregular in 26/139 (19%) and clustered in 5/139 (4%). Different firing patterns were not significantly modified by increasing the amplitude of depolarizing current pulses (data not shown). In both regular and irregular firing neurons, spike repolarization was followed by a small but consistent slow membrane hyperpolarization (sAHP, amplitude 5.7 ± 0.5 mV; decay time constant: 1.1 ± 0.19 s; $n = 10$; see also Zhang & McBain, 1995). The passive and active membrane properties of each group of neurons were very similar, except for the input resistance of regular firing neurons, which was higher than that of irregular and clustered neurons (Table 1). In the following experiments the role of nicotine on the firing properties of stratum oriens interneurons was tested mainly on regular firing cells, which were those occurring more frequently.

TABLE 1. Membrane properties according to neuron type

	Regular	Irregular	Clustered	Total
Number of cells (n)	108	26	5	139
R_i (MΩ)	305 ± 23*	197 ± 26	203 ± 24	281 ± 19
C_m (pF)	52 ± 1.6	59 ± 4	55.3 ± 4.1	53 ± 1.4
V_m (mV)	−66 ± 0.3	−66 ± 1.1	−64.1 ± 2.8	−66 ± 0.3
Spike amplitude (mV)	71 ± 1.1	66 ± 2.2	61.4 ± 8.8	70 ± 1
Spike width (ms)	0.76 ± 0.02	0.78 ± 0.05	0.67 ± 0.1	0.76 ± 0.02

*$P = 0.007$, Mann–Whitney rank sum test.

Low doses of nicotine strongly reduced the firing rate of stratum oriens interneurons

In agreement with previous studies (McQuiston & Madison, 1999; Jia *et al.*, 2009), a brief puff of nicotine (50–100 ms) from a patch pipette localized close to a patched neuron (intrapipette concentration of nicotine 2 mM) held at −75 mV caused fast inward currents (mean peak amplitude 85 ± 35 pA; $n = 5$) followed by slow ones. The fast components were blocked by αBGT (100 nM; $n = 5$; Fig. 1B) and the slow components by DHβE (1 μM; $n = 4$), indicating that they were mediated by α7 and non-α7 nAChRs, respectively. In addition, pressure application of choline, a selective α7 nAChR agonist (Papke *et al.*, 1996; intrapiptte concentration 10 mM), evoked only fast inward currents (Fig. 1B) that were selectively blocked by the α7 nAChR antagonist MLA (100 nM; data not shown). In current clamp experiments, puff application of nicotine from a holding potential ranging from −65 to −60 mV (below the threshold for action potential generation) induced a slow membrane depolarization which triggered repetitive action potential firing. These effects were partially reduced by application of MLA (10 nM) and completely blocked when DHβE (500 nM) was added to MLA ($n = 7$; Fig. 1C). In another group of neurons ($n = 5$) incubated for at least 1 h in the presence of αBGT, pressure application of nicotine induced sustained firing that was blocked by DHβE (Fig. 1D), indicating that functional non-α7 receptors, probably containing the α2 subunits, are also expressed in O-LM interneurons (see Jia *et al.*, 2009).

To investigate whether nicotine was able to modulate the firing of these cells, a low concentration of nicotine (1–3 μM) was applied in the bath for 5 min. In a few cases ($n = 3$) nicotine was applied also by pressure from a glass pipette localized close to the patched cell. Similar effects were found and therefore data were pooled. In 21/35 (60%) of regular firing cells, nicotine strongly reduced the firing frequency (from 28 ± 2 to 17 ± 2 Hz, $n = 21$, $t_{20} = 6.99$, $P < 0.001$; Fig. 2). In a small group of irregularly firing neurons ($n = 4/8$), nicotine reduced firing frequency from 20 ± 1.6 to 7.8 ± 1.3 Hz ($n = 4$, $t_3 = 20.5$, $P < 0.001$; data not shown). Only in 2/21 cases was a complete recovery obtained 20 min after washing out nicotine. Nicotine-induced reduction of firing rate was associated with a significant decrease in the amplitude of the AHP following the action potentials (the peak amplitude of the AHP was 3.4 ± 0.3 mV; and the decay time constant 1.5 ± 0.8 s; $n = 5$, $t_4 = -3.14$, $P = 0.035$ with respect to controls). As shown in Fig. 2B, nicotine significantly increased the adaptation index $A(t)$ ($n = 17$; P values ranged from 0.03 to < 0.001).

To assess the involvement of nAChRs in the observed effects, we repeated the same experiments in the presence of nAChR antagonists. Bath application of selective α7 and non-α7 nAChR antagonists MLA (10 nM, $n = 15$) and DHβE (500 nM; $n = 12$), respectively, *per se* did not modify the firing of EGFP-positive cells. This allows us to exclude the possibility that the tonic activation of nAChRs by endogenous ACh present in the extracellular space contributes to set different firing

© The Authors (2009). Journal Compilation © Federation of European Neuroscience Societies and Blackwell Publishing Ltd

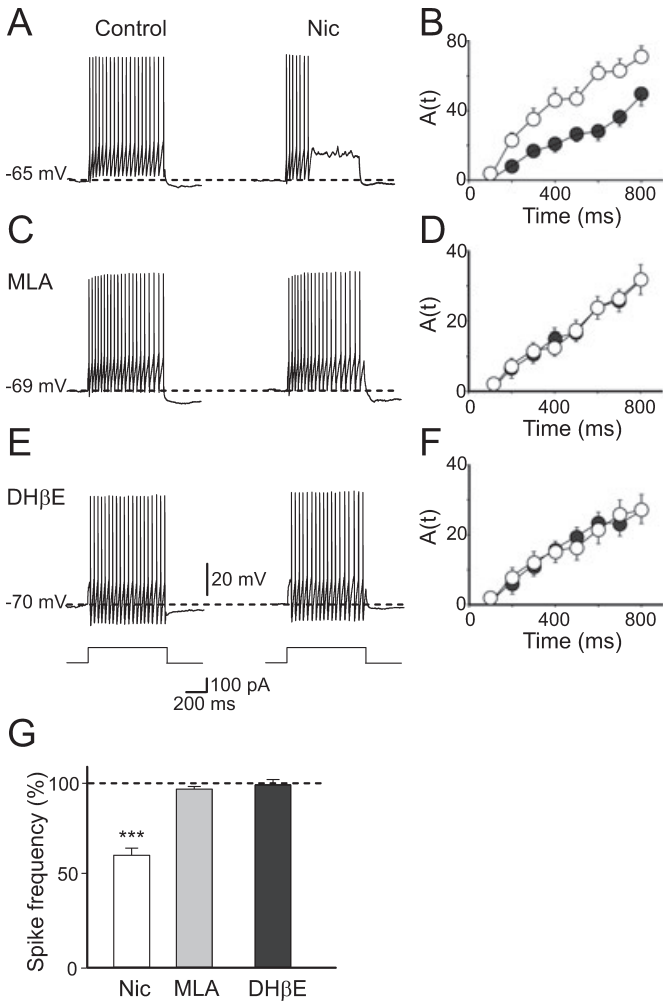


FIG. 2. Nicotine reduces the firing frequency of O-LM interneurons. (A) Regular spiking interneuron in control (left) and after bath application of nicotine (1 μM, right). (B) Mean firing adaptation values [$A(t)$] obtained in control (closed circles) or during nicotine (open circles) are plotted vs. time (n = 17 for each). Paired t-test through data points obtained in the absence or in the presence of nicotine were significantly different (P values varied from 0.01 to < 0.001). In this and in the following figures vertical bars refer to SEM (often these are within the symbols). (C–F) As in A but in the presence of MLA (100 nM; C and D) or DHbE (0.5 mM; E and F). (G) Each column represents the mean spike frequency values (as percentage of control, dashed line), obtained in the presence of nicotine (n = 21) and nicotine plus MLA (n = 16) or DHβE (n = 16). ***P < 0.001.

patterns in stratum oriens interneurons. However, these substances fully prevented nicotine effects on the firing rate (before and after MLA, firing frequency was 36 ± 2 and 35 ± 2 Hz, respectively, n = 16, t_{15} = 2.11, P = 0.06; Fig. 2C–G; before and after DHβE, firing frequency was 35 ± 10 and 34 ± 10 Hz, n = 16, t_{15} = 0.75, P = 0.47; Fig. 2E–G) and on $A(t)$ (Fig. 2D–F). The possibility of blocking nicotine-induced firing frequency adaptation with either α7 or non-α7 nAChR antagonists suggests that a certain degree of cooperation is needed to produce the observed effects. In seven neurons treated with MLA or DHβE, application of nicotine 30 min after wash out of the antagonists induced a significant reduction of firing rate (from 25 ± 2 to 15 ± 2.4 Hz, n = 7, t_6 = 4.73, P = 0.003). Taken together, these results suggest that nicotine-induced reduction in firing rate was mediated by α7 and non-α7 nAChRs.

Nicotine reduces the firing rate of stratum oriens interneurons by enhancing an apamin-sensitive Ca^{2+}-activated K^+ conductance

In stratum oriens interneurons, action potentials are followed by an sAHP, which is generated by the activation of small Ca^{2+}-activated K^+ channels (SK channels; Sah, 1996). These channels, which are selectively blocked by the bee venom toxin apamin (Sah & McLachlan, 1991), contribute to regulate cell excitability and are responsible for spike frequency adaptation (Zhang & McBain, 1995). Therefore, in the following experiments we tested whether nicotine-induced changes in firing rate and in $A(t)$ involved an apamin-sensitive Ca^{2+}-activated K^+ conductance. First we blocked the sAHP with apamin. Apamin (100 nM) caused an increase in firing frequency from 34 ± 6 to 47 ± 8 Hz (n = 6, t_5 = −3.55, P = 0.016). The effects of apamin did not recover after washing out the drug. Addition of nicotine to apamin did not modify the firing rate or $A(t)$ (the firing rate was 46 ± 8 and 51 ± 10 Hz, before and after nicotine, respectively; n = 6, W = 9 Wilcoxon signed rank test, P = 0.44; Fig. 3). To elucidate this point further, nicotine effects were directly tested on sI_{AHP}, the current underlying the sAHP. Voltage steps (100-ms duration) from −50 to +10 mV delivered in the presence of TTX, linopirdine and paxilline (see Materials and methods) gave rise to characteristic slow tail currents following robust and unclamped Ca^{2+} action currents. Application of nicotine caused a significant increase of sI_{AHP} from 118 ± 17 to 147 ± 16 pA (130 ± 12%; n = 6, t_5 = -4.75, P = 0.005; Fig. 4A, left, and Fig. 4B). It is worth noting that the increase in amplitude of sI_{AHP}

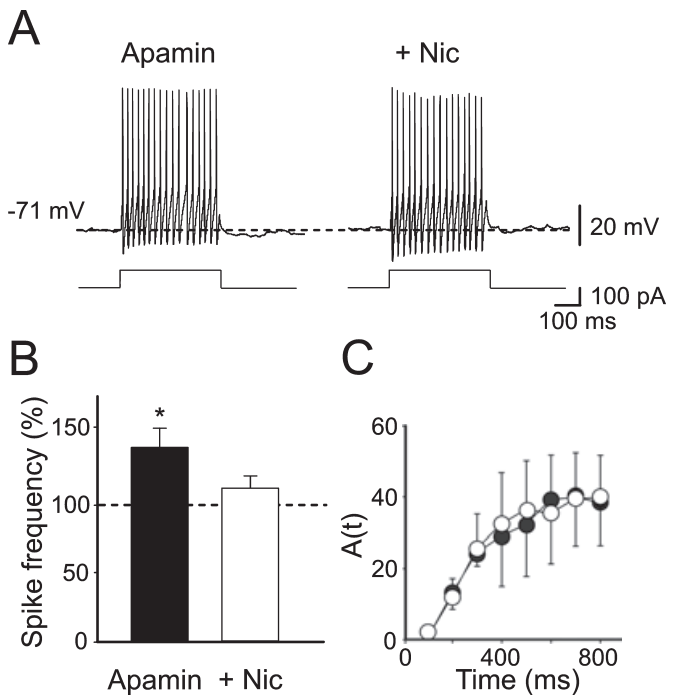


FIG. 3. The effects of nicotine on the firing rate of O-LM interneurons are prevented by apamin. (A) Representative example of a regular spiking neuron recorded in the presence of apamin (100 nM, left) and apamin plus nicotine (1 μM, right). Note that in the presence of apamin nicotine was unable to modify the firing rate. (B) Each column represents the mean spike frequency (as percentage of control, dashed line), obtained in the presence of apamin (n = 6) and apamin plus nicotine (n = 6). With respect to controls, the increase in firing frequency induced by apamin was significant (P = 0.016). No significant differences were found between apamin and apamin plus nicotine (P = 0.438). (C) Mean firing adaptation $A(t)$ values obtained in the presence of apamin (closed circles) or apamin plus nicotine (open circles) are plotted vs. time (n = 6 for each). *P < 0.05.

© The Authors (2009). Journal Compilation © Federation of European Neuroscience Societies and Blackwell Publishing Ltd

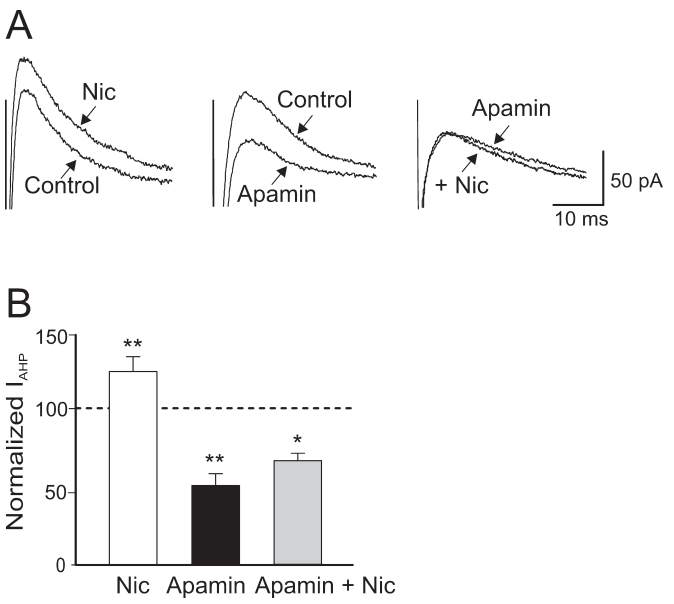


FIG. 4. Nicotine enhances the apamin-sensitive sI_{AHP}. (A) Representative examples of slow outward tail currents elicited in three different O-LM interneurons by voltage steps (100-ms duration) from −50 to +10 mV in the presence of TTX (1 μM), linopirdine (10 μM) and paxilline (10 μM) to block fast sodium channels, KCQN/M and BK channels, respectively. Each trace is the average of three samples. Whereas nicotine increased the tail current (left), apamin reduced it (middle). In addition, nicotine applied in the presence of apamin was ineffective (right). (B) Each column represents the mean peak amplitude of sI_{AHP} (as percentage of control, dashed line), obtained in the presence of nicotine (n = 6), apamin (n = 7) and apamin plus nicotine (n = 5). With respect to controls, P values were 0.005, 0.002 and 0.015 for nicotine, apamin and apamin plus nicotine, respectively. *P < 0.05; **P ≤ 0.005.

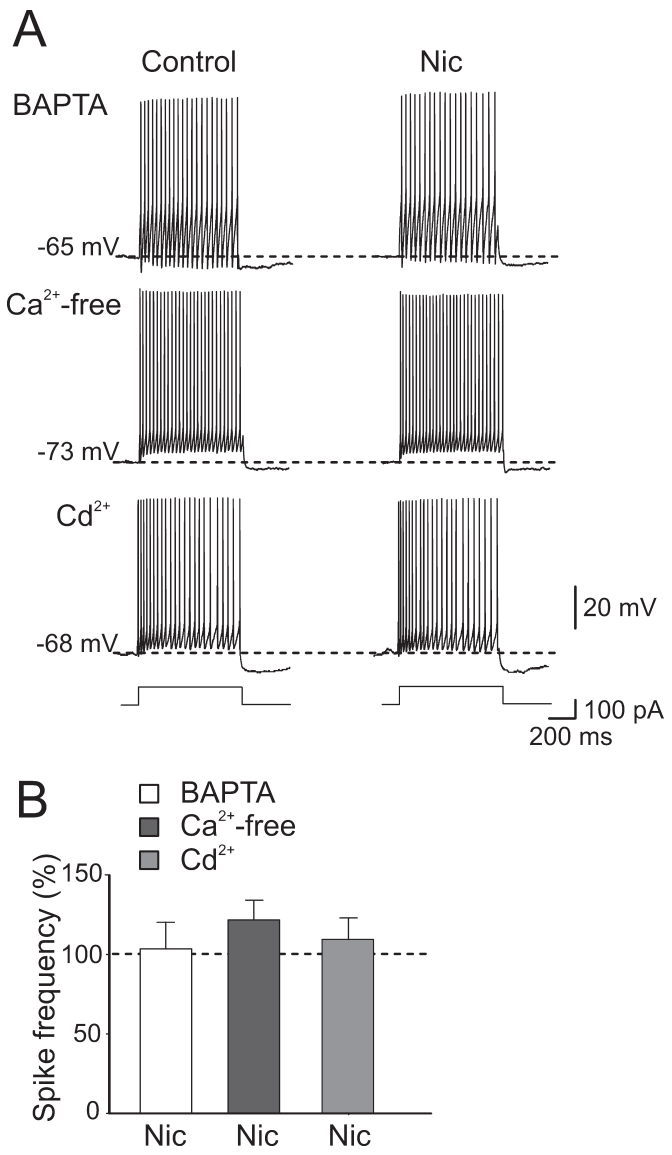


FIG. 5. The effects of nicotine on firing rate of O-LM interneurons require calcium increase via nAChRs and voltage-dependent calcium channels. (A) Representative examples of regular firing O-LM interneurons recorded with a patch pipette containing BAPTA (10 mM, top) or with an extracellular solution devoid of calcium and containing EGTA (100 μM, middle) or containing cadmium (200 μM, bottom). Traces on the left and on the right are in the absence or in the presence of nicotine (1 μM), respectively. (B) Each column represents mean spike frequency (as percentage of control, dashed line) obtained in the presence of nicotine in cells patched with an intracellular solution containing BAPTA (n = 5), or perfused with an extracellular solution devoid of calcium and containing EGTA (n = 5) or containing cadmium (n = 7).

was associated with a reduction in the numbers of unclamped Ca^{2+} action currents (from three to one). Unlike nicotine, bath application of apamin (100 nM) significantly reduced the amplitude of tail currents from 134 ± 16 to 74 ± 19 pA (52 ± 9%; n = 7, t_6 = 5.02, P = 0.002, Fig. 4A, middle, and Fig. 4B), an effect associated with an increased number of unclamped Ca^{2+} action currents. In the presence of apamin, nicotine was unable to modify the peak amplitude of sI_{AHP} (on average, tail current amplitude was 67 ± 10 pA in apamin and 64 ± 11 pA in apamin plus nicotine; 94 ± 6%; n = 5, t_4 = 1.18, P = 0.304; Fig. 4A, right, and Fig. 4B), indicating that nicotine and apamin exert their effect on the same target.

Nicotine reduces the firing rate of stratum oriens interneurons by increasing Ca^{2+} entry via nAChRs and voltage-activated calcium channels

The sAHP that follows spike repolarization results from the activation of a Ca^{2+}-dependent K^+ conductance which is gated by calcium entering into the cell during the action potentials (Sah, 1996). The underlying sI_{AHP} peaks quickly and decays with a time course which depends on the amount of calcium influx, and therefore the time course of the macroscopic current reflects the dissipation of calcium gradients at the plasmalemma (Sah, 1996). nAChRs are highly permeable to Ca^{2+}, particularly the homomeric α7 (Tsuneki *et al.*, 2000; Fucile, 2004; Fayuk & Yakel, 2005). In addition, calcium may enter into the cell via voltage-dependent calcium channels, activated by the depolarizing action of nicotine (Kulak *et al.*, 2001). Therefore, different sets of experiments were performed to assess whether a direct or indirect increase of calcium following activation of nAChRs may account for nicotine-induced reduction in firing rate and in $A(t)$ of stratum oriens interneurons. First, patch pipettes were loaded with an intracellular solution containing the fast calcium buffer BAPTA. Application of nicotine did not modify the firing frequency, which was 21 ± 5 and 20 ± 6 Hz before and during nicotine, respectively (n = 5, t_4 = 0.47, P = 0.66; Fig. 5A and B). In another set of experiments, nicotine was applied to cells bathed with an extracellular solution devoid of calcium and containing EGTA (100 μM). In these conditions, firing frequency increased from 10 ± 5 to 22 ± 3 Hz

© The Authors (2009). Journal Compilation © Federation of European Neuroscience Societies and Blackwell Publishing Ltd

(n = 4, t_3 = −5.44, P = 0.012; data not shown). Addition of nicotine failed to modify the firing frequency, which was 37 ± 4 and 45 ± 7 Hz before and during nicotine, respectively (n = 5, t_4 = −2.04, P = 0.110; Fig. 5A and B). Finally, in another set of experiments, we added to the extracellular solution cadmium, a non-selective voltage-dependent calcium channel blocker. Cadmium (200 μM) significantly enhanced the firing rate of stratum oriens interneurons from 21 ± 4 to 33 ± 3.5 Hz (n = 6, W = 91 Wilcoxon signed rank test, P = 0.016; data not shown). However, addition of nicotine failed to alter the firing rate, which was 34 ± 5 and 36 ± 5 Hz before and during nicotine application, respectively (n = 7, t_6 = −0.5, P = 0.634; Fig. 5A and B). These experiments demonstrate that calcium increase via nAChRs and voltage-dependent calcium channels is responsible for the nicotine-induced increase of sI_{AHP} and reduction in firing rate.

Nicotine increases the basal level of intracellular calcium

To evaluate directly whether nicotine-induced reduction of firing rate is associated with an increase in intracellular calcium concentration, in one set of experiments the intracellular calcium increase following nAChRs activation was directly measured using the calcium-sensitive dye Fura-2 in the patch pipette. As shown in the example in Fig. 6, nicotine application induced an increase in fluorescence (Fig. 6A) which was associated with a rise in basal intracellular calcium level (see the two dashed lines in Fig. 6B) and a reduction in firing rate (Fig. 6D). This was assessed by delivering depolarizing current pulses before and during nicotine application (arrows in Fig. 6B). Overall, in six cells, nicotine enhanced the basal Fura-2 fluorescence ratio from 334 ± 6 to 442 ± 20 a.u. (W = 13593 Wilcoxon signed rank test, P < 0.001; Fig. 6C). This was accompanied by a reduction in firing

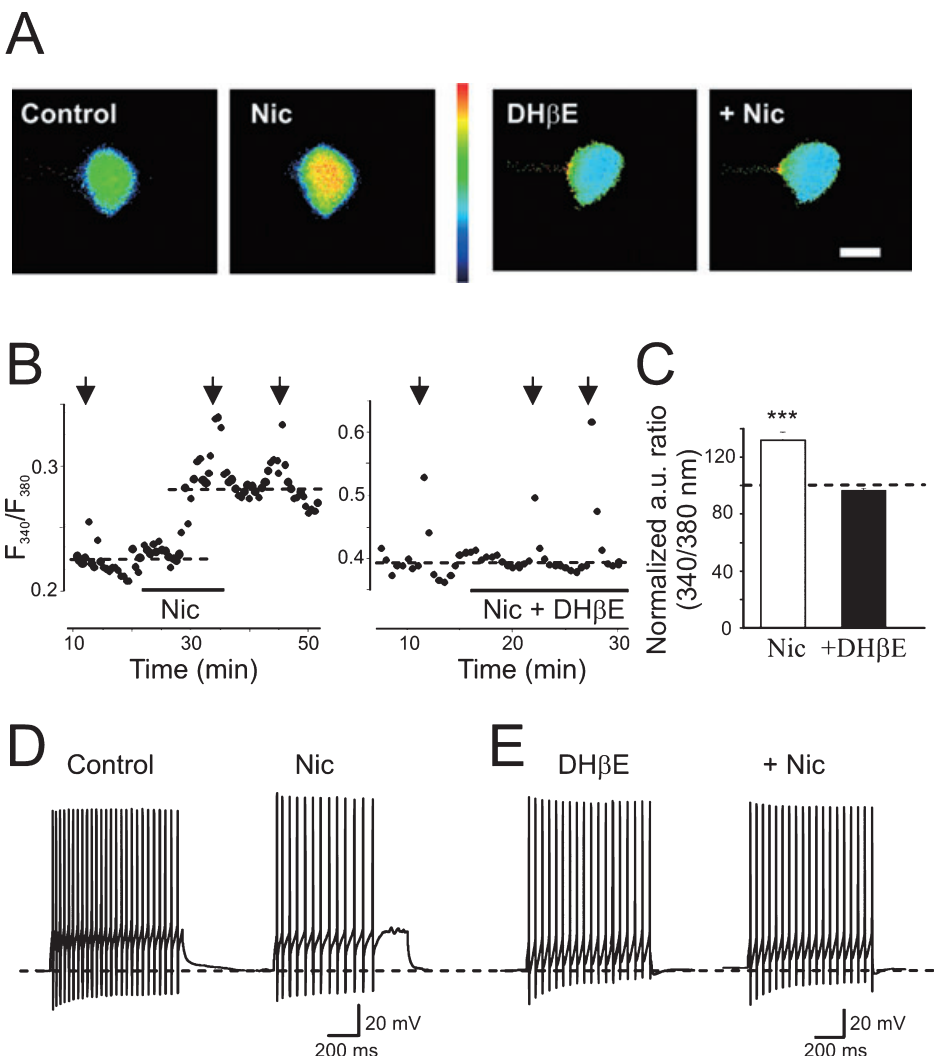


FIG. 6. Nicotine-induced reduction of firing rate is associated with an increase in basal intracellular calcium level. (A) Sample images representing fluorescence ratio (F_{340}/F_{380}) before and after nicotine application (3 μM) in the absence (left) and in the presence (right) of DHβE (50 μM), as indicated. Scale bar: 20 μm. (B) Time course of fluorescence increase induced by nicotine in the Fura-2-loaded voltage-clamped neuron shown in A; arrows indicate the time of cell stimulation with firing protocol; dashed lines refer to average basal fluorescence values. Fluorescence transients induced by firing are cut. Fluorescence calibration bar represents ratio variation 0–0.4 in D and 0–1.2 in E. (C) Each column represents the mean basal fluorescence ratio (in arbitrary units, a.u., measured over 3 min in each experiment) calculated in six neurons during nicotine application in the absence (white) or in the presence of DHβE (black), normalized to controls; ***P < 0.001. (D and E) Representative examples of two regular firing cells (the same as in A) before and after nicotine application in the absence (left) and in the presence (right) of DHβE.

© The Authors (2009). Journal Compilation © Federation of European Neuroscience Societies and Blackwell Publishing Ltd

rate from 29 ± 4 to 17 ± 4 Hz (n = 6, t_5 = 0.32, P = 0.01). Both nicotine-induced reduction in firing rate and increase in fluorescence ratio were prevented by a high concentration of DHβE (50 μM), which blocks all nAChR subtypes (Fig. 6A and B). In the presence of DHβE the firing rate was 27 ± 5 and 26 ± 5 Hz (n = 5, t_4 = 3.42, P = 0.77) while the fluorescence ratio was 370 ± 2 and 368 ± 3 a.u. before and during nicotine application, respectively (W = −1461 Wilcoxon signed rank test, P = 0.09, Fig. 6C). These experiments further indicate that nicotine effects on cell firing adaptation are strictly dependent on the intracellular calcium increase via nAChRs and/or voltage-dependent calcium channels activated by the depolarizing action of nicotine.

Ca^{2+} entering through nAChRs and/or voltage-dependent calcium channels induces Ca^{2+} release from intracellular calcium stores

The apparent paradoxical effect of nicotine on the firing rate of stratum oriens interneurons can be caused by a delayed effect related to calcium-induced calcium release (CICR) from intracellular stores (Verkhratsky, 2002) following calcium flux through nAChRs and/or voltage-activated calcium channels. It is well established that the increase in cytoplasmatic calcium concentration consecutive to the opening of homomeric α7 and heteromeric non-α7 nAChR channels activates ryanodine receptors that gate endoplasmatic reticulum calcium stores (Tsuneki *et al.*, 2000; Shoop *et al.*, 2001; Dajas-Bailador *et al.*, 2002). Therefore, the following experiments were performed to verify whether CICR contributes to nicotine-induced reduction in firing rate of O-LM interneurons. First, slices were incubated for at least 1 h in the extracellular solution containing 100 μM ryanodine, a concentration known to block ryanodine receptors irreversibly (Llano *et al.*, 2000). Depolarizing current pulses elicited action potential firing that was unaffected by nicotine (the firing frequency was 18 ± 4 and 20 ± 8 Hz before and during nicotine, respectively; n = 4, t_3 = -0.61, P = 0.58; Fig. 7A and B). In a second set of experiments we used thapsigargin, which selectively blocks sarcoplasmic–endoplasmic reticulum calcium ATPase, a protein that controls refilling of calcium stores (Thastrup *et al.*, 1990). Thapsygargin was applied in the bath at 10 μM (after pre-incubation for at least 1 h). In the presence of thapsigargin, nicotine failed to reduce the firing rate of stratum oriens interneurons (the firing frequency was 13 ± 2 and 11 ± 1 Hz in the absence and in the presence of nicotine, respectively; n = 4, W = −10 Wilcoxon signed rank test, P = 0.125; Fig. 7A and B). As thapsygargin may exert its effect by inhibiting calcium entry via voltage-activated calcium channels (Rossier *et al.*, 1993; Nelson *et al.*, 1994; Shmigol *et al.*, 1995), we tested another blocker of sarcoplasmic–endoplasmic reticulum calcium ATPase (SERCA), namely CPA (Seidler *et al.*, 1989). CPA (applied at 30 μM after a pre-incubation period of at least 1 h) fully prevented the effects of nicotine on stratum oriens interneuron firing (spike frequency was 28 ± 6 and 26 ± 6 Hz before and during nicotine application, respectively; n = 7, t_6 = 1.77, P = 0.13; Fig. 7A and B). Overall these results indicate that the effects of nicotine on the firing properties of EGFP-positive cells present on stratum oriens, including O-LM interneurons, are strictly dependent on mobilization of calcium from intracellular stores consequent to CICR mechanisms.

Endogenously released ACh from cholinergic fibres mimics the effects of nicotine on reduction in spike frequency

As mentioned, pyramidal cells and interneurons in the hippocampus receive strong cholinergic innervation from the medial septum-diagonal band complex of the basal forebrain (Frotscher & Léránth, 1985). Activation of nAChRs by ACh, endogenously released from cholinergic fibres, may mimic the effect of nicotine on the reduction of firing rate of O-LM interneurons. Therefore, to see whether this was the case, in the following experiments, depolarizing current steps were applied before and immediately after stimulating cholinergic fibres in the alveus. Stimulation trains were delivered in the presence of atropine (1 μM) to block muscarinic AChRs. In eight of 13 cells (61%), stimulation of cholinergic fibres induced a significant reduction in firing rate (from 40 ± 4 to 20 ± 3; n = 8, t_7 = 4.66, P = 0.002; Fig. 8A and B). This effect was prevented by DHβE (50 μM), a concentration that blocks all nAChR subtypes (in the presence of DHβE, firing frequency was 37 ± 2 and 38 ± 3 Hz before and after

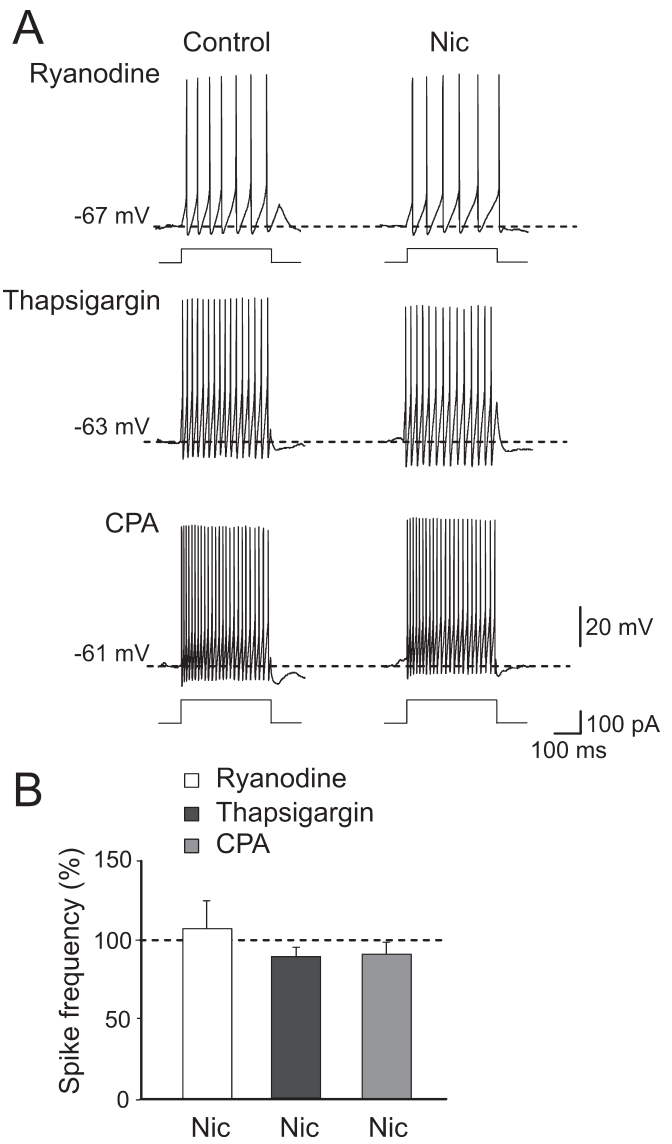


FIG. 7. Nicotine-induced reduction of firing rate requires mobilization of calcium from internal stores through CICR. (A) Representative examples of regular firing O-LM interneurons recorded in the presence of ryanodine (100 μM, top), thapsigargin (10 μM, middle) or CPA (30 μM, bottom). Traces on the left and on the right are in the absence or in the presence of nicotine (1 μM), respectively. (B) Each column represents mean spike frequency (as percentage of control, dashed line) obtained in the presence of nicotine in cells bathed with an extracellular solution containing ryanodine (n = 4), thapsigargin (n = 4) or CPA (n = 7). These drugs did not alter the firing properties of O-LM interneurons.

© The Authors (2009). Journal Compilation © Federation of European Neuroscience Societies and Blackwell Publishing Ltd

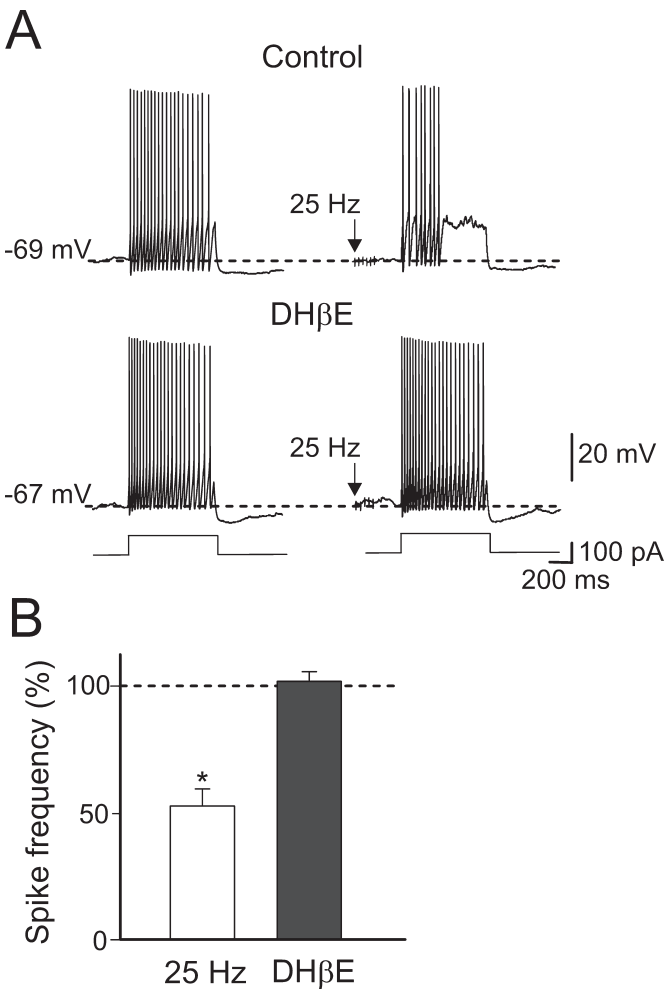


FIG. 8. Activation of nAChRs by endogenously released ACh mimics the effect of nicotine on spike frequency adaptation. (A) Upper traces: example of a regular spiking neuron recorded before (left) and immediately after delivering one train of stimuli (2-s duration at 25 Hz, 200-μs duration each; right) to cholinergic fibres in the alveus (in the presence of atropine 1 μM). Lower traces: regular spiking neuron recorded before (left) and immediately after stimulation of cholinergic fibres in the alveus (right) in the presence of atropine (1 μM) and DHβE (50 μM). (B) Each column represents the mean spike frequency expressed as percentage of control (dashed line, before stimulation of cholinergic fibers) immediately after stimulation of cholinergic fibers in the absence (white, $n = 8$) or in the presence (black, $n = 8$) of DHβE. *$P = 0.002$.

stimulation of cholinergic fibres, respectively; $n = 8$, $t_7 = 0.56$, $P = 0.59$; Fig. 8A and B).

Discussion

We have demonstrated that in stratum oriens interneurons, calcium increase through calcium-permeable nAChRs and/or voltage-dependent calcium channels activated by the depolarizing action of nicotine facilitates the mobilization of calcium from intracellular stores. This in turn activates apamin-sensitive calcium-dependent potassium conductances responsible for cell firing adaptation. Interestingly, a similar effect was produced by endogenously released acetylcholine following repetitive stimulation of cholinergic fibres in the alveus. Pharmacological experiments indicate that the action of nicotine on spike frequency adaptation was mediated by α7 and non-α7 nAChRs.

Of the four classes of nAChRs described in the central nervous system (Zoli *et al.*, 1998), the α7 and non-α7, α2 and α4 containing nAChRs, have been detected in O-LM interneurons (McQuiston & Madison, 1999; Ishii *et al.*, 2005; Jia *et al.*, 2009). Of particular interest are the α2-containing nAChRs because their activation induces a sustained firing and they exhibit little desensitization. In the present experiments, it is unlikely that nicotine-induced increase in firing adaptation was dependent on nAChR desensitization as nicotine effects were fully prevented by nAChR antagonists. In the case of desensitization, both nicotine and nAChR antagonists should have been produced similar effects.

It is commonly accepted that activation of nAChRs opens cationic channels leading to depolarization and excitation of tagged cells; indeed, in accordance with previous studies (McQuiston & Madison, 1999; Jia *et al.*, 2009), short pulses of nicotine were able to depolarize stratum oriens interneurons, making them fire. How could this effect be reconciled with nicotine-induced firing inhibition? EGFP-positive cells in stratum oriens, including O-LM interneurons, are endowed with α7 and non-α7 nAChRs, which to a different degree are both permeable to calcium (Tsuneki *et al.*, 2000; Fucile, 2004; Fayuk & Yakel, 2005). The rise of calcium in the cytosol may occur via nAChRs and/or voltage-dependent calcium channels, activated by the depolarizing action of nicotine. In our current clamp conditions, the amount of calcium entering through voltage-dependent calcium channels would prevail over that entering through nAChRs, as demonstrated for calcium permeability of α7 nAChRs present on stratum radiatum and stratum oriens interneurons (Fayuk & Yakel, 2005). Calcium in turn would initiate a variety of signal transduction cascades having different temporal profiles, leading sometimes to opposite effects. In stratum radiatum interneurons it has been shown that activation of nAChRs enhances GABA release and at the same time reduces the amplitude of inhibitory postsynaptic currents, an effect caused by a postsynaptic increase in calcium, known to alter $GABA_A$ receptor phosphorylation and/or internalization (Wanaverbecq *et al.*, 2007; see also Zhang & Berg, 2007). Therefore, it is not surprising that an initial transient excitatory effect of nicotine can be followed by an inhibitory one. Modulation of SK channels by nAChRs is not completely new. Auditory outer hair cells in the cochlea present a unique inhibitory synapse that uses a calcium-permeable excitatory acetylcholine receptor to activate hyperpolarizing potassium currents mediated by SK channels (Art *et al.*, 1984; Housley & Ashmore, 1991; Fuchs & Murrow, 1992; Blanchet *et al.*, 1996; Evans, 1996; Yuhas & Fuchs, 1999). In addition, in human neuroblastoma cells, calcium entry via nAChRs has been shown to regulate SK channels (Noronha-Blob *et al.*, 1989). SK channels are widely expressed in the central nervous system where they play a crucial role in regulating a variety of neuronal functions including cell excitability, pacemaking, dendritic integration, shaping of postsynaptic responses, plasticity processes (for a review see Fakler & Adelman, 2008). GABAergic interneurons in stratum oriens bear SK channels, which are responsible for the sAHP that limits the firing frequency of repetitive action potentials (Zhang & McBain, 1995). It is worth noting that in the absence of nAChR activation, little accommodation is present in these cells (Lacaille *et al.*, 1987; McBain, 1994; Zhang & McBain, 1995). This may depend on the relative briefness of action potentials, which may limit the amount of calcium entering into the cell during single spikes (Zhang & McBain, 1995). In the present experiments, the involvement of SK channels in nicotine-induced reduction of firing rate was supported by the observation that apamin, a selective blocker of SK channels (Sah, 1996), was able to prevent nicotine-induced firing frequency adaptation fully. Although apamin did not completely block the sAHP, it considerably increased cell

© The Authors (2009). Journal Compilation © Federation of European Neuroscience Societies and Blackwell Publishing Ltd

firing, indicating that the sAHP is essential for determining the rate of repetitive action potential firing in these neurons (see also Zhang & McBain, 1995). SK channels are contained within a microdomain with more than a single calcium source providing calcium ions for their activation. These include voltage-dependent calcium channels, nAChRs and NMDA receptors. Due to their intrinsically higher calcium sensitivity, these calcium channels can be located at some distance from calcium sources and still provide essential saturating calcium concentrations at rates that are faster than their intrinsic activation kinetics (Fakler & Adelman, 2008). This means that SK channels should not necessarily be co-localized with nAChRs. In the present case, calcium supply was via nAChRs and voltage-dependent calcium channels, activated by the depolarizing action of nicotine, as assessed by the possibility of preventing nicotine-induced spike frequency adaptation by loading the cell with BAPTA or by applying in the bath a solution devoid of calcium or containing cadmium. In addition, calcium imaging experiments directly showed that nicotine-induced decrease in firing rate was correlated with a large increase in the basal level of intracellular calcium. Our results also demonstrate that calcium signalling via nAChRs and/or voltage-dependent calcium channels was involved in mobilization of calcium from intracellular stores through a mechanism known as CICR (Verkhratsky, 2002). Thus, CICR following calcium rise via pre- and postsynaptic nAChRs has been well documented (Tsuneki *et al.*, 2000; Shoop *et al.*, 2001; Dajas-Bailador *et al.*, 2002; Sharma & Vijayaraghavan, 2003). This process, which once primed is self-sustained, may considerably prolong the effects of nicotine. In a previous study from the neonatal hippocampus we have demonstrated that at low probability Schaffer collateral-CA1 synapses, activation of nicotine receptors persistently upregulates glutamate release, an effect that involves mobilization of calcium from intracellular stores through CICR in presynaptic nerve terminals (Le Magueresse & Cherubini, 2007). Moreover, mobilization of calcium from internal stores through CICR mechanisms is required for regulating sI_{AHP} and cell firing in cortical pyramidal neurons (Yamada *et al.*, 2004; Hagenston *et al.*, 2008) and midbrain dopamine neurons (Fiorillo & Williams, 1998; Morikawa *et al.*, 2003). Interestingly, in neocortical pyramidal cells (Gulledge & Stuart, 2005) and in basolateral amygdala projection neurons (Power & Sah, 2008), mobilization of calcium from internal stores was shown to be triggered by inositol 1,4,5-triphosphate (IP_3) following stimulation of mAChRs by ACh. As in the present experiments, calcium increase induced activation of SK channels and an inhibitory effect on cell firing. In the present case, the ability fully to prevent nicotine action on the firing of stratum oriens interneurons with drugs known to interfere with ryanodine receptors or with SERCA fully supports the involvement of CICR in the action of nicotine.

In conclusion, this study demonstrates that activation of nAChRs by nicotine or endogenously released ACh changes the firing properties of stratum oriens interneurons including O-LM interneurons. These cells are crucial for synchronizing large populations of neurons and initiating oscillatory activities at different frequencies. Therefore, overstimulation or deficits in cholinergic signalling may influence rhythmogenesis, leading to impairment of high cognitive functions. This may be particularly relevant during senescence and in age-related neurodegenerative disorders (Selkoe, 2002; Mansvelder *et al.*, 2006).

Acknowledgements

We are grateful to Drs Laura Lagostena and Marcelo Rosato-Siri for helpful suggestions. This work was supported by a grant from the Ministero Istruzione Universita' e Ricerca (MIUR) to E.C. We thank Micaela Grandolfo for help with confocal microscopy.

Abbreviations

αBGT, α-bungarotoxin; ACh, acetylcholine; AHP, membrane afterhyperpolarization; BAPTA, 1,2-bis (2-aminophenoxy) ethane-N,N,N′,N′-tetraacetic acid; CICR, calcium-induced calcium release; CPA, cyclopiazonic acid; DHβE, dihydro-β-eritroidine; EGFP, enhanced green fluorescent protein; GABA, γ-aminobutyric acid; mAChRs, muscarinic acetylcholine receptors; MLA, methyllycaconitine; nAChRs, nicotinic acetylcholine receptors; NMDA, *N*-methyl-D-aspartate; O-LM, oriens-lacunosum moleculare; sAHP, slow membrane afterhyperpolarization; SERCA, sarcoplasmic–endoplasmic reticulum calcium ATP-ase; SK, small calcium-dependent potassium channels; TTX, tetrodotoxin.

References

Ali, A.B. & Thomson, A.M. (1998) Facilitating pyramid to horizontal oriens-alveus interneurone inputs: dual intracellular recordings in slices of rat hippocampus. *J. Physiol.*, **507**, 185–199.

Alkondon, M. & Albuquerque, E.X. (2001) Nicotinic acetylcholine receptor alpha7 and alpha4beta2 subtypes differentially control GABAergic input to CA1 neurons in rat hippocampus. *J. Neurophysiol.*, **86**, 3043–3055.

Alkondon, M. & Albuquerque, E.X. (2004) The nicotinic acetylcholine receptor subtypes and their function in the hippocampus and cerebral cortex. *Prog. Brain Res.*, **145**, 109–120.

Alkondon, M., Pereira, E.F. & Albuquerque, E.X. (1998) Alpha-bungarotoxin- and methyllycaconitine-sensitive nicotinic receptors mediate fast synaptic transmission in interneurons of rat hippocampal slices. *Brain Res.*, **810**, 257–263.

Alkondon, M., Pereira, E.F., Eisenberg, H.M. & Albuquerque, E.X. (1999) Choline and selective antagonists identify two subtypes of nicotinic acetylcholine receptors that modulate GABA release from CA1 interneurons in rat hippocampal slices. *J. Neurosci.*, **19**, 2693–2705.

Art, J.J., Fettiplace, R. & Fuchs, P.A. (1984) Synaptic hyperpolarization and inhibition of turtle cochlear hair cells. *J. Physiol.*, **356**, 525–550.

Avossa, D., Rosato-Siri, M.D., Mazzarol, F. & Ballerini, L. (2003) Spinal circuits formation: a study of developmentally regulated markers in organotypic cultures of embryonic mouse spinal cord. *Neuroscience*, **122**, 391–405.

Blanchet, C., Erósteguí, C., Sugasawa, M. & Dulon, D. (1996) Acetylcholine-induced potassium current of guinea pig outer hair cells: its dependence on a calcium influx through nicotinic-like receptors. *J. Neurosci.*, **16**, 2574–2584.

Buzsáki, G. (2002) Theta oscillations in the hippocampus. *Neuron*, **33**, 325–340.

Changeux, J.P. & Edelstein, S.J. (2005) *Nicotinic Acetylcholine Receptors*. Odile Jacob, New York.

Dajas-Bailador, F.A., Soliakov, L. & Wonnacott, S. (2002) Nicotine activates the extracellular signal-regulated kinase 1/2 via the alpha7 nicotinic acetylcholine receptor and protein kinase A, in SH-SY5Y cells and hippocampal neurones. *J. Neurochem.*, **80**, 520–530.

Descarries, L., Gisiger, V. & Steriade, M. (1997) Diffuse transmission by acetylcholine in the CNS. *Prog. Neurobiol.*, **53**, 603–625.

Evans, M.G. (1996) Acetylcholine activates two currents in guinea-pig outer hair cells. *J. Physiol.*, **491**, 563–578.

Fakler, B. & Adelman, J.P. (2008) Control of K(Ca) channels by calcium nano/microdomains. *Neuron*, **59**, 873–881.

Fayuk, D. & Yakel, J.L. (2005) Ca^{2+} permeability of nicotinic acetylcholine receptors in rat hippocampal CA1 interneurones. *J. Physiol.*, **566**, 759–768.

Fiorillo, C.D. & Williams, J.T. (1998) Glutamate mediates an inhibitory postsynaptic potential in dopamine neurons. *Nature*, **394**, 78–82.

Frazier, C.J., Rollins, Y.D., Breese, C.R., Leonard, S., Freedman, R. & Dunwiddie, T.V. (1998) Acetylcholine activates an alpha-bungarotoxin-sensitive nicotinic current in rat hippocampal interneurons, but not pyramidal cells. *J. Neurosci.*, **18**, 1187–1195.

Frotscher, M. & Léránth, C. (1985) Cholinergic innervation of the rat hippocampus as revealed by choline acetyltransferase immunocytochemistry: a combined light and electron microscopic study. *J. Comp. Neurol.*, **239**, 237–246.

Fuchs, P.A. & Murrow, B.W. (1992) Cholinergic inhibition of short (outer) hair cells of the chick's cochlea. *J. Neurosci.*, **12**, 800–809.

Fucile, S. (2004) Ca^{2+} permeability of nicotinic acetylcholine receptors. *Cell Calcium*, **35**, 1–8.

Goldin, M., Epsztein, J., Jorquera, I., Represa, A., Ben-Ari, Y., Crépel, V. & Cossart, R. (2007) Synaptic kainate receptors tune oriens-lacunosum moleculare interneurons to operate at theta frequency. *J. Neurosci.*, **27**, 9560–9572.

© The Authors (2009). Journal Compilation © Federation of European Neuroscience Societies and Blackwell Publishing Ltd

Gulledge, A.T. & Stuart, G.J. (2005) Cholinergic inhibition of neocortical pyramidal neurons. *J. Neurosci.*, **25**, 10308–10320.
Hagenston, A.M., Fitzpatrick, J.S. & Yeckel, M.F. (2008) MGluR-mediated calcium waves that invade the soma regulate firing in layer V medial prefrontal cortical pyramidal neurons. *Cereb. Cortex*, **18**, 407–423.
Housley, G.D. & Ashmore, J.F. (1991) Direct measurement of the action of acetylcholine on isolated outer hair cells of the guinea pig cochlea. *Proc. Biol. Sci.*, **244**, 161–167.
Ishii, K., Wong, J.K. & Sumikawa, K. (2005) Comparison of alpha2 nicotinic acetylcholine receptor subunit mRNA expression in the central nervous system of rats and mice. *J. Comp. Neurol.*, **493**, 241–260.
Jia, Y., Yamazaki, Y., Nakauchi, S. & Sumikawa, K. (2009) Alpha2 nicotine receptors function as a molecular switch to continuously excite a subset of interneurons in rat hippocampal circuits. *Eur. J. Neurosci.*, **8**, 1588–1603.
Klausberger, T. & Somogyi, P. (2008) Neuronal diversity and temporal dynamics: the unity of hippocampal circuit operations. *Science*, **321**, 53–57.
Klausberger, T., Magill, P.J., Marton, L.F., Roberts, J.D., Cobden, P.M., Buzsaki, G. & Somogyi, P. (2003) Brain-state- and cell-type-specific firing of hippocampal interneurons in vivo. *Nature*, **421**, 844–848.
Klausberger, T., Marton, L.F., Baude, A., Roberts, J.D., Magill, P.J. & Somogyi, P. (2004) Spike timing of dendrite-targeting bistratified cells during hippocampal network oscillations in vivo. *Nat. Neurosci.*, **7**, 41–47.
Kulak, J.M., McIntosh, J.M., Yoshikami, D. & Olivera, B.M. (2001) Nicotine-evoked transmitter release from synaptosomes: functional association of specific presynaptic acetylcholine receptors and voltage-gated calcium channels. *J. Neurochem.*, **77**, 1581–1589.
Lacaille, J.C., Mueller, A.L., Kunkel, D.D. & Schwartzkroin, P.A. (1987) Local circuit interactions between oriens/alveus interneurons and CA1 pyramidal cells in hippocampal slices: electrophysiology and morphology. *J. Neurosci.*, **7**, 1979–1993.
Lawrence, J.J., Grinspan, Z.M., Statland, J.M. & McBain, C.J. (2006a) Muscarinic receptor activation tunes mouse stratum oriens interneurones to amplify spike reliability. *J. Physiol.*, **571**, 555–562.
Lawrence, J.J., Statland, J.M., Grinspan, Z.M. & McBain, C.J. (2006b) Cell type-specific dependence of muscarinic signalling in mouse hippocampal stratum oriens interneurones. *J. Physiol.*, **570**, 595–610.
Le Magueresse, C. & Cherubini, E. (2007) Presynaptic calcium stores contribute to nicotine-elicited potentiation of evoked synaptic transmission at CA3-CA1 connections in the neonatal rat hippocampus. *Hippocampus*, **17**, 316–325.
Levey, A.I., Edmunds, S.M., Koliatsos, V., Wiley, R.G. & Heilman, C.J. (1995) Expression of m1-m4 muscarinic acetylcholine receptor proteins in rat hippocampus and regulation by cholinergic innervation. *J. Neurosci.*, **15**, 4077–4092.
Llano, I., Gonzalez, J., Caputo, C., Lai, F.A., Blayney, L.M., Tan, Y.P. & Marty, A. (2000) Presynaptic calcium stores underlie large-amplitude miniature IPSCs and spontaneous calcium transients. *Nat. Neurosci.*, **3**, 1256–1265.
Maccaferri, G. (2005) Stratum oriens horizontal interneurone diversity and hippocampal network dynamics. *J. Physiol.*, **562**, 73–80.
Maccaferri, G. & McBain, C.J. (1996) The hyperpolarization-activated current (Ih) and its contribution to pacemaker activity in rat CA1 hippocampal stratum oriens-alveus interneurones. *J. Physiol.*, **497**, 119–130.
Maccaferri, G., Roberts, J.D., Szucs, P., Cottingham, C.A. & Somogyi, P. (2000) Cell surface domain specific postsynaptic currents evoked by identified GABAergic neurones in rat hippocampus in vitro. *J. Physiol.*, **524**, 91–116.
Maggi, L., Le Magueresse, C., Changeux, J.P. & Cherubini, E. (2003) Nicotine activates immature "silent" connections in the developing hippocampus. *Proc. Natl Acad. Sci. USA*, **100**, 2059–2064.
Mansvelder, H.D., van Aerde, K.I., Couey, J.J. & Brussaard, A.B. (2006) Nicotinic modulation of neuronal networks: from receptors to cognition. *Psychopharmacology*, **184**, 292–305.
McBain, C.J. (1994) Hippocampal inhibitory neuron activity in the elevated potassium model of epilepsy. *J. Neurophysiol.*, **72**, 2853–2863.
McQuiston, A.R. & Madison, D.V. (1999) Nicotinic receptor activation excites distinct subtypes of interneurons in the rat hippocampus. *J. Neurosci.*, **19**, 2887–2896.
Minneci, F., Janahmadi, M., Migliore, M., Dragicevic, N., Avossa, D. & Cherubini, E. (2007) Signaling properties of stratum oriens interneurons in the hippocampus of transgenic mice expressing EGFP in a subset of somatostatin-containing cells. *Hippocampus*, **17**, 538–553.
Morikawa, H., Khodakhah, K. & Williams, J.T. (2003) Two intracellular pathways mediate metabotropic glutamate receptor-induced Ca^{2+} mobilization in dopamine neurons. *J. Neurosci.*, **23**, 149–157.
Nelson, E.J., Li, C.C., Bangalore, R., Benson, T., Kass, R.S. & Hinkle, P.M. (1994) Inhibition of L-type calcium-channel activity by thapsigargin and 2,5-t-butylhydroquinone, but not by cyclopiazonic acid. *Biochem. J.*, **302**, 147–154.
Noronha-Blob, L., Gover, R. & Baumgold, J. (1989) Calcium influx mediated by nicotinic receptors and voltage sensitive calcium channels in SK-N-SH human neuroblastoma cells. *Biochem. Biophys. Res. Commun.*, **162**, 1230–1235.
Oliva, A.A.. Jr, Jiang, M., Lam, T., Smith, K.L. & Swann, J.W. (2000) Novel hippocampal interneuronal subtypes identified using transgenic mice that express green fluorescent protein in GABAergic interneurons. *J. Neurosci.*, **20**, 3354–3368.
Papke, R.L., Bencherif, M. & Lippiello, P. (1996) An evaluation of neuronal nicotinic acetylcholine receptor activation by quaternary nitrogen compounds indicates that choline is selective for the alpha 7 subtype. *Neurosci. Lett.*, **213**, 201–204.
Parra, P., Gulyas, A.I. & Miles, R. (1998) How many subtypes of inhibitory cells in the hippocampus? *Neuron*, **20**, 983–993.
Power, J.M. & Sah, P. (2008) Competition between calcium-activated K^+ channels determines cholinergic action on firing properties of basolateral amygdala projection neurons. *J. Neurosci.*, **28**, 3209–3220.
Rosato-Siri, M., Cattaneo, A. & Cherubini, E. (2006) Nicotine-induced enhancement of synaptic plasticity at CA3-CA1 synapses requires GABAergic interneurons in adult anti-NGF mice. *J. Physiol.*, **576**, 361–377.
Rossier, M.F., Python, C.P., Burnay, M.M., Schlegel, W., Vallotton, M.B. & Capponi, A.M. (1993) Thapsigargin inhibits voltage-activated calcium channels in adrenal glomerulosa cells. *Biochem. J.*, **296**, 309–312.
Rózsa, B., Katona, G., Kaszás, A., Szipöcs, R. & Vizi, E.S. (2008) Dendritic nicotinic receptors modulate backpropagating action potentials and long-term plasticity of interneurons. *Eur. J. Neurosci.*, **27**, 364–377.
Sah, P. (1996) $Ca^{(2+)}$-activated K^+ currents in neurones: types, physiological roles and modulation. *Trends Neurosci.*, **19**, 150–154.
Sah, P. & McLachlan, E.M. (1991) $Ca^{(2+)}$-activated K^+ currents underlying the afterhyperpolarization in guinea pig vagal neurons: a role for $Ca^{(2+)}$-activated Ca^{2+} release. *Neuron*, **7**, 257–264.
Seidler, N.W., Jona, I., Vegh, M. & Martonosi, A. (1989) Cyclopiazonic acid is a specific inhibitor of the Ca^{2+}-ATPase of sarcoplasmic reticulum. *J. Biol. Chem.*, **264**, 17816–17823.
Selkoe, D.J. (2002) Alzheimer's disease is a synaptic failure. *Science*, **298**, 789–791.
Sharma, G. & Vijayaraghavan, S. (2003) Modulation of presynaptic store calcium induces release of glutamate and postsynaptic firing. *Neuron*, **38**, 929–939.
Shmigol, A., Kostyuk, P. & Verkhratsky, A. (1995) Dual action of thapsigargin on calcium mobilization in sensory neurons: inhibition of Ca^{2+} uptake by caffeine-sensitive pools and blockade of plasmalemmal Ca^{2+} channels. *Neuroscience*, **65**, 1109–1118.
Shoop, R.D., Chang, K.T., Ellisman, M.H. & Berg, D.K. (2001) Synaptically driven calcium transients via nicotinic receptors on somatic spines. *J. Neurosci.*, **21**, 771–781.
Somogyi, P. & Klausberger, T. (2005) Defined types of cortical interneurone structure space and spike timing in the hippocampus. *J. Physiol.*, **562**, 9–26.
Sudweeks, S.N. & Yakel, J.L. (2000) Functional and molecular characterization of neuronal nicotinic ACh receptors in rat CA1 hippocampal neurons. *J. Physiol.*, **527**, 515–528.
Thastrup, O., Cullen, P.J., Drobak, B.K., Hanley, M.R. & Dawson, A.P. (1990) Thapsigargin, a tumor promoter, discharges intracellular Ca^{2+} stores by specific inhibition of the endoplasmic reticulum $Ca^{2(+)}$-ATPase. *Proc. Natl Acad. Sci. USA*, **87**, 2466–2470.
Tribollet, E., Bertrand, D., Marguerat, A. & Raggenbass, M. (2004) Comparative distribution of nicotinic receptor subtypes during development, adulthood and aging: an autoradiographic study in the rat brain. *Neuroscience*, **124**, 405–420.
Tsuneki, H., Klink, R., Léna, C., Korn, H. & Changeux, J.P. (2000) Calcium mobilization elicited by two types of nicotinic acetylcholine receptors in mouse substantia nigra pars compacta. *Eur. J. Neurosci.*, **12**, 2475–2485.
Umbriaco, D., Garcia, S., Beaulieu, C. & Descarries, L. (1995) Relational features of acetylcholine, noradrenaline, serotonin and GABA axon terminals

© The Authors (2009). Journal Compilation © Federation of European Neuroscience Societies and Blackwell Publishing Ltd

in the stratum radiatum of adult rat hippocampus (CA1). *Hippocampus*, **5**, 605–620.

Verkhratsky, A. (2002) The endoplasmic reticulum and neuronal calcium signalling. *Cell Calcium*, **32**, 393–404.

Wanaverbecq, N., Semyanov, A., Pavlov, I., Walker, M.C. & Kullmann, D.M. (2007) Cholinergic axons modulate GABAergic signaling among hippocampal interneurons via postsynaptic alpha 7 nicotinic receptors. *J. Neurosci.*, **27**, 5683–5693.

Yamada, S., Takechi, H., Kanchiku, I., Kita, T. & Kato, N. (2004) Small-conductance Ca^{2+}-dependent K^{+} channels are the target of spike-induced Ca^{2+} release in a feedback regulation of pyramidal cell excitability. *J. Neurophysiol.*, **91**, 2322–2329.

Yuhas, W.A. & Fuchs, P.A. (1999) Apamin-sensitive, small-conductance, calcium-activated potassium channels mediate cholinergic inhibition of chick auditory hair cells. *J. Comp. Physiol. [A]*, **185**, 455–462.

Zhang, J. & Berg, D.K. (2007) Reversible inhibition of GABAA receptors by alpha7-containing nicotinic receptors on the vertebrate postsynaptic neurons. *J. Physiol.*, **579**, 753–763.

Zhang, L. & McBain, C.J. (1995) Potassium conductances underlying repolarization and after-hyperpolarization in rat CA1 hippocampal interneurones. *J. Physiol.*, **488**, 661–672.

Zoli, M., Léna, C., Picciotto, M.R. & Changeux, J.P. (1998) Identification of four classes of brain nicotinic receptors using beta2 mutant mice. *J. Neurosci.*, **18**, 4461–4472.

© The Authors (2009). Journal Compilation © Federation of European Neuroscience Societies and Blackwell Publishing Ltd

Results

Paper N. 2.

Nicotine blocks the hyperpolarization-activated current I_h and severely impairs the oscillatory activity of O-LM interneurons in the hippocampus.

Marilena Griguoli, Alena Maul, Chuong Nguyen, Alejandro Giorgetti, Paolo Carloni, and Enrico Cherubini

The Journal of Neuroscience, August 11, 2010 • 30(32):10773–10783 • 10773

Neurobiology of Disease

Nicotine Blocks the Hyperpolarization-Activated Current I_h and Severely Impairs the Oscillatory Behavior of Oriens-Lacunosum Moleculare Interneurons

Marilena Griguoli,[1] Alena Maul,[1] Chuong Nguyen,[2] Alejandro Giorgetti,[3] Paolo Carloni,[2] and Enrico Cherubini[1]

[1]Neurobiology Department and Italian Institute of Technology Unit, International School for Advanced Studies (SISSA), 34014 Trieste, Italy, [2]Statistical and Biological Physics Department, SISSA, 34151 Trieste, Italy, and [3]Department of Biotechnology, University of Verona, 37134 Verona, Italy

In the brain, high cognitive functions are encoded by coherent network oscillations. Key players are inhibitory interneurons that, by releasing GABA into principal cells, pace targeted cells. Among these, oriens-lacunosum moleculare (O-LM) interneurons that provide a theta frequency patterned output to distal dendrites of pyramidal cells are endowed with HCN channels responsible for the slowly activating inwardly rectifying I_h current and their pacemaking activity. Here we show that, in transgenic mice expressing EGFP (enhanced green fluorescent protein) in a subset of stratum oriens somatostatin-containing interneurons that mostly comprise O-LM cells, nicotine, the active component of tobacco, reduced I_h and the oscillatory behavior of O-LM interneurons. In cells hyperpolarized at −90 mV, nicotine suppressed the theta resonance in the same way as ZD 7288 (4-ethylphenylamino-1,2-dimethyl-6-methylaminopyrimidinium chloride), a selective blocker of I_h. Nicotine blocked I_h in a concentration-dependent way with an EC_{50} of 62 nM. Similar effects were produced by epibatidine, a structural analog of nicotine. The effects of nicotine and epibatidine were independent on nicotinic ACh receptor (nAChR) activation because they persisted in the presence of nAChR antagonists. Furthermore, nicotine slowed down the interspike depolarizing slope and the firing rate, thus severely disrupting the oscillatory behavior of O-LM cells. Molecular modeling suggests that, similarly to ZD 7288, nicotine and epibatidine directly bind to the inner pore of the HCN channels. It is therefore likely that nicotine severely influences rhythmogenesis and high cognitive functions in smokers.

Introduction

The hippocampal network comprises a large variety of distinct locally connected GABAergic cells that exert a powerful control on network excitability and are responsible for the oscillatory behavior crucial for information processing in the brain. GABAergic interneurons selectively innervate different domains of pyramidal cells, thus providing the main source of feedback and feedforward inhibition (Freund and Buzsáki, 1996; Miles et al., 1996). Because of their extensive axonal arborization, they can phase the output of principal cells giving rise to coherent oscillations (McBain and Fisahn, 2001; Klausberger et al., 2003, 2004; Somogyi and Klausberger, 2005) occurring at different frequencies (Buzsáki, 2002; Whittington and Traub, 2003). Oscillatory rhythms are facilitated by the intrinsic properties of GABAergic interneurons (Maccaferri and McBain, 1996) and by their electrical coupling via gap junctions (Hestrin and Galarreta, 2005; Zsiros and Maccaferri, 2005; Minneci et al., 2007).

Oriens-lacunosum moleculare (O-LM) cells constitute a subpopulation of GABAergic interneurons containing somatostatin. They have the soma and horizontal dendrites localized in stratum oriens and the axons targeting distal dendrites of CA1 pyramidal cells in stratum-lacunosum moleculare (Lacaille et al., 1987; Ali and Thomson, 1998; Maccaferri et al., 2000; Maccaferri, 2005). These neurons participate in hippocampal theta activity *in vivo* (Buzsáki, 2002; Klausberger et al., 2003) and *in vitro* (Pike et al., 2000; Gillies et al., 2002; Hájos et al., 2004; Gloveli et al., 2005).

O-LM interneurons receive an important cholinergic innervation from the medial septum–diagonal band complex of the basal forebrain (Frotscher and Léránth, 1985) and are endowed with a variety of muscarinic acetylcholine receptors and nicotinic acetylcholine receptors (nAChRs) (Levey et al., 1995; Tribollet et al., 2004) that regulate their activity (Lawrence et al., 2006; Griguoli et al., 2009). An *in vivo* study has demonstrated a key role of cholinergic activity in amplifying theta oscillations (Lee et al., 1994), and a recent *in vitro* work has outlined the role of muscarinic receptors in enhancing spike reliability and precision to theta frequency input (Lawrence et al., 2006). Whether activation of nAChRs by nicotine affects rhythmogenesis in the hippocampus is not known. Nicotine is the major substance of tobacco, responsible for the elevated risk of cardiovascular and neurological disorders, including attention and memory deficits associated with smoking.

This study was aimed at elucidating whether activation of nAChRs by nicotine may interfere with I_h and rhythmogenesis in the hippocampus. We focused on somatostatin-expressing stratum oriens interneurons and in particular on O-LM cells, the predominant horizontal cell type in the CA1 hippocampal area (Ali and Thomson, 1998; Maccaferri, 2005), because these cells exhibit intrinsic resonance and spike transfer frequency preference in the theta range (Pike et al., 2000) and have been shown to contribute to the generation of the theta rhythm *in vivo* (Klausberger et al.,

Received May 13, 2010; revised June 9, 2010; accepted June 17, 2010.

This work was supported by Ministero Istruzione Università e Ricerca Grant PRIN 2009 (E.C.). We thank M. Dibattista and L. Lagostena for useful discussions during the preparation of this manuscript.

Correspondence should be addressed to Enrico Cherubini, Neurobiology Sector, International School for Advanced Studies, Area Science Park, 34012 Basovizza, Trieste, Italy. E-mail: cher@sissa.it.

DOI:10.1523/JNEUROSCI.2446-10.2010

Copyright © 2010 the authors 0270-6474/10/3010773-11$15.00/0

2003). To target this subpopulation, we used transgenic mice expressing enhanced green fluorescent protein (EGFP) in a subset of somatostatin-containing interneurons that mostly comprise O-LM cells in the CA1 stratum oriens (Oliva et al., 2000). Surprisingly, we found that nicotine blocked I_h by directly interfering with the channel protein responsible for this current independently of nAChR activation. The inhibitory effect of nicotine on I_h resulted in a severe impairment of the pacemaker properties of these cells.

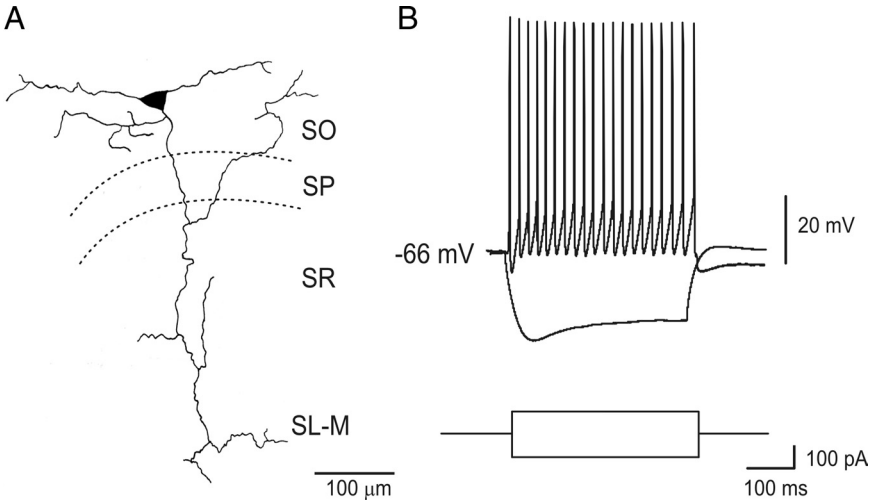


Figure 1. Identification of EGFP-positive O-LM interneurons. ***A***, *Post hoc* camera lucida reconstruction of an EGFP-positive cell recorded with patch pipette containing Neurobiotin, showing characteristic horizontal dendrites and long axon projecting to stratum-lacunosum moleculare. ***B***, Voltage responses obtained by injecting depolarizing and hyperpolarizing current steps. Note the prominent sag and the repetitive firing in the electrotonic potentials. SO, Stratum oriens; SP, stratum pyramidale; SR, stratum radiatum; SL-M, stratum-lacunosum moleculare.

Materials and Methods

Hippocampal slice preparation. All experiments were performed in accordance with the European Community Council Directive of November 24, 1986 (86/609EEC) and were approved by the local authority veterinary service. All efforts were made to minimize animal suffering and to reduce the number of animal used.

We used transgenic mice (both male and female) expressing EGFP in a subpopulation of somatostatin-containing GABAergic interneurons (GIN mice; The Jackson Laboratory) (Oliva et al., 2000; Minneci et al., 2007). To confer EGFP expression to GABAergic interneurons, an upstream regulatory sequence from the murine *Gad1* gene was used for the transgene construction (Oliva et al., 2000). Hippocampal slices were obtained from juvenile (postnatal day 14–21) using a standard protocol (Griguoli et al., 2009). Briefly, after being anesthetized with an intraperitoneal injection of urethane (2 g/kg), the brain was quickly removed from the skull and placed in ice-cold artificial CSF (ACSF) containing the following (in mM): 130 NaCl, 25 glucose, 3.5 KCl, 1.2 NaH_2PO_4, 25 $NaHCO_3$, 2 $CaCl_2$, and 1.3 $MgCl_2$ (Sigma), pH 7.3–7.4 (saturated with 95% O_2 and 5% CO_2). Transverse hippocampal slices (300 μm thick) were cut with a vibratome and stored at room temperature (22–24°C) in a holding bath containing the same solution as above. After incubation for at least 1 h, an individual slice was transferred to a submerged recording chamber and continuously superfused at 33–34°C with oxygenated ACSF at a rate of 2–3 ml/min.

Electrophysiological recordings. Whole-cell patch-clamp recordings (in current- and voltage-clamp mode) were routinely obtained from visually identified EGFP-positive cells localized in stratum oriens of the CA1 hippocampal region. We patched only those cells exhibiting round or fusiform cell bodies and horizontal dendrites, often close to the alveus border that exhibited a prominent sag in electrotonic potentials evoked by hyperpolarizing currents (Fig. 1*A*) (Zemankovics et al., 2010). Neurons were visualized using an upright fluorescent microscope (Nikon E600 FN) equipped with differential interference contrast optics and infrared video camera. Recordings were made from 166 stratum oriens EGFP-positive cells with a Multiclamp 700A amplifier (Molecular Devices) in the presence of DL-2-amino-5-phosphonopentaoic acid (DL-AP-5) (50 μM), 6,7-dinitroquinoxaline-2,3-dione (DNQX) (20 μM), and gabazine (SR 95531 hydrobromide [6-imino-3-(4-methoxyphenyl)-1(6*H*)-pyridazinebutanoic acid hydrobromide]) (10 μM) to block ionotropic glutamatergic and GABAergic synaptic currents, respectively. Patch electrodes were pulled from borosilicate glass capillaries (Hingelberg). They had a resistance of 4–6 MΩ when filled with an intracellular solution containing the following (in mM): 135 $KMeSO_4$, 10 KCl, 10 HEPES, 0.5 EGTA, 2 Na_2ATP, and 0.4 Na_2GTP, pH 7.2–7.3 with KOH (osmolarity, 280–300 mOsm). Series resistance was assessed repetitively every 5 min throughout the experiment. Series resistance values varied between 20 and 25 MΩ; cells exhibiting >15–20% changes were excluded from the analysis. Membrane potential values were corrected for a liquid junction potential of 15.1 mV.

In some experiments, the impedance (Z) amplitude profile (ZAP) was used to measure the electric resonance behavior of O-LM cells (Puil et al., 1986; Hutcheon and Yarom, 2000). The voltage response during injection through the patch pipette of a sinusoidal current (the ZAP current) with constant amplitude and linearly increasing frequency (0.5–30 Hz for 30 s; using Matlab; MathWorks) was recorded in current-clamp conditions. Resonance was manifested as a distinct and reproducible peak in the voltage response corresponding to a certain frequency. The magnitude of the ratio of the fast Fourier transform (FFT) of the voltage response to the fast Fourier transform of the ZAP stimulus formed the impedance amplitude profile. The frequency at which the impedance amplitude reached its maximum was the resonance frequency.

In current-clamp experiments, the hyperpolarization-activated current I_h gives rise to a sag in the electrotonic potentials (obtained by injecting steady hyperpolarizing currents into the cell), followed by a rebound depolarization at the end of the pulses, which often triggered action potentials. The sag was measured from the normalized steady state to peak voltage response of the cell to a hyperpolarizing current step of 250 pA (400 ms duration, from a holding potential of −70 mV) and was defined as follows: $100 \times (1 - V_{ss}/V_{peak})$, where V_{ss} is the steady-state voltage deflection from baseline, and V_{peak} is the peak voltage deflection from baseline (Narayanan and Johnston, 2007).

Currents mediated by I_h were measured in voltage-clamp conditions by applying hyperpolarizing voltage steps (2 s duration) from a holding potential of −50 mV up to −120 mV (in 10 mV increment) in the presence of tetrodotoxin (TTX) (1 μM) and cadmium (200 μM) to block fast Na^+ channels and voltage-dependent Ca^{2+} channels, respectively.

In the experiments with cadmium, NaH_2PO_4 was omitted from the bathing solution. The current–voltage (I–V) relationship was obtained by measuring the steady-state current values at the end of 2 s voltage steps after subtracting the instantaneous current at the beginning of the voltage steps. The activation curve was determined from tail current amplitudes (at the end of each hyperpolarized voltage step from −50 to −120 mV), measured after subtracting current responses obtained in the presence of nicotine and ZD 7288 (4-ethylphenylamino-1,2-dimethyl-6-methylaminopyrimidinium chloride) from their respective controls (Janigro et al., 1997). Current values at each voltage were normalized by current value obtained at −120 mV. The resulting values were plotted versus the hyperpolarization step voltages and were fitted with the following Boltzmann equation: $I/I_{MAX} = 1/\{1 + \exp[(V_{1/2} - V_m)/k]\}$, where $V_{1/2}$ is the voltage for half-maximum activation and deactivation, V_m is the pulse potential, and k is the slope factor.

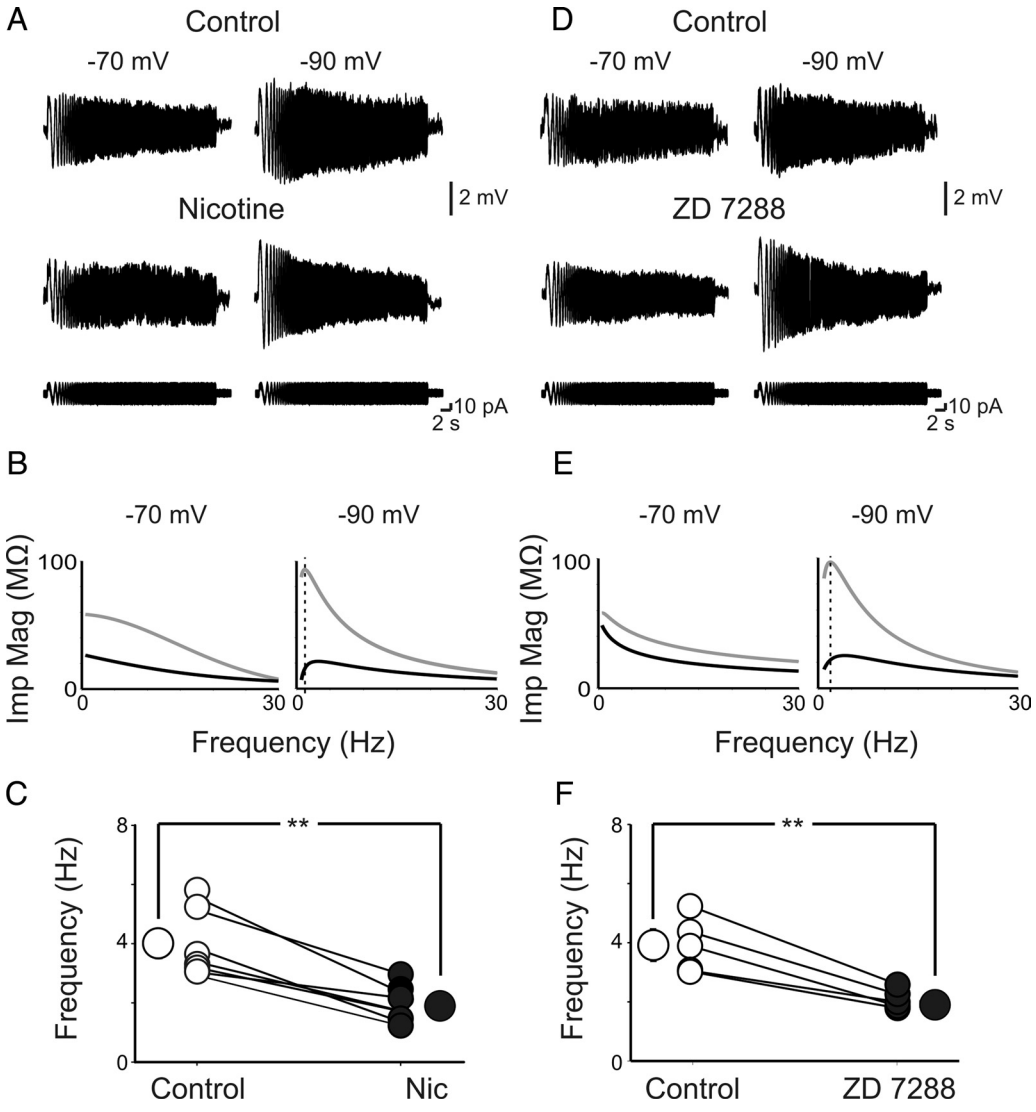


Figure 2. Nicotine affects theta resonance of O-LM interneurons. ***A***, Voltage response of an O-LM interneuron to the injection of a ZAP current at −70 mV (left) and −90 mV (right), in the absence (top traces) or presence (bottom traces) of nicotine (1 μM). Note that nicotine abolished the resonance at −90 mV but not at −70 mV. ***B***, Impedance magnitude (Imp Mag) profiles calculated from the data in ***A*** are plotted as a function of input frequencies before (black) and during (gray) nicotine application. Note the shift in the impedance magnitude peak at −90 mV (right) but not at −70 mV (left). ***C***, Each symbol represents the frequency of the impedance magnitude peak of individual cells obtained at −90 mV in control (open circles) and in the presence of nicotine (Nic; filled circles). Bigger symbols represent averaged values. Error bars are within the symbols. ***D–F***, As for ***A–C*** but in the absence or presence of ZD 7288. $^{**}p < 0.01$.

Time constants were determined by fitting currents using pClamp with a double-exponential function of the following form: $I_h(t) = A_f \exp(-t/\tau_f) + A_s \exp(-t/\tau_s)$, where $I_h(t)$ is the amplitude of the current at time t, and A_f and A_s are the initial amplitudes of the fast (τ_f) and slow (τ_s) activation time constant components, respectively.

The dose–response curve for nicotine was constructed by applying hyperpolarizing voltage steps from −50 to −120 mV in the absence or presence of the alkaloid. The amplitudes of the steady-state currents (measured at the end of the voltage steps) obtained in the presence of increasing concentrations of nicotine (from 10 nM to 10 μM) and normalized to those obtained in controls were plotted as I_h block (percentage) for different nicotine concentrations.

To investigate whether nicotine affected the intrinsic oscillatory properties of O-LM interneurons, sinusoidal currents were injected into the cells at the frequency of 4–7 Hz (in the presence of blockers of synaptic transmission) before and during application of nicotine and slopes (millivolts per millisecond) of the voltage responses during the upswing of cycle were measured.

Drugs. The following drugs were used: DL-AP-5, DNQX, SR 95531 hydrobromide, ZD 7288, forskolin, bromo-cAMP (Br-cAMP), mecamylamine, and epibatidine were all purchased from Tocris Bioscience; nicotine, dihydro-β-erytroidine (DHβE), atropine, acetylcholine, and edrophonium were purchased from Sigma; TTX was from Latoxan.

Stock solutions were made in distilled water and then aliquoted and frozen at −20°C. DNQX was dissolved in dimethylsulfoxide (DMSO). The final concentration of DMSO in the bathing solution was 0.1%. At this concentration, DMSO alone did not modify the membrane potential, input resistance, or the firing properties of O-LM interneurons. Drugs were applied in the bath via a three-way tap system, by changing the superfusion solution to one differing only in its content of drug(s). The ratio of flow rate to bath volume ensured complete exchange within 1–2 min. Nicotine was applied in the bath (for 5–7 min).

Data analysis. Data were acquired with pClamp 9.2 software (Molecular Devices) and transferred to a computer hard disk after digitization with an analog-to-digital converter (Digidata 1322; Molecular Devices). Data were digitized at 20 kHz, filtered at 2 kHz, and analyzed offline with Clampfit 9.2 (Molecular Devices). Input resistance and capacitance of the cells were measured online with the membrane test feature of the pClamp software.

Values are given as mean ± SEM. Significance of differences was assessed by Student's paired *t* test and ANOVA as indicated; $p < 0.05$ was taken as significant.

Morphology. Slices were processed for *post hoc* identification of EGFP-positive stratum oriens interneurons filled with Neurobiotin (0.2%; Vector Laboratories) during patch recordings using a standard procedure (Goldin et al., 2007; Cossart et al., 2006). Briefly, slices were fixed overnight at 4°C in a solution containing 4% paraformaldehyde in 0.1 M phosphate buffer (PB), pH 7.4. After fixation, slices were rinsed in PB, cryoprotected in sucrose (30% in PBS), and quickly frozen on dry ice. To neutralize endogenous peroxidase, slices were pretreated for 30 min in 1% H_2O_2. After several rinses in 0.01 M PBS, pH 7.4, slices were incubated for 24 h at room temperature, in 1:100 avidin–biotin peroxidase complex (Vector Laboratories) diluted in PBS containing 0.3% Triton X-100. After 30 min rinses in PBS, slices were processed with 0.04% 3–3-diaminobenzidine- HCl (Sigma) and 0.006% H_2O_2 diluted in PBS. All labeled neurons ($n = 20$) except one that was excluded from this study showed complete axonal and dendritic labeling characteristics of O-LM interneurons (McBain et al., 1994). Neurons were reconstructed using a camera lucida.

Homology model. A homology model of the pore region of HCN channels has been developed (Giorgetti et al., 2005) based on the following assumptions. (1) In the closed state, the topology of the inner pore of HCN channels is similar to that of K^+ channels. In particular, the orientation of the S5 and S6 helices is very similar to that of the corresponding helices of the K^+ KcsA and K^+ KirBac1.1 channels. Thus, we have used as templates the x-ray structure of these K^+ channels. (2) In the open state, the S6 helix is supposed to bend further than it is in the closed state. For this reason, the template of the open conformation was the x-ray structure of the MthK channel (Jiang et al., 2002). The structural models of the closed and open states turned out to be consistent with all the available electrophysiological data. Our modeling suggests that the bending amplitude of the S6 helix during gating is significantly smaller than that found in MthK channels (Jiang et al., 2002). The model has been further validated by a recent study (Cheng et al., 2007), in which the amino acids involved in the interaction between ZD 7288 and cilobradine with HCN channels has been identified.

Docking procedure. Nicotine and epibatidine were docked onto the modeled open structure of HCN channels, using the AUTODOCK 4.0 program. The parameters for the molecules were calculated using the AUTODOCK standard parameterization procedure (Morris et al., 1998). The Lamarckian Genetic Algorithm and 25 million energy evaluations per run were applied as a search method for the different docking results. The potential grid map for each atom type was calculated using a cubic box centered in the channel cavity, with a distance of 0.375 Å between grid points. For each complex, 100 docking runs were performed, resulting in a total of 300 calculations. The lowest energy conformations within the most populated clusters were used to hypothesize the location of the ligands. The cluster analyses were based on the root-mean-square deviation distance among the ligands on each run (root-mean-square deviation cutoff of 2 Å).

Results

In agreement with previous studies (Minneci et al., 2007; Griguoli et al., 2009), O-LM interneurons exhibited a mean resting membrane potential (measured in nonspontaneously active neurons) of 65 ± 0.4 mV and a mean input resistance of 326 ± 16 MΩ ($n = 166$). Some of them (122 of 166, 73%) fired spontaneously (the firing frequency ranged between 4 and 9.5 Hz). In addition, these cells exhibited different firing patterns in response to long (400 ms) depolarizing current pulses applied from holding potentials of −65 and −75 mV (Minneci et al., 2007; Griguoli et al., 2009), which were maintained with similar characteristics after blocking AMPA/kainate, NMDA, and $GABA_A$ receptors with DNQX (20 μM), DL-AP-5 (50 μM), and gabazine (10 μM), respectively. Hyperpolarizing current pulses of different amplitude revealed a sag in the electrotonic potentials, which was mediated by the time-dependent inwardly rectifying cationic current I_h (Fig. 1*B*) (Maccaferri and McBain, 1996; Minneci et al., 2007).

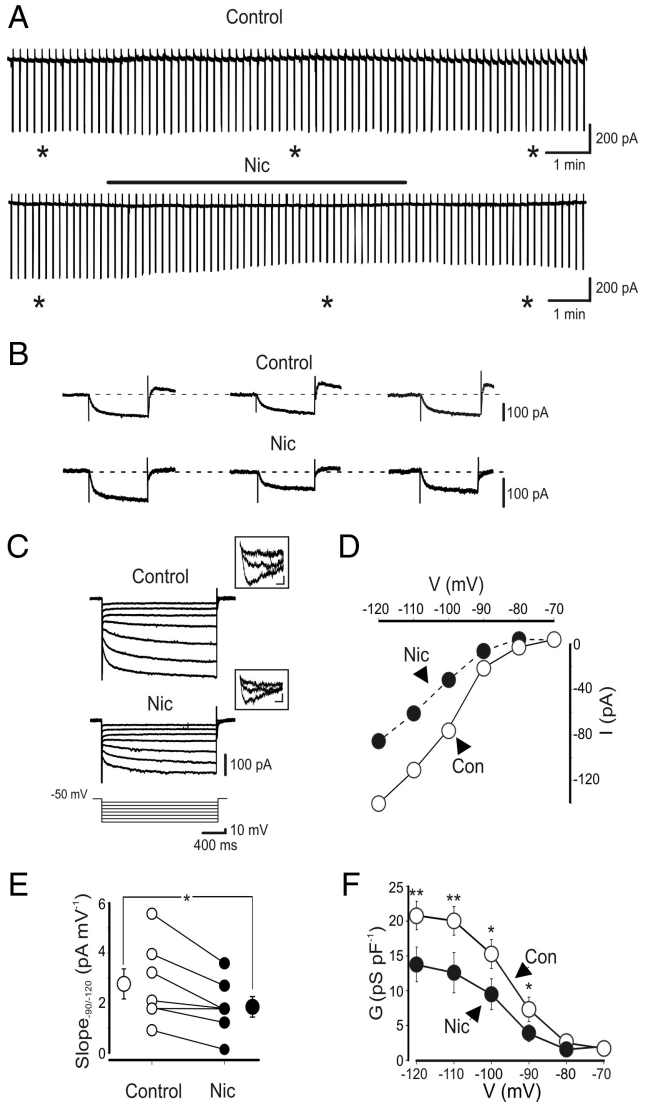


Figure 3. Nicotine reduces I_h in O-LM interneurons. ***A***, Continuous recordings of current responses evoked by hyperpolarizing voltage steps (from −60 to −120 mV, 1 s duration) repetitively delivered at 0.1 Hz, in the absence (top trace) and presence (bottom trace) of nicotine (1 μM; black bar). Note reduction of I_h amplitude with nicotine. ***B***, Leak-subtracted current responses (obtained from the traces in ***A***, asterisks) are shown in an expanded timescale. ***C***, Current responses evoked by hyperpolarizing voltage steps (10 mV increment) from a holding potential of −50 to −120 mV, in the absence (Control) or presence of nicotine (Nic) 1 μM. In the insets above the traces, tail currents evoked by voltage steps from −50 to −60, −80, and −120 mV, respectively. Calibration: 10 pA, 10 ms. ***D***, Current–voltage relationship obtained in the absence (open circles) or presence (filled circles) of nicotine for the cell shown in ***B***. Current amplitudes were measured at the end of the voltage steps. ***E***, Each symbol represents the *I–V* slope of individual cells, measured between −90 and −120 mV in the absence (open circles) or presence (filled circles) of nicotine. Bigger symbols represent averaged values. ***F***, Membrane conductances, normalized to cell capacitances, are plotted as a function of voltages in the absence (open circle) or presence (filled circles) of nicotine ($n = 6$). *$p < 0.05$, **$p < 0.01$. In this and in the following figures, vertical bars represent SEM (sometimes they are within the symbols). Con, Control.

Nicotine suppresses the theta resonance of O-LM interneurons

O-LM interneurons are known to exhibit intrinsic resonance and spike transfer frequency preferences in the theta range (Pike et al., 2000; Whittington and Traub, 2003; Gloveli et al., 2005). Reso-

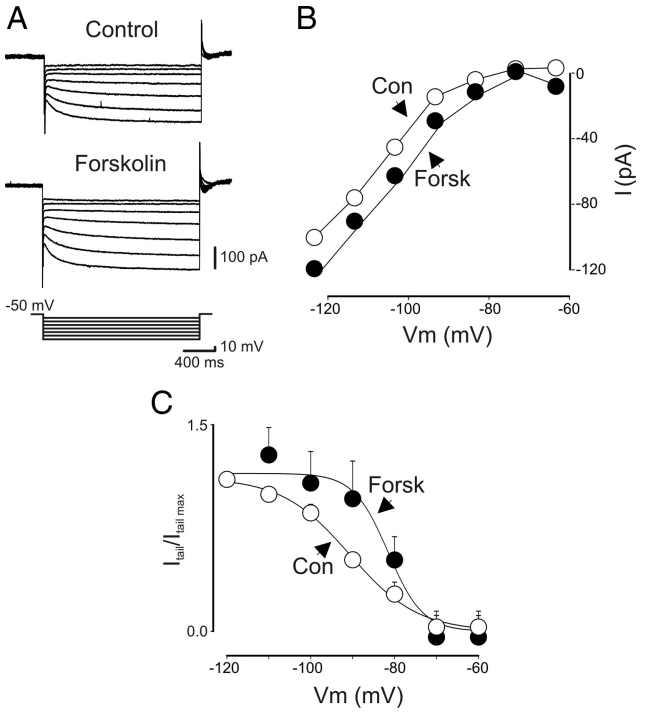


Figure 4. In a subset of O-LM interneurons, forskolin enhances I_h. ***A***, Current responses evoked by hyperpolarizing voltage steps (10 mV increments) from a holding potential of −50 to −120 mV, in the absence (Control) or presence (50 μM) of forskolin. ***B***, Current–voltage relationship obtained in the absence (open circles) or presence (filled circles) of forskolin (Forsk) for the cell shown in ***A***. ***C***, Activation curves obtained in the absence (Con) and presence of forskolin. Data points obtained from three of eight cells were fitted with the Boltzmann equation. The two curves were significantly different ($p < 0.001$, one-way ANOVA).

nance is the property by which a given neuron oscillates with maximal amplitude at certain "preferred" input frequencies (Hutcheon and Yarom, 2000). Voltage-dependent conductances underlying resonance at theta frequency are those that actively oppose changes in membrane voltages known to be mediated by Kv7/M and HCN channels, respectively. Therefore, in a first set of experiments, we have tested whether nicotine affects the subthreshold resonance behavior of O-LM interneurons. We have applied the ZAP method (Puil et al., 1986; Hutcheon and Yarom, 2000) during whole-cell current-clamp recordings. Because subthreshold resonance strictly depends on HCN channels, responsible for I_h (Hu et al., 2002), the membrane potential of the cells was manually clamped at −70 and −90 mV, respectively, by injecting a steady current through the recording electrode. As shown in the top traces of Figure 2*A*, resonance was clearly voltage dependent. Thus, a sinusoidal current with constant amplitude and linearly increasing frequency (0.5–30 Hz during 30 s; ZAP current) injected into O-LM interneurons induced a reproducible peak in the amplitude of voltage responses only at −90 mV but not at −70 mV. At this membrane potential, the impedance profile (the relationship between the voltage response and the input current as a function of the frequency) calculated by dividing the FFT of the voltage response by the FFT of input ZAP current peaked within the theta frequency range (Fig. 2*B*). Nicotine applied in the bath at the concentration of 1 μM (for 5 min) enhanced the voltage response obtained at −90 mV without significantly modifying that detected at −70 mV (Fig. 2*A*, bottom traces). The impedance magnitude increased from 22 to 97 MΩ (Fig. 2*B*). Figure 2*C* summarizes the data obtained from six cells held at −90 mV in the absence or presence of nicotine. Overall nicotine reduced the frequency of the impedance peak from 4.0 ± 0.5 to 1.8 ± 0.2 Hz ($p < 0.01$). The increase in input resistance induced by nicotine at −90 mV suggests the block of a membrane conductance active at hyperpolarized membrane potentials. To see whether I_h, which activates negative to −65 mV, was the target of nicotine action, we applied the I_h channel blocker ZD 7288 (100 μM) (Maccaferri and McBain, 1996) to the bathing solution. As shown in the bottom traces of Figure 2*D*, although ZD 7288 did not produce any significant effect at −70 mV, it almost doubled the voltage response at −90 mV. The peak of the impedance magnitude increased from 25 to 98 MΩ (Fig. 2*E*). On average, in five O-LM cells held at −90 mV, ZD 7288 reduced the frequency of the impedance magnitude peak from 4.0 ± 0.4 to 1.9 ± 0.13 Hz ($p < 0.01$) (Fig. 2*F*).

Together, these data indicate that nicotine affects resonance properties of O-LM interneurons in a way similar to ZD 7288 possibly by interfering with the slowly activating, non-inactivating inward rectifying cationic current I_h.

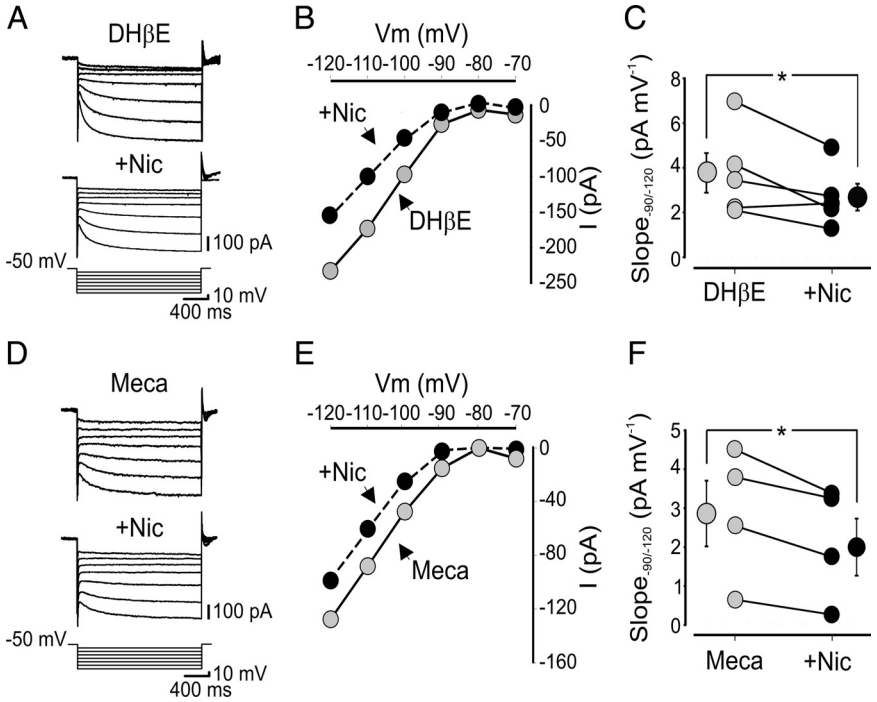


Figure 5. The effect of nicotine on I_h is independent of the activation of nAChRs. ***A***, Current responses evoked by hyperpolarizing voltage steps (10 mV increments) from a holding potential of −50 to −120 mV, in the presence of DHβE (50 μM) or DHβE plus nicotine (Nic; 1 μM). ***B***, Current–voltage relationship obtained in the presence of DHβE (gray) or DHβE plus nicotine (black) for the cell shown in ***A***. ***C***, Each symbol represents the *I–V* slope of individual cells, measured between −90 and −120 mV in the presence of DHβE and DHβE plus nicotine ($n = 5$). ***D–F***, As in ***A–C*** but in the presence of mecamylamine (Meca, 100 μM; gray) or mecamylamine plus nicotine (black). In ***C*** and ***F***, bigger symbols represent averaged values. *$p < 0.05$.

Nicotine blocks I_h by directly interfering with HCN channels

To further assess whether nicotine affects I_h, voltage-clamp experiments were performed in the presence of cadmium (200

μM) and TTX (1 μM) to block voltage-gated Ca^{2+} channels, calcium-dependent K^+ channels, and Na^+ channels, respectively. First we examined whether, in the absence of nicotine, inward currents induced by repetitive hyperpolarizing voltage steps (from −60 to −120 mV, 1 s duration, delivered at 0.1 Hz for at least 10 min) exhibited rundown. As shown in the top traces of Figure 3, *A* and *B*, current responses were stable for a prolonged period of time (>10 min). In nine O-LM cells examined, at the end of the experiments, a small nonsignificant reduction in the amplitude of I_h of 7 ± 4% ($p > 0.05$) was observed. In contrast, bath application of nicotine (1 μM, for 5–7 min) caused always a gradual reduction in amplitude of I_h (39 ± 3%; $n = 11$; $p < 0.001$). In five cells, a partial recovery of current amplitude to 78 ± 3% was observed 3–5 min after washing out nicotine ($n = 5$) (Fig. 3*A*,*B*, bottom traces). In additional experiments, hyperpolarizing voltage steps (2 s duration) of increasing amplitude (10 mV increment) were delivered to O-LM interneurons from a holding potential of −50 to −120 mV in the absence or presence of nicotine. In agreement with a previous study (Maccaferri and McBain, 1996), this protocol elicited slowly activating inward currents, followed at the end of the voltage pulses by transient tail currents (Fig. 3*C*). The current–voltage relationship revealed an inward rectifying current with a slope measured in the range −90 to −120 mV of 2.4 ± 0.3 pA/mV ($n = 16$) (Fig. 3*D*,*E*).

The activation kinetics of I_h (following a voltage step from −50 to −120 mV) was fitted with two exponentials: a fast one (τ_f) of 139 ± 10 ms ($n = 14$) and a slow one (τ_s) of 839 ± 82 ms ($n = 14$). These values were similar to those described by Maccaferri and McBain (1996).

I_h is known to be mediated by HCN channels (Biel et al., 2009) The HCN channel subunits are encoded by at least four different genes (HCN1–4, Biel et al., 2009) that are differentially distributed among cortical and subcortical structures (Robinson and Siegelbaum, 2003). Changes in homomeric and heteromeric expression of HCN subunits would determine differences in the biophysical properties of I_h as well as its sensitivity to cAMP (Pedarzani and Storm, 1995; Santoro et al., 1998; Kanyshkova et al., 2009). To assess whether native HCN channels present on O-LM interneurons contain the cAMP-sensitive subunits, hyperpolarizing voltage steps of increasing amplitude were delivered in the absence or presence of forskolin ($n = 8$), which activates adenylate cyclase, or in the presence of the long-acting cAMP derivative Br-cAMP ($n = 4$). Forskolin (50 μM) induced in three of eight cells a slight increase in amplitude of I_h (from 101 ± 27 to 116 ± 24 pA; $p < 0.05$) and a positive shift in the activation curve (Fig. 4), which reached a significant level ($p < 0.001$) (Pedarzani and Storm, 1995; Santoro et al., 1998). Br-cAMP (250 μM) (Gasparini and DiFrancesco, 1999) produced a similar effect only in one of four neurons tested (from 58 to 71 pA), suggest-

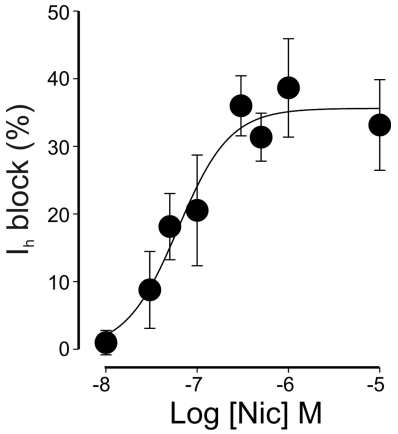


Figure 6. Nicotine reduces I_h in a concentration-dependent way. Each point represents the nicotine-induced I_h block (I_h evoked by hyperpolarizing voltage steps from −50 to −120 mV; see Materials and Methods), in the presence of increasing concentrations of nicotine (Nic) and normalized to their respective controls. Data points were fitted with the Hill equation. The EC_{50} value was 62 nM. Each point is the average of four to seven cells (total number of cells 45).

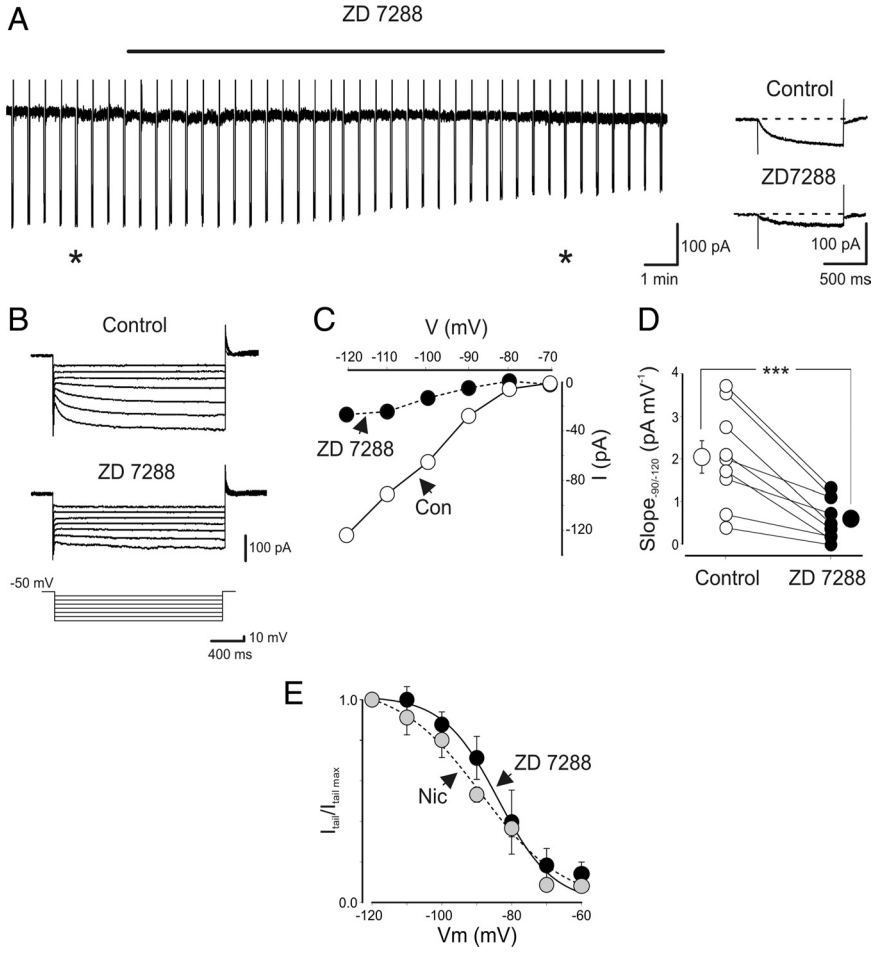


Figure 7. Nicotine reduces I_h similarly to ZD 7288. ***A***, Continuous recordings of current responses evoked by hyperpolarizing voltage steps (from −60 to −120 mV, 1 s duration) repetitively delivered at 0.1 Hz, in the absence and presence of ZD 7288 (100 μM; black bar). Individual responses obtained before and during ZD 7288 from the trace on the left (asterisks) are shown on the right with an expanded timescale. ***B***, Current responses evoked by hyperpolarizing voltage steps (10 mV increments) from a holding potential of −50 to −120 mV in the absence (Control) or presence of ZD 7288 (100 μM). ***C***, Current–voltage relationship for the cell shown in ***B***. Con, Control. ***D***, Each symbol represents *I–V* slope (measured between −90 and −120 mV) of individual cells obtained in the absence (open circles) or presence (filled circles) of ZD 7288. Bigger symbols represent averaged values. ***E***, Activation curves of nicotine-sensitive (gray circles; $n = 6$) and ZD 7288-sensitive (black circles; $n = 9$) responses obtained by subtracting tail currents recorded in the presence of nicotine (Nic) or ZD 7288 from their respective controls. ***$p < 0.001$.

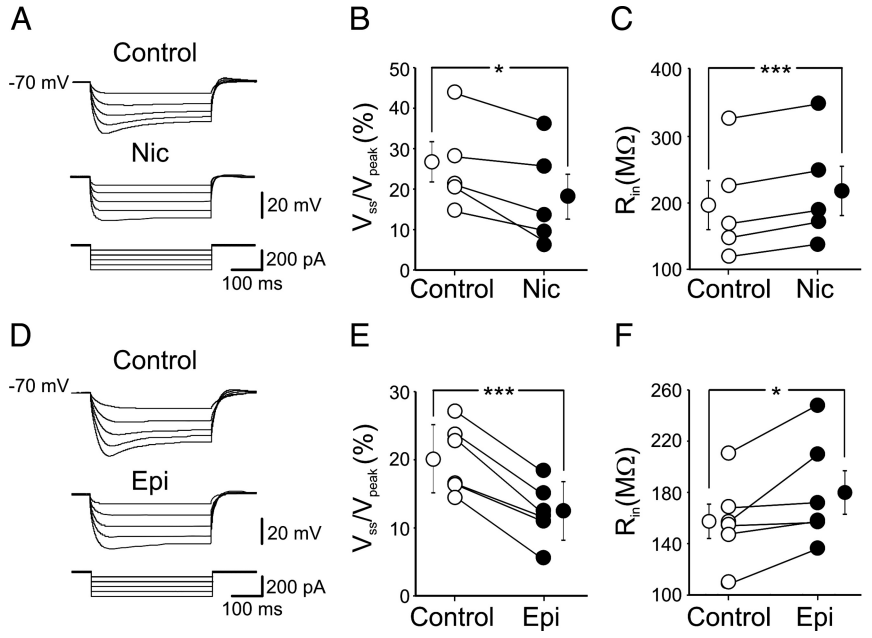


Figure 8. Epibatidine mimics the effects of nicotine on voltage sags evoked by hyperpolarizing current steps. ***A***, Voltage responses of a representative O-LM cell to injected current steps of increasing intensity (bottom) in control (top traces) or in the presence of nicotine (Nic; middle traces). ***B***, Each symbol represents the percentage ratio between the steady state and the peak values of voltage responses obtained in individual cells by hyperpolarizing current steps of 250 pA in control (open circles) or in the presence of nicotine (filled circles). ***C***, Each symbol represents the input resistance value measured in individual cells at the end of hyperpolarizing current pulses, in control (open circles) and during application of nicotine (filled circles; $n = 5$). ***D–F***, As in ***A–C*** but for epibatidine (Epi; 300 nM). Bigger symbols represent the mean ± SEM (vertical bars). $^*p < 0.05$; $^{***}p < 0.001$.

ing that, in O-LM interneurons, cAMP-sensitive HCN subunits are relatively rare.

Nicotine (applied in the bath at the concentration of 1 μM for 5 min) readily reduced I_h (Fig. 3*C*,*D*). In the −90 to −120 mV range, the slope of the current was reduced 35 ± 10% (from 2.4 ± 0.3 to 1.8 ± 0.4 pA/mV; $n = 7$; $p < 0.05$) (Fig. 3*D*,*E*).

The blocking effect of nicotine on channel conductance was more pronounced at more hyperpolarized membrane potentials. Although at −70 mV the conductance values (normalized to the cell capacitance) obtained in the absence and presence of nicotine were similar (1.8 ± 0.5 and 2.0 ± 0.4 pS/pF, respectively), at −120 mV, these were significantly different (20.9 ± 2.2 and 13.8 ± 2.7 pS/pF, respectively; $p < 0.01$) (Fig. 3*F*). Interestingly, nicotine effect on I_h was independent on nAChR activation because a similar block was observed when nicotine was applied in the presence of DHβE (50 μM) (Fig. 5*A*,*B*) or mecamylamine (100 μM) (Fig. 5*D*,*E*), known to block, at these concentrations, all nAChRs. In the presence of DHβE, nicotine induced a reduction of current slope (measured in the range −90 to −120 mV) of 27 ± 7% (from 3.8 ± 0.9 to 2.7 ± 0.6 pA/mV; $n = 5$; $p < 0.05$) (Fig. 5*B*,*C*) but in mecamylamine of 33 ± 8% (from 2.9 ± 0.8 to 2.2 ± 0.7 pA/mV; $n = 4$; $p < 0.05$) (Fig. 5*E*,*F*). These values were not significantly different from those obtained when nicotine was applied in the absence of nAChR antagonists ($p > 0.05$). It should be stressed that, in the absence of nicotine, DHβE or mecamylamine per se did not affect I_h.

To assess the minimal concentration at which nicotine affects I_h, a dose–response curve was constructed by applying hyperpolarizing voltage steps from −50 to −120 mV in the absence or presence of increasing concentrations of nicotine (from 10 nM to 10 μM). The value for the steady-state amplitude of I_h, normalized to control, was plotted versus different nicotine concentrations. Although at 30 nM the blocking effect on I_h was ~9% at 10 μM, it reached its maximum of 39 ± 7.3%. A saturating effect was found at the concentration of 1 μM. Fitting the experimental points (obtained from 45 cells, in 18 slices from 10 different animals) with the Hill equation gave an EC_{50} value of 62 nM and a Hill coefficient of 7.3, suggesting cooperativity (Fig. 6).

The blocking effect of nicotine on I_h was compared with that obtained with ZD 7288. In Figure 7*A*, the time course of ZD 7288 on I_h is illustrated. In agreement with a previous study on O-LM interneurons (Maccaferri and McBain, 1996), ZD 7288 at the concentration of 100 μM fully blocked I_h (Fig. 7*A–C*). ZD 7288 strongly reduced the slope of the *I–V* curve from 2.0 ± 0.4 to 0.59 ± 0.2 pA/mV ($n = 9$; $p < 0.001$) (Fig. 7*D*). The activation curves of nicotine- and ZD 7288-sensitive tail currents obtained at different voltages and normalized to maximal currents obtained at −120 mV were fitted with the Boltzmann equation. The $V_{1/2}$ values were −95.5 ± 1 and −85.8 ± 2.5 mV for nicotine ($n = 6$) and ZD 7288 ($n = 7$), respectively. These values were not significantly different ($p > 0.05$, one-way ANOVA). The corresponding slope factors (k) were 14.9 ± 2.5 and 6.8 ± 1.4 for nicotine and ZD 7288, respectively (Fig. 7*E*).

Epibatidine mimics the effect of nicotine on I_h

To assess whether nicotine effect on I_h is dependent on its chemical structure, we tested epibatidine, a nicotine analog, originally isolated from the frog skin, which binds with a high affinity to nAChRs (Badio and Daly, 1994). To this aim, in current-clamp conditions, hyperpolarizing current steps of increasing intensity (400 ms duration) were applied to O-LM interneurons held −70 mV. As shown in Figure 8*A* (top traces), at hyperpolarized membrane potentials, a slowly activating rectification, apparent as depolarizing sags in the electrotonic potential appeared. The amplitude of the rectification and its activation increased markedly with hyperpolarizing current steps. At the end of the current pulse, rebound depolarizing potentials were often detected. Bath application of nicotine (1 μM) almost halved the sag of the voltage response and the amplitude of the rebound depolarization (Fig. 8*A*, bottom traces). Summary data showing the percentage ratio between the steady-state and the peak values of voltage responses to hyperpolarizing current steps of 250 pA obtained in control and in the presence of nicotine are represented in Figure 8*B* (the mean normalized V_{ss}/V_{peak} values obtained before and during nicotine were 25 ± 5 and 18 ± 6, respectively; $n = 5$; $p < 0.05$). The nicotine-induced reduction of the normalized V_{ss}/V_{peak} was associated with a significant increase in membrane input resistance of 13 ± 2% (from 197 ± 37 MΩ in control to 219 ± 38 MΩ in the presence of nicotine; $n = 5$; $p < 0.001$) (Fig. 8*C*).

Like nicotine, epibatidine, at the concentration of 300 nM, reduced the sag of voltage responses and the rebound depolarization in a voltage-dependent way (Fig. 8*D*). The mean normalized V_{ss}/V_{peak} values obtained before and during epibatidine were 20 ± 5 and 12 ± 4, respectively; $n = 6$; $p < 0.001$) (Fig. 8*E*). The epibatidine-induced reduction of the normalized V_{ss}/V_{peak} was associated with a significant increase in membrane input resis-

tance of 17 ± 5% (from 157 ± 13 MΩ in control to 180 ± 17 MΩ in the presence of epibatidine; $n = 6$; $p < 0.05$) (Fig. 8*F*).

In contrast to nicotine and epibatidine, the endogenous ligand of nAChRs, acetylcholine (100 μM), applied in the presence of atropine (1 μM) to block muscarinic AChRs did not affect the voltage sag induced by hyperpolarizing current steps. The mean normalized V_{ss}/V_{peak} values obtained in the absence and presence of acetylcholine were 16 ± 3 and 14 ± 2, respectively ($n = 6$; $p > 0.05$; data not shown). Because in the brain acetylcholine is rapidly degraded by acetylcholinesterase, experiments were repeated in the presence of the acetylcholinesterase inhibitor edrophonium (20 μM; $n = 3$). Also in this case ACh failed to affect I_h.

Nicotine disrupts the oscillatory behavior of O-LM interneurons

As mentioned previously, a large number of O-LM interneurons (122 of 166) fire spontaneously in the range of 4–9.5 Hz. In 8 of 10 neurons, bath application of nicotine (1 μM) in the presence of the nAChR antagonists mecamylamine (100 μM) or DHβE (50 μM) and synaptic blockers caused a slowdown of the firing frequency from 6.1 ± 0.6 to 1.3 ± 0.6 Hz ($n = 8$; $p < 0.01$) (Fig. 9*A*,*B*). In five of eight neurons, nicotine completely blocked the firing and caused a strong membrane hyperpolarization (12 ± 0.1 mV; $n = 5$; $p < 0.001$) (Fig. 9*C*). Nicotine-induced depression of the firing rate was still present when the membrane potential was set back to the predrug membrane potential level via injection of a steady depolarizing current (in these conditions, the firing rate was reduced from 6.9 ± 0.7 to 3.8 ± 0.5 Hz; $n = 4$; $p < 0.05$) (Fig. 9*A*, arrow). This effect was similar to that obtained with ZD 7288 (Maccaferri and McBain, 1996). To elucidate whether nicotine-induced reduction of the firing rate involved I_h, the activation threshold for I_h was estimated by plotting peak amplitudes of nicotine-sensitive components of inward currents at various hyperpolarizing voltage steps versus membrane potentials. Data points through the linear portion of the *I–V* curve (in the range of −80/−110 mV) were fitted with a regression line (Kilb and Luhmann, 2000), which intercepted the *x*-axis at −67 mV, a value very close to the resting membrane potential of these cells (Fig. 9*D*). This suggests that, in our preparation, I_h is already active at rest and therefore can influence the spontaneous firing (Lupica et al., 2001).

In additional experiments, to evaluate whether nicotine affects the intrinsic oscillatory properties of O-LM interneurons, a subthreshold sinusoidal current at the theta frequency (4–7 Hz) was injected into the cells. The amplitude of the currents was adjusted to evoke spikes at the top of the sinusoidal wave.

Nicotine (1 μM) significantly reduced the rotation number [average spike per cycle (Lawrence et al., 2006)] from 1.37 ± 0.6 to 0.5 ± 0.3 ($n = 6$; $p < 0.05$) (Fig. 10*A*,*E*) and slowed down the interspike depolarizing slope from 0.26 ± 0.04 to 0.23 ± 0.03 mV/ms ($n = 5$; $p < 0.001$) (Fig. 10*A*,*B*,*D*) without altering the amplitude, duration, and shape of the action potentials (Fig. 10*C*). This indicates that nicotine severely alters the intrinsic oscillatory properties of O-LM cells and rhythmogenesis.

Similarly to nicotine, bath application of epibatidine (300 nM) in the presence of the nAChR antagonist DHβE (50 μM) and synaptic blockers significantly reduced the firing of O-LM interneurons from 4.4 ± 0.8 to 1 ± 0.7 Hz ($n = 5$; $p < 0.05$; data not shown).

A homology model predicts nicotine binding site within the HCN channel pore

To estimate nicotine binding site within the HCN channel, we docked the three-dimensional structures of nicotine and epibatidine (Fig. 11) inside our previously reported models of the HCN channels in their open configuration (Giorgetti et al., 2005). Although the docking of the ligands from the outer mouth of the channels did not show highly populated clusters, the docking from the inside of the cell, which is from the inner mouth of the channels, produced a set of highly populated clusters. The ones with the lower energies showed the ligands bound inside the inner cavity of the channel, in coincidence with the mid region of the S6 domain. The rings of the ligands were predominantly aligned with the axis of the central cavity of the channel (Fig. 11).

It can be therefore hypothesized that, to block the channels, both ligands should form hydrophobic interactions with the Ile432 and Ala425 residues. However, this hypothesis should be validated with point-directed mutagenesis experiments. Interestingly, the poses of the ligands are highly similar to those described recently for ZD 7288 and cilobradine (Cheng et al., 2007).

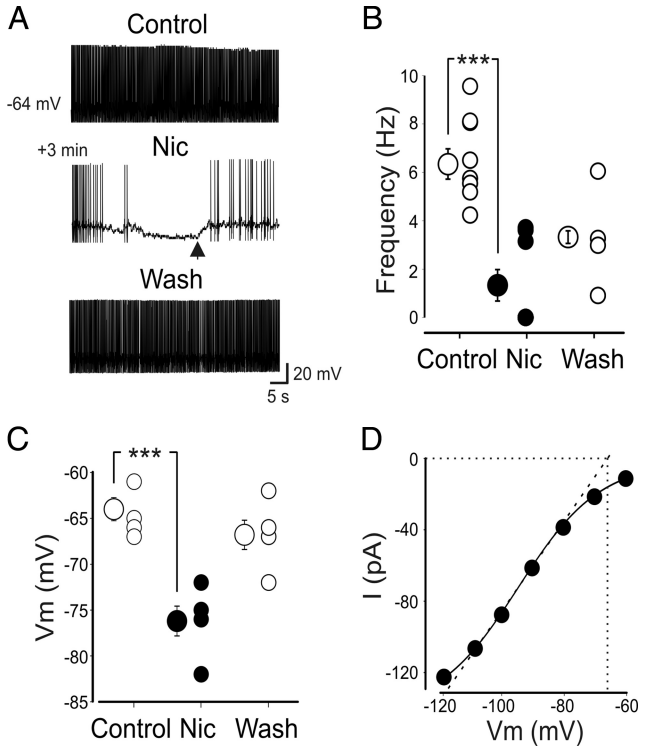


Figure 9. Nicotine reduces the spontaneous firing of O-LM cells. ***A***, Representative traces of one O-LM cell showing spontaneous firing before (Control), during (Nic; horizontal bar), and after (Wash) nicotine application. Note that the block of firing induced by nicotine was only partially restored by injecting a depolarizing steady current through the patch pipette (arrow). Full recovery was obtained 4 min after wash. ***B***, Each symbol represents the frequency value of individual cells recorded before (Control), during (Nic), and after (Wash) nicotine application. Bigger symbols represent mean values. A partial recovery was observed in five of eight cells 3–5 min after washing out nicotine. ***C***, As in ***B*** but for the resting membrane potential (V_m). ***D***, Plot of peak amplitudes of nicotine-sensitive components of inward currents at various hyperpolarizing voltage steps versus membrane potentials. Data points were fitted with the Boltzmann equation (solid line). Data points through the linear portion of the *I–V* curve (in the range of −80/−110 mV) were fitted with a regression line (dotted line) to obtain the activation threshold of I_h (*x* intercept). *$p < 0.05$; ***$p < 0.001$.

Discussion

The present data clearly show that, in O-LM interneurons, nicotine, the active component of tobacco, at a very low concentration and independently of nAChR activation, is able to reversibly reduce the time-dependent inwardly rectifying cationic current I_h responsible for the oscillatory behavior of these cells.

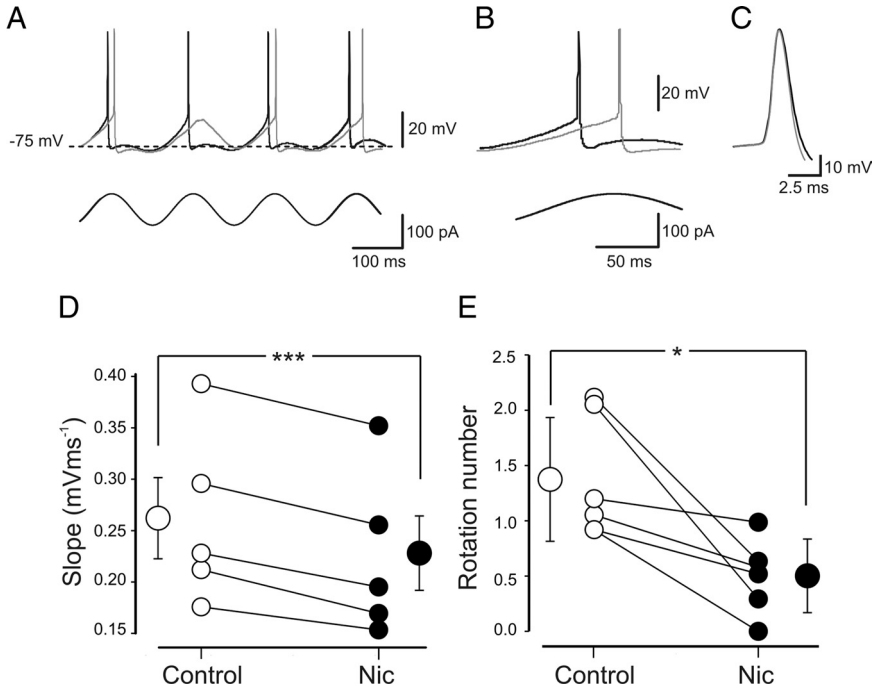


Figure 10. Nicotine slows down the depolarizing voltage slopes induced by subthreshold oscillations in the theta frequency range. ***A***, Two superimposed traces of voltage responses to injected steady subthreshold sinusoidal currents in control (black) or in the presence of nicotine (gray). Nicotine slowed down the slope and reduced the number of action potentials. ***B***, The reduction in the depolarizing voltage slope shown in ***A*** is represented on an expanded timescale. ***C***, Two action potentials from the traces in ***A*** are superimposed at a different timescale. ***D***, Each symbol represents the slope value of individual cells measured in control (open circles) or in the presence of nicotine (Nic; filled circles). ***E***, Each symbol represents the rotation number (average spikes per cycle) of individual cells obtained in control (open circles) or in the presence of nicotine (filled circles). $*p < 0.05$; $***p < 0.001$.

In a first set of experiments, using the patch-clamp technique in current-clamp mode, we have demonstrated that nicotine affects the resonance properties of O-LM interneurons. Previous work from CA1 pyramidal cells has shown the existence of two forms of slow electrical resonance occurring at the theta frequency: one at depolarizing membrane potentials (between −50 and −70 mV) dominated by I_M and the other prevailing at hyperpolarizing membrane potentials (between −70 and −95 mV) dominated by I_h (Hu et al., 2002). Blocking I_M or I_h channels with selective blockers enhanced the input resistance at their respective activation voltages and abolished the respective resonance peaks. In the present experiments from O-LM interneurons, resonance was studied only at hyperpolarizing membrane potentials in which I_h is particularly pronounced (Maccaferri and McBain, 1996). In agreement with a previous study (Pike at al. 2000), we found that O-LM interneurons optimally responded to theta inputs with maximum spiking activity occurring at input frequency at ~3–5 Hz. Surprisingly, nicotine blocked resonance at −90 mV but not at −70 mV in a way similar to ZD 7288, a selective blocker of I_h, implying that it was acting on this conductance (BoSmith et al., 1993).

In a second set of experiments, we provided direct evidence that indeed nicotine affected I_h. Similarly to ZD 7288, nicotine strongly reduced the slowly activating rectification apparent as a depolarizing sag in the electrotonic potentials evoked by hyperpolarizing current steps, further indicating that I_h was the target of this alkaloid. In voltage-clamp experiments, nicotine significantly reduced the steady-state amplitude of the currents evoked by hyperpolarizing voltage steps. The effect of nicotine on I_h did not involve activation of nAChRs because its action persisted in the presence of nAChR antagonists. Interestingly, the structurally analog of nicotine epibatidine had similar effect, whereas the physiological ligand for nAChRs, acetylcholine, was ineffective.

I_h is a mixed cationic (Na^+ and K^+) current mediated by HCN channels. Four different subunits have been so far cloned, which may assemble to form homotetramers and heterotetramers with different biophysical properties (Biel et al., 2009). In particular, the HCN2 and HCN4 subunits have been shown to confer high sensitivity to cAMP (Biel et al., 2009). The composition of native HCN channels in O-LM cells is unknown. However, the observation that both forskolin and Br-cAMP were, in the majority of cases, unable to potentiate I_h suggest that these subunits, if present, exert only a minor contribution. Alternatively, the possibility that the whole-cell condition may disrupt in some cells the cAMP-dependent regulatory pathway cannot be excluded.

The similarity of action between nicotine and ZD 7288 strongly suggest that this alkaloid blocks I_h by directly interfering with the channel protein. Molecular docking calculations have allowed estimating nicotine putative binding site within the HCN channel pore, in a position close to the one identified for ZD 7288. Based on a previous HCN channel model (Giorgetti et al., 2005) and mutagenesis experiments, Cheng et al. (2007) have found that the phenyl ring of ZD 7288 occupies a hydrophobic cavity formed by Ala425 and Ile432. The charged ring aligns with the axis of the inner pore closely corresponding to the localization of the K^+ ions, observed in the KcsA K^+ channel crystal structure. Similarly to our results, a direct interaction of nicotine with voltage-dependent K^+ channels has been described in the heart in which this alkaloid affects the shape of cardiac action potentials, independently of nAChRs activation (Greenspan et al., 1969; Pappano and Rembish, 1970; Carryl et al., 1992; Satoh H., 1997), thus contributing to cardiac arrhythmias. In particular, in canine ventricular myocytes, nicotine has been shown to reduce the transient outward K^+ current I_A (Wang et al., 2000a) and the inward rectifier potassium current mediated by Kir channels, which in cardiac cells contribute to stabilize the resting membrane potential at relatively negative values and to regulate cell excitability (Wang et al., 2000b). In a previous study aimed at clarifying whether the chronic exposure of pregnant mothers to cigarette smoke affects the intrinsic membrane properties of pedunculopontine nucleus neurons in brainstem slices of the offspring, an increase of I_h was detected (Good et al., 2006). It should be stressed however that, in contrast with the present data, in pedunculopontine nucleus neurons, I_h was studied without blocking synaptic transmission and/or nAChRs. In the present experiments, the reduction of I_h by nicotine severely affected the firing properties of O-LM interneurons and their oscillatory properties. How does nicotine-induced reduction of I_h affect the firing properties of O-LM interneurons?

One likely explanation is that nicotine reduces an inward current already active at rest that exerts a tonic depolarizing action on O-LM cells. The activation threshold of −67 mV for nicotine-sensitive inward currents found in the present experiments, very close to the resting membrane potential of O-LM cells, strongly

suggests that indeed this is the case. Therefore, similarly to ZD 7288, nicotine could affect spontaneous firing of O-LM interneurons by directly interfering with I_h. This effect was independent of nicotine-induced membrane hyperpolarization, because it persisted when the membrane was repolarized to the control level. It should be stressed, however, that this conductance becomes fully activated during the afterhyperpolarization after action potential firing. Nicotine-induced firing attenuation was dependent on the slow-down of the interspike depolarizing slope, which brings the membrane potential back to threshold for action potential firing. Interestingly, these effects occurred in the absence of any change in the shape of the action potentials, indicating a selective action of nicotine on the pacemaker current I_h. O-LM interneurons are key players in the generation of the theta rhythm (Somogyi and Klausberger, 2005) and a recent study on an *in vivo* animal model of epilepsy has clearly demonstrated that reducing I_h in O-LM interneurons severely impairs rhythmogenesis in the hippocampus (Dugladze et al., 2007).

It is worth noting that, in the present experiments, nicotine affected I_h at very low concentrations. In regular smokers, the average blood concentration of nicotine is ~220 nM/L (Varanda et al., 1985; Tang et al., 1999). In addition, with an average half-life of 2–3 h, nicotine can accumulate into the blood of smokers to reach higher concentrations (Benowitz et al., 1989). The EC_{50} value for nicotine effects on I_h (~60 nM) was well below the level found in the blood of smokers and below the level necessary to block multiple K^+ currents in the heart (Tang et al., 1999; Wang et al., 2000b).

In conclusion, nicotine, by directly blocking I_h in O-LM interneurons, disrupts the temporal coding necessary for network synchronization and for generation of the theta rhythm crucial for the processing and storage of information in the brain (Buzsáki, 2002). This may be relevant for smokers.

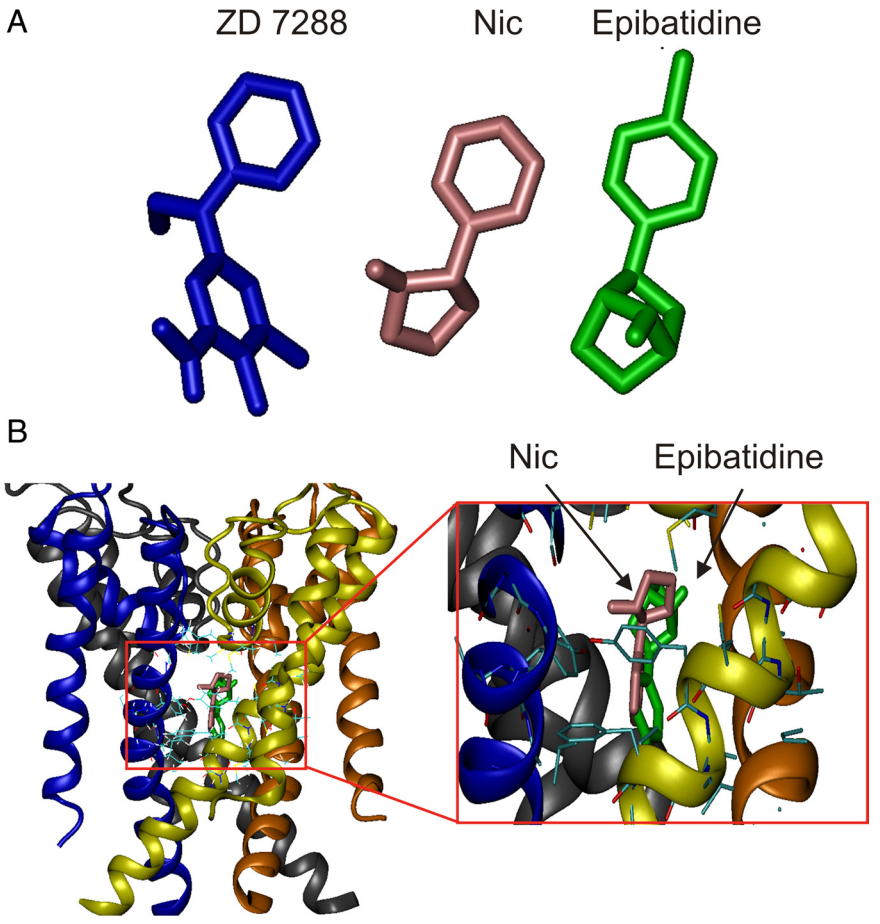


Figure 11. Putative binding site of nicotine and epibatidine into the inner pore of HCN channels. ***A***, Three-dimensional structures of ZD 7288, nicotine (Nic), and epibatidine, respectively. ***B***, Model of the tetrameric HCN channel pore structure with nicotine (pink arrow) and epibatidine (green arrow), docked in the internal cavity of the channel. Surrounding amino acids are shown in stick representation. For clarity, the four monomers are shown in different colors.

References

Ali AB, Thomson AM (1998) Facilitating pyramid to horizontal oriens-alveus interneurone inputs: dual intracellular recordings in slices of rat hippocampus. J Physiol 507:185–199.

Badio B, Daly JW (1994) Epibatidine, a potent analgetic and nicotinic agonist. Mol Pharmacol 45:563–569.

Benowitz NL, Jacob P 3rd, Yu L (1989) Daily use of smokeless tobacco: systemic effects. Ann Intern Med 111:112–116.

Biel M, Wahl-Schott C, Michalakis S, Zong X (2009) Hyperpolarization-activated cation channels: from genes to function. Physiol Rev 89:847–885.

BoSmith RE, Briggs I, Sturgess NC (1993) Inhibitory actions of ZENECA ZD 7288 on whole-cell hyperpolarization activated inward current (If) in guinea-pig dissociated sino atrial node cells. Br J Pharmacol 110:343–349.

Buzsáki G (2002) Theta oscillations in the hippocampus. Neuron 33:325–340.

Carryl OR, Gallardo-Carpentier A, Carpentier RG (1992) Effects of nicotine and ethanol on rat atrial membrane potentials. Alcohol 9:87–92.

Cheng L, Kinard K, Rajamani R, Sanguinetti MC (2007) Molecular mapping of the binding site for a blocker of hyperpolarization-activated, cyclic nucleotide-modulated pacemaker channels. J Pharmacol Exp Ther 322:931–939.

Cossart R, Petanjek Z, Dumitriu D, Hirsch JC, Ben-Ari Y, Esclapez M, Bernard C (2006) Interneurons targeting similar layers receive synaptic inputs with similar kinetics. Hippocampus 16:408–420.

Dugladze T, Vida I, Tort AB, Gross A, Otahal J, Heinemann U, Kopell NJ, Gloveli T (2007) Impaired hippocampal rhythmogenesis in a mouse model of mesial temporal lobe epilepsy. Proc Natl Acad Sci U S A 104:17530–17535.

Freund TF, Buzsáki G (1996) Interneurons of the hippocampus. Hippocampus 6:347–470.

Frotscher M, Léránth C (1985) Cholinergic innervation of the rat hippocampus as revealed by choline acetyltransferase immunocytochemistry: a combined light and electron microscopic study. J Comp Neurol 239:237–246.

Gasparini S, DiFrancesco D (1999) Action of serotonin on the hyperpolarization-activated cation current (I_h) in rat CA1 hippocampal neurons. Eur J Neurosci 11:3093–3100.

Gillies MJ, Traub RD, LeBeau FE, Davies CH, Gloveli T, Buhl EH, Whittington MA (2002) A model of atropine-resistant theta oscillations in rat hippocampal area CA1. J Physiol 543:779–793.

Giorgetti A, Carloni P, Mistrik P, Torre V (2005) A homology model of the pore region of HCN channels. Biophys J 89:932–944.

Gloveli T, Dugladze T, Saha S, Monyer H, Heinemann U, Traub RD, Whittington MA, Buhl EH (2005) Differential involvement of oriens/pyramidale interneurones in hippocampal network oscillations in vitro. J Physiol 562:131–147.

Goldin M, Epsztein J, Jorquera I, Represa A, Ben-Ari Y, Crépel V, Cossart R

(2007) Synaptic kainate receptors tune oriens-lacunosum moleculare interneurons to operate at theta frequency. J Neurosci 27:9560–9572.
Good CH, Bay KD, Buchanan RA, McKeon KA, Skinner RD, Garcia-Rill E (2006) Prenatal exposure to cigarette smoke affects the physiology of pedunculopontine nucleus (PPN) neurons in development. Neurotoxicol Teratol 28:210–219.
Greenspan K, Edmands RE, Knoebel SB, Fisch C (1969) Some effects of nicotine on cardiac automaticity, conduction, and inotropy. Arch Intern Med 123:707–712.
Griguoli M, Scuri R, Ragozzino D, Cherubini E (2009) Activation of nicotinic acetylcholine receptors enhances a slow calcium-dependent potassium conductance and reduces the firing of stratum oriens interneurons. Eur J Neurosci 30:1011–1022.
Hájos N, Pálhalmi J, Mann EO, Németh B, Paulsen O, Freund TF (2004) Spike timing of distinct types of GABAergic interneuron during hippocampal gamma oscillations *in vitro*. J Neurosci 24:9127–9137.
Hestrin S, Galarreta M (2005) Electrical synapses define networks of neocortical GABAergic neurons. Trends Neurosci 28:304–309.
Hu H, Vervaeke K, Storm JF (2002) Two forms of electrical resonance at theta frequencies, generated by M-current, h-current and persistent Na^+ current in rat hippocampal pyramidal cells. J Physiol 545:783–805.
Hutcheon B, Yarom Y (2000) Resonance, oscillation and the intrinsic frequency preferences of neurons. Trends Neurosci 23:216–222.
Janigro D, Martenson ME, Baumann TK (1997) Preferential inhibition of Ih in rat trigeminal ganglion neurons by an organic blocker. J Membr Biol 160:101–109.
Jiang Y, Lee A, Chen J, Cadene M, Chait BT, MacKinnon R (2002) Crystal structure and mechanism of a calcium-gated potassium channel. Nature 417:515–522.
Kanyshkova T, Pawlowski M, Meuth P, Dubé C, Bender RA, Brewster AL, Baumann A, Baram TZ, Pape HC, Budde T (2009) Postnatal expression pattern of HCN channel isoforms in thalamic neurons: relationship to maturation of thalamocortical oscillations. J Neurosci 29:8847–8857.
Kilb W, Luhmann HJ (2000) Characterization of a hyperpolarization-activated inward current in Cajal-Retzius cells in rat neonatal neocortex. J Neurophysiol 84:1681–1691.
Klausberger T, Magill PJ, Márton LF, Roberts JD, Cobden PM, Buzsáki G, Somogyi P (2003) Brain-state- and cell-type-specific firing of hippocampal interneurons in vivo. Nature 421:844–848.
Klausberger T, Márton LF, Baude A, Roberts JD, Magill PJ, Somogyi P (2004) Spike timing of dendrite-targeting bistratified cells during hippocampal network oscillations in vivo. Nat Neurosci 7:41–47.
Lacaille JC, Mueller AL, Kunkel DD, Schwartzkroin PA (1987) Local circuit interactions between oriens/alveus interneurons and CA1 pyramidal cells in hippocampal slices: electrophysiology and morphology. J Neurosci 7:1979–1993.
Lawrence JJ, Grinspan ZM, Statland JM, McBain CJ (2006) Muscarinic receptor activation tunes mouse stratum oriens interneurones to amplify spike reliability. J Physiol 571:555–562.
Lee MG, Chrobak JJ, Sik A, Wiley RG, Buzsáki G (1994) Hippocampal theta activity following selective lesion of the septal cholinergic system. Neuroscience 62:1033–1047.
Levey AI, Edmunds SM, Koliatsos V, Wiley RG, Heilman CJ (1995) Expression of m1–m4 muscarinic acetylcholine receptor proteins in rat hippocampus and regulation by cholinergic innervation. J Neurosci 15:4077–4092.
Lupica CR, Bell JA, Hoffman AF, Watson PL (2001) Contribution of the hyperpolarization-activated current I(h) to membrane potential and GABA release in hippocampal interneurons. J Neurophysiol 86:261–268.
Maccaferri G (2005) Stratum oriens horizontal interneurone diversity and hippocampal network dynamics. J Physiol 562:73–80.
Maccaferri G, McBain CJ (1996) The hyperpolarization-activated current (Ih) and its contribution to pacemaker activity in rat CA1 hippocampal stratum oriens-alveus interneurones. J Physiol 497:119–130.
Maccaferri G, Roberts JD, Szucs P, Cottingham CA, Somogyi P (2000) Cell surface domain specific postsynaptic currents evoked by identified GABAergic neurones in rat hippocampus in vitro. J Physiol 524:91–116.
McBain CJ, Fisahn A (2001) Interneurons unbound. Nat Rev Neurosci 2:11–23.
McBain CJ, DiChiara TJ, Kauer JA (1994) Activation of metabotropic glutamate receptors differentially affects two classes of hippocampal interneurons and potentiates excitatory synaptic transmission. J Neurosci 14:4433–4445.
Miles R, Tóth K, Gulyás AI, Hájos N, Freund TF (1996) Differences between somatic and dendritic inhibition in the hippocampus. Neuron 16:815–823.
Minneci F, Janahmadi M, Migliore M, Dragicevic N, Avossa D, Cherubini E (2007) Signaling properties of stratum oriens interneurons in the hippocampus of transgenic mice expressing EGFP in a subset of somatostatin-containing cells. Hippocampus 17:538–553.
Morris GM, Goodsell DS, Halliday RS, Huey R, Hart WE, Belew RK, Olson AJ (1998) Automated docking using a Lamarckian genetic algorithm and an empirical binding free energy function. J Comput Chem 19:1639–1662.
Narayanan R, Johnston D (2007) Long-term potentiation in rat hippocampal neurons is accompanied by spatially widespread changes in intrinsic oscillatory dynamics and excitability. Neuron 56:1061–1075.
Oliva AA Jr, Jiang M, Lam T, Smith KL, Swann JW (2000) Novel hippocampal interneuronal subtypes identified using transgenic mice that express green fluorescent protein in GABAergic interneurons. J Neurosci 20:3354–3368.
Pappano AJ, Rembish RA (1970) Nicotine-induced restoration of action potentials to cardiac tissue depolarized by potassium. Life Sci I 9:1381–1388.
Pedarzani P, Storm JF (1995) Protein kinase A-independent modulation of ion channels in the brain by cyclic AMP. Proc Natl Acad Sci U S A 92:11716–11720.
Pike FG, Goddard RS, Suckling JM, Ganter P, Kasthuri N, Paulsen O (2000) Distinct frequency preferences of different types of rat hippocampal neurones in response to oscillatory input currents. J Physiol 529:205–213.
Puil E, Gimbarzevsky B, Miura RM (1986) Quantification of membrane properties of trigeminal root ganglion neurons in guinea pigs. J Neurophysiol 55:995–1016.
Robinson RB, Siegelbaum SA (2003) Hyperpolarization-activated cation currents: from molecules to physiological function. Annu Rev Physiol 65:453–480.
Santoro B, Liu DT, Yao H, Bartsch D, Kandel ER, Siegelbaum SA, Tibbs GR (1998) Identification of a gene encoding a hyperpolarization-activated pacemaker channel of brain. Cell 93:717–729.
Satoh H (1997) Effects of nicotine on spontaneous activity and underlying ionic currents in rabbit sinoatrial nodal cells. Gen Pharmacol 28:39–44.
Somogyi P, Klausberger T (2005) Defined types of cortical interneurone structure space and spike timing in the hippocampus. J Physiol 562:9–26.
Tang G, Hanna ST, Wang R (1999) Effects of nicotine on K^+ channel currents in vascular smooth muscle cells from rat tail arteries. Eur J Pharmacol 364:247–254.
Tribollet E, Bertrand D, Marguerat A, Raggenbass M (2004) Comparative distribution of nicotinic receptor subtypes during development, adulthood and aging: an autoradiographic study in the rat brain. Neuroscience 124:405–420.
Varanda WA, Aracava Y, Sherby SM, VanMeter WG, Eldefrawi ME, Albuquerque EX (1985) The acetylcholine receptor of the neuromuscular junction recognizes mecamylamine as a noncompetitive antagonist. Mol Pharmacol 28:128–137.
Wang H, Shi H, Zhang L, Pourrier M, Yang B, Nattel S, Wang Z (2000a) Nicotine is a potent blocker of the cardiac A-type K^+ channels. Effects on cloned Kv4.3 channels and native transient outward current. Circulation 102:1165–1171.
Wang H, Yang B, Zhang L, Xu D, Wang Z (2000b) Direct block of inward rectifier potassium channels by nicotine. Toxicol Appl Pharmacol 164:97–101.
Whittington MA, Traub RD (2003) Interneuron diversity series: inhibitory interneurons and network oscillations in vitro. Trends Neurosci 26:676–682.
Zemankovics R, Káli S, Paulsen O, Freund TF, Hájos N (2010) Differences in subthreshold resonance of hippocampal pyramidal cells and interneurons: the role of h-current and passive membrane characteristics. J Physiol 588:2109–2132.
Zsiros V, Maccaferri G (2005) Electrical coupling between interneurons with different excitable properties in the stratum lacunosum-moleculare of the juvenile CA1 rat hippocampus. J Neurosci 25:8686–8695.

Conclusions and future perspectives

Network-driven oscillations in the cortex and in the hippocampus have been implicated in high cognitive functions including encoding, consolidation and retrieval of information. Rhythmic neuronal synchronization occurring at the theta-frequency, which constitutes the major operational mode of the hippocampus, is thought to govern temporal integration of synaptic inputs (Buzsaki & Chrobak, 1995) and the mechanisms mediating memory formation (Larson & Lynch, 1986; Huerta & Lisman, 1995). Although no consensus has yet emerged regarding the specific behavioral correlates of theta rhythm, theta waves are most consistently present during REM sleep (Jouvet, 1969) and during various types of locomotor activities described by the subjective terms "voluntary", "preparatory", "orienting" or "exploratory" (Vanderwolf, 1969).

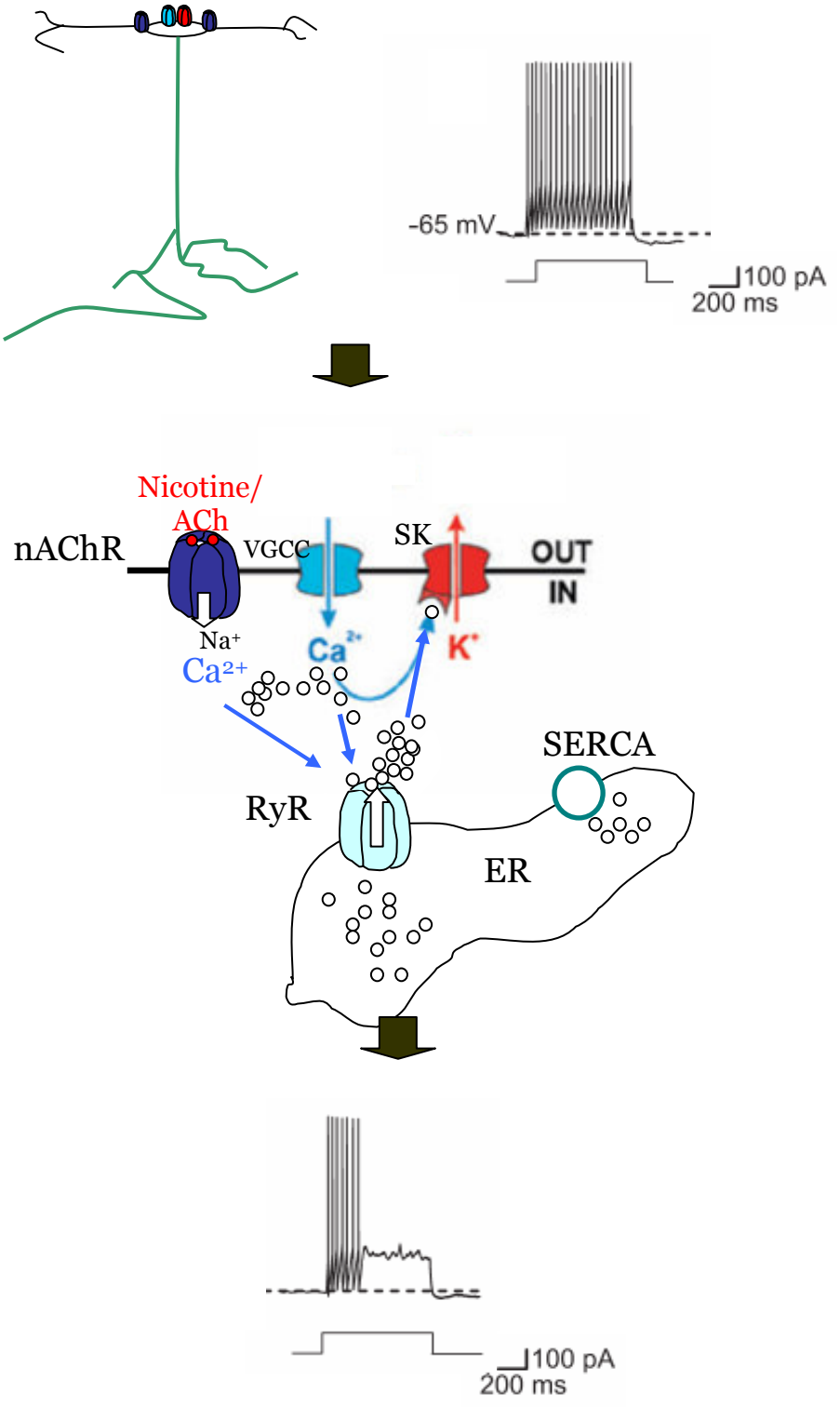
Neuronal oscillatory activity arises from the interplay between synaptic network activity and intrinsic conductances underling the firing and the resonance properties of the participating neurons. Cholinergic and GABAergic medial septal afferents contribute to hippocampal theta rhythm in part by regulating the activity of local interneurons. Hippocampal inhibitory interneurons play a central role in theta activity by rhythmically inhibiting pyramidal cells (Leung, 1984; Fox, 1989; Ylinen et al., 1995; Toth et al., 1997). $GABA_A$-mediated chloride conductances are activated during each theta cycle (Fox et al., 1986; Leung & Yim, 1986; Buzsaki et al., 1986; Soltesz and Deschenes, 1993; Ylinen et al., 1995), and rhythmic stimulation of basket and axo-axonic interneurons sets the phase of theta wave in pyramidal cells *in vitro* (Cobb et al., 1995). By innervating the distal dendrites of principal cells, O-LM interneurons fire in phase with the trough of theta oscillation suggesting their contribution to theta rhythm generation. O-LM interneurons receive a strong cholinergic innervation from the septum and express functional nAChRs.

In my thesis work I have identified two different mechanisms by which nicotine affects the firing of O-LM cells and influences rhythmogenesis, one dependent and the other independent on the activation of nAChRs.

In the first study, I found that activation of nAChRs by nicotine or endogenously released acetylcholine enhances a calcium dependent potassium conductance responsible for spike accommodation. This effect depends on the elevation of intracellular calcium *via* nAChRs activation. The reduced firing rate would lead to a reduction in GABA release. This in turn would affect principal cells synchronization and oscillatory activity (see Figure 7). Therefore, the possibility that in smokers, the persistent activation of non-desensitizing nAChRs by nicotine alters rhythmogenesis by interfering with O-LM firing can not be ruled out.

Figure 7

First question: Does Ca^{2+} entering through nAChRs modulate the firing properties of O-LM interneurons?



Nicotine- or ACh-induced increase in intracellular Ca^{2+} enhances SK-mediated outward current leading to O-LM firing adaptation.

Therefore.....

Endogenous ACh or Nicotine

↓

O-LM firing adaptation

↓

Reduction of GABA release at pyramidal cell distal dendrites

↓

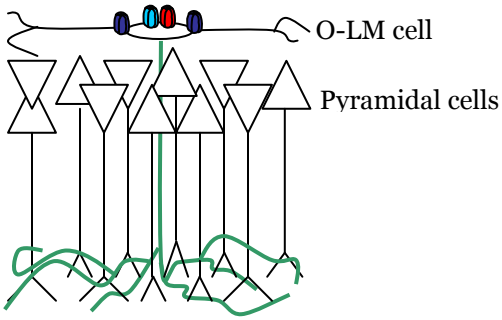
Disinhibition of dendritic calcium spikes

↓

Changes in spatial-temporal integration properties of principal cells and network synchronization

?



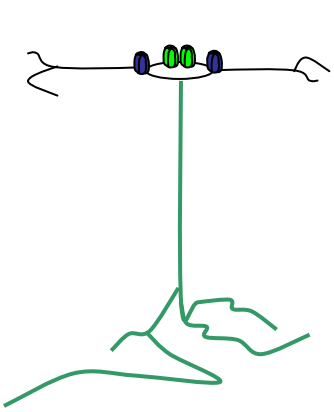


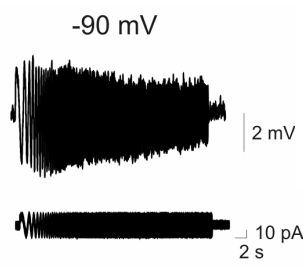
In the second study, I found that a low concentration of nicotine strongly reduces I_h, the pacemaker current carried by HCN channels. This conductance which underlies the subthreshold resonance properties of O-LM cells contributes to bring the membrane potential towards the threshold for action potential generation. Unexpectedly, I found that nicotine reduces I_h independently of nAChRs activation. This effect leads to alterations in the firing properties and oscillatory behavior of O-LM cells.

All these pieces of evidence highlight the intriguing possibility that nicotine either directly or indirectly *via* nAChRs activation alters rhythmogenesis in smokers (see Figure 8).

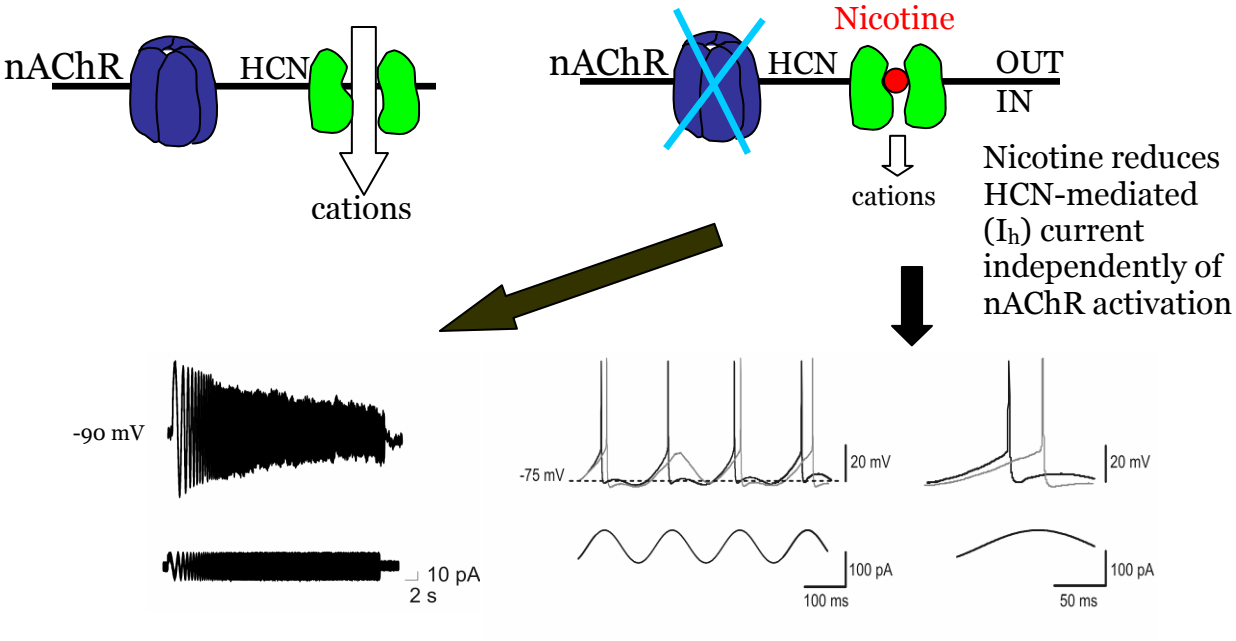
Figure 8

Second question: Does nicotine directly affect the oscillatory properties of O-LM interneurons?





Theta resonance (3-7 Hz) at hyperpolarized membrane potential



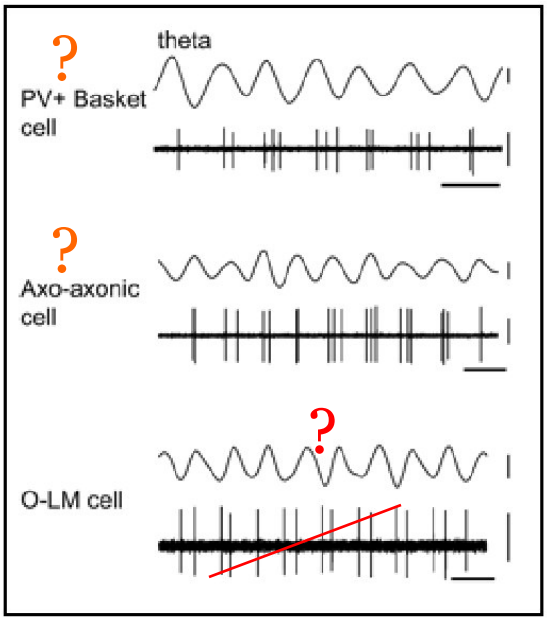
Nicotine-mediated decrease of I_h current disrupts the theta resonance of O-LM cells (left), slows down the depolarizing slope and the number of action potential (grey trace; right).

Therefore……

Exogenous Nicotine



May alter rythmogenesis in smokers



(Modified from Somogyi & Klausberger, 2005)

It would be of interest to investigate whether the action of nicotine on I_h which is independent of nAChRs affects other cell types and how this influence brain rhythms and cognitive functions.

The integrative properties of neurons are strongly influenced by their synaptic inputs (Pouille & Scanziani, 2004; Oren et al., 2006) which can be modified in an activity-dependent manner. Therefore, in future experiments it would be of interest to investigate whether activation of nAChRs in O-LM cells can modulate activity-dependent synaptic plasticity processes through calcium-dependent mechanisms.

Unlike other hippocampal interneurons (Ouardouz & Lacaille, 1995; Lamsa et al., 2005; 2007b), O-LM cells exhibit two different NMDA-independent forms of LTP. The first one consists in an associative type of learning (Hebbian type) mediated by mGluRs (Perez et al., 2001) while the second one in a non-associative type of learning (anti-Hebbian) mediated by Ca^{2+}-permeable AMPARs (Oren et al., 2009). The anti-Hebbian form of LTP can be induced in voltage clamp conditions, holding the cell at a relatively hyperpolarized membrane potential, using a non-associative stimulation paradigm (Lamsa et al., 2007). According to Lamsa et al. (2007), this process would play distinct roles in neurons exhibiting characteristic phase relationships in different network states. During sharpe-wave ripples, O-LM cells are typically silent while many of their input pyramidal cells fire at high frequency (Klusberger et al., 2003) possibly satisfying the ideal conditions for an anti-Hebbian form of LTP. This would contribute to remapping and creating new place fields and to rearrange the temporal relationship within activated neuronal ensembles (Dragoi et al. 2003).

In contrast, during theta activity which is associated with exploratory behavior, O-LM interneurons fire in phase with pyramidal cells, thus contributing to this rhythm through phase locked dendritic inhibition (Klusberger et al., 2003; Gillies et al., 2002).. The anti-Hebbian LTP, induced during ripples may result in long-term alteration of pyramidal cell excitation of O-LM interneurons, which persist during theta activity further contributing to spatial memory formation.

The same condition utilized for inducing an anti-Hebbian form of LTP, namely the hyperpolarized membrane potential allows the maximal flow of cations (including calcium) into the cell also *via* nAChRs. Calcium entry *via* nAChRs may interfere with synaptic plasticity processes and may affect rhythmogenesis.

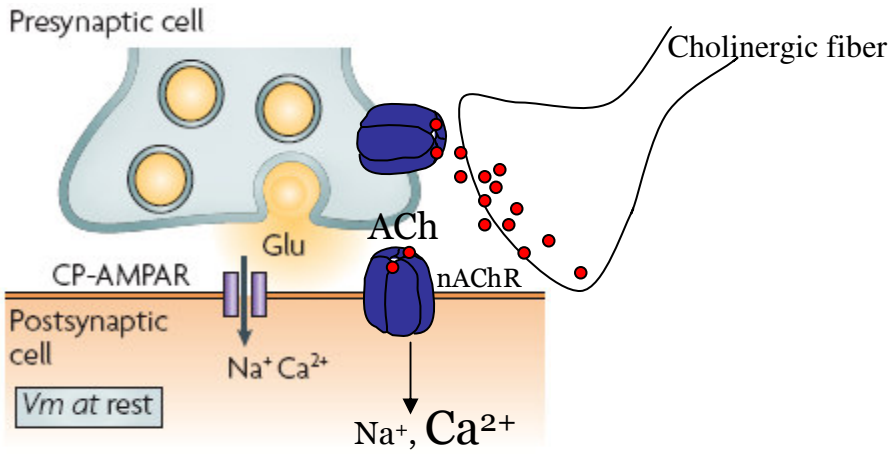
In a recent study, Jia et al. (2010) have reported that activation of non-desensitizing α2 nAChRs by nicotine facilitates the induction of a NMDA-independent form of LTP in O-LM cells voltage-clamped at -70 mV (possibly anti-Hebbian). This form of LTP persisted in the presence of ryanodine and nifedipine, indicating that calcium-induced calcium release from ryanodine-sensitive stores and voltage-dependent calcium channels were not involved. However, whether endogenous activation of nAChRs by ACh or nicotine induces similar effects remains to be elucidated.

We aim at investigating whether α7 and/or non-α7 nAChR antagonists affect the anti-Hebbian form of LTP. In affirmative case we shall identify the nAChR subtypes involved using also genetically modified mice (lacking the α7 or the β2 subunits of nAChRs). Additional experiments will be performed to see whether activation of nAChRs by endogenously released acetylcholine, following stimulation of cholinergic fibers in the alveus (in the presence of muscarinic receptor antagonists), produces similar effects. Chelating calcium in the postsynaptic cell with BAPTA will allow dissecting out pre *versus* postsynaptic expression mechanisms. A fluorimetric technique will be used to measure changes in intracellular calcium levels following LTP induction, in the absence or in the presence of selective nAChR antagonists. In additional experiments, we shall identify possible intracellular second messenger cascades activated by Ca^{2+} influx through nAChRs. Long-term changes in neuronal function often require changes in gene transcription. In cultured hippocampal neurons activation of nAChRs by nicotine has been shown to switch on the transcription factor CREB (Hu et al., 2002), which in turn activates the immediate early gene *c-fos*. This transcriptional activation requires CaMKII/IV and MAP kinases, as well as Ca^{2+} release from internal stores (Hu et al., 2002). This combination of events immediately increases phosphorylated CREB (pCREB), whose levels remain elevated for at least one hour. CREB, and in particular pCREB, has been implicated in various forms of learning and memory (Nguyen & Wo, 2003; Mizuno & Giese, 2005). Therefore, the possible involvement of CAMKII/IV and

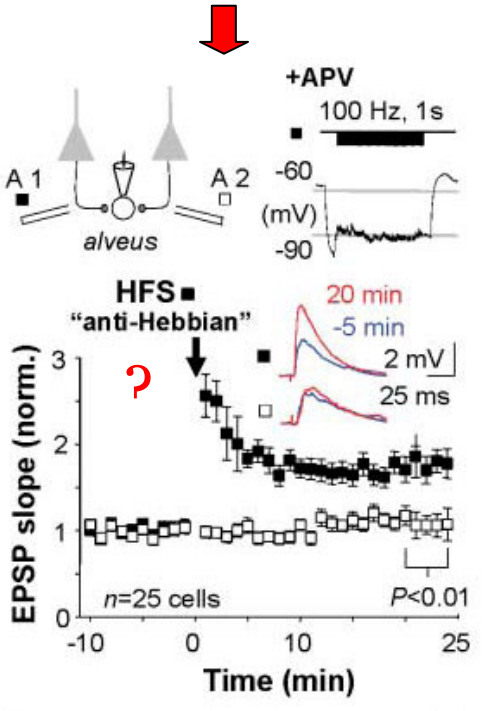
MAP kinases in nicotine-induced potentiation of anti-Hebbian LTP in O-LM cells will be tested using selective kinase inhibitors in the patch pipette.
A similar approach will be used to test the involvement of nAChRs in the Hebbian form of LTP induced by activation of mGluR, which requires a different induction protocol (see Perez et al., 2001).
These experiments may contribute to shed light on the functional role exerted by nAChRs in regulating synaptic plasticity processes and information processing in O-LM interneurons (see Figure 9).

Figure 9

First question: does Ca^{2+} entering through nAChRs modulate long-term plasticity processes in O-LM cells?



CP-AMPAR=Ca^{2+} permeable AMPA receptor



Modified from Lamsa et al., 2007

Anti-Hebbian form of LTP: high frequency stimulation paired with postsynaptic hyperpolarization

It would be of interest:

1. to repeat the same protocol in the presence of nAChR antagonists
2. to verify whether endogenously released ACh from cholinergic terminals can modulate anti-Hebbian LTP
3. to elucidate whether nAChRs are involved in other forms of LTP (Hebbian type).

Often neurons orchestrate their activity *via* gap junctions which are the structural correlates of electrical synapses in the brain (MacVicar & Dudek, 1981; Galarreta & Hestrin, 1999). The electrotonic coupling between neurons plays a significant role in neuronal oscillations (Draguhn et al., 1998; Buhl et al., 2003). Gap junctions are formed by proteins called connexins, membrane spanning proteins, six of which combine to form a hemichannel called connexon. Two connexons that span the apposing plasma membranes of two cells align to form intercellular channels, which become organized into a gap junction (White & Paul, 1999). Different connexin molecules have been identified in different tissues and among these connexin 36 is of particular interest because its expression is restricted to neurons (Condorelli et al., 1998; Sohl et al., 1998). Interestingly a recent work highlighted the role of this molecule in learning and memory processes (Frisch et al., 2005).

Different studies have evaluated the presence of gap junction between *stratum oriens* interneurons including O-LM cells (Zhang et al., 2004; Minneci et al., 2007). In particular Zhang et al., (2004) stated that the electrotonic coupling between these interneurons is due to gap junctions which connect distal dendrites. Hence, low pass filter properties of electrotonic signals *via* gap junctions would favor synchronization of O-LM cells. In a recent study Minneci et al. (2007) have clearly demonstrated that the dynamic interaction between electrically coupled O-LM interneurons, exhibiting different firing patterns, can differentially affect target cells. In the same study, these authors have found that principal cells establish reliable connections with O-LM cells, particularly efficient in the gamma frequency range. The overlapping of two type of signaling (theta and gamma) within the inhibitory network may be crucial for encoding complex information in the same way as described for short-term memory processing (Lisman and Idiart, 1995; Bragin et al. 1995).

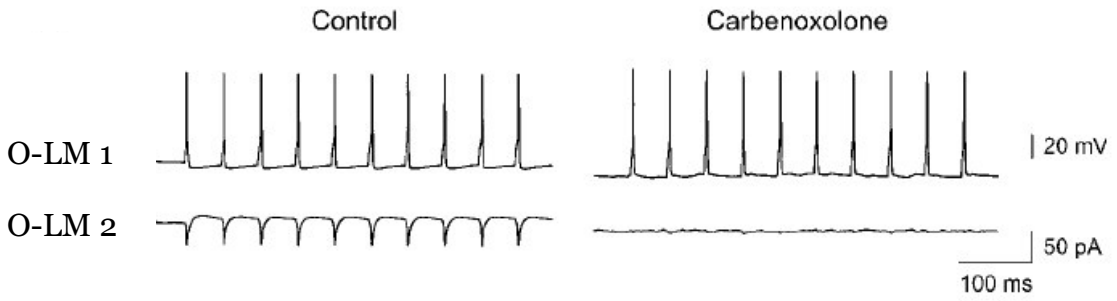
It would be of interest to study whether connexins are co-localized with nAChRs and whether the activation of nAChRs can affect the electrical coupling between O-LM cells. It has been known for long time that an increase in cytosolic Ca^{2+} can close gap junctions (Rose et al., 1977; Peracchia, 1978). Recent studies indicate that Ca^{2+} action on gap junction conductance is dependent on calmodulin, which

interacts directly with connexin subunits (DeVries, & Schwartz, 1989; Peracchia et al., 2000). Our hypothesis is that nAChR-mediated Ca^{2+} entering could change the electrotonic coupling between interneurons affecting network synchronization. Furthermore, since most mammalian gap junctions are sensitive to the voltage difference across the junctional membranes (Spray et al., 1981, Srinivas et al., 1999) the depolarizing action of nAChR activation could affect the conductance of the junctional channel. Interestingly, in a recent study on human endothelial cells, nicotine was found to down-regulate connexin gene expression (Haussing et al., 2008).

We intend to use nAChR antagonists on electrically coupled O-LM interneurons in *stratum oriens* to verify the hypothesis that endogenously released acetylcholine acting on nAChRs can modulate gap junctions. Similar experiments will be performed using low concentrations of nicotine. The coupling index between interconnected neurons will be measured before and after application of nAChR antagonists as well as the gap junction inhibitor carbenoxolone. Moreover, single cell PCR study will allow testing the possibility that nicotine affects the expression of connexin genes, like in endothelial cells (Haussing et al., 2008). Eventual changes in the electrical coupling between two O-LM cells could have important consequences on the synchronization of principal cell activity and theta oscillations (see Figure 10).

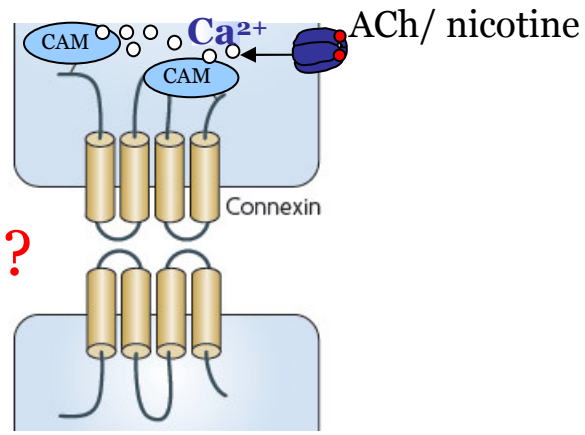
Figure 10

Second question: does nicotine via nAChRs affect the electrotonic coupling between O-LM interneurons?



Minneci et al., 2007

The rationale behind is that Ca^{2+} entering through nAChRs may reduce the electrical coupling via calmodulin (CAM)/connexin interaction



Modified from Stewart et al., 2009

.....this would lead to network desynchronization

It would be of interest to see whether:

1. application of nAChR antagonists alter the electric coupling between O-LM interneurons
2. uncoupling could be mimicked by endogenously released acetylcholine

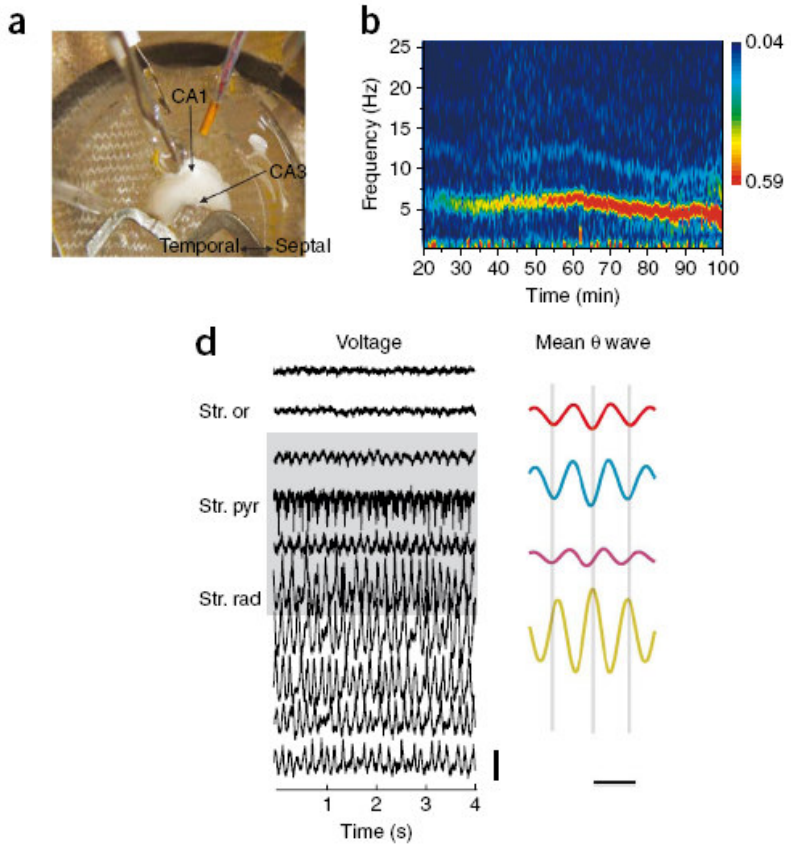
From the work of this thesis (and from the proposed experiments) it emerges that one of the main effect of nicotine, the main component of tobacco, on O-LM cells is the alteration of the firing rate which probably leads to the disruption of rhythmogenesis. This massive effect which may alter high cognitive functions occurs either dependently or independently of nAChRs activation. However, these studies have not directly addressed the effects of nicotine on rhythmic oscillations including those occurring in the theta frequency range. Therefore, it will be crucial to evaluate how nicotine affects theta oscillations at the network level.

Network oscillations have been extensively studied *in vitro*, in the hippocampal slice preparation, using pharmacological induction either with kainate or charbacol (Williams & Kauer, 1997; Glovely et al., 2005; Hájos et al., 2004). However, the *in vitro* preparation, due to the disruption of intrinsic and extrinsic network connectivity, is inadequate for this type of study. A recent work has highlighted the possibility to record self-generating theta oscillations in the intact hippocampus thus circumventing this problem (Goutagny et al. 2009). This preparation allows maintaining the integrity of all intrinsic networks, but specifically the wide branching horizontally oriented interneurons which are most likely damaged in the slice preparation (Maccaferri, 2005). Furthermore, the number of pyramidal cells is important for maintaining a tonic excitation as sparsely firing pyramidal cells may not be sufficient to consistently excite interneurons in the hippocampal slice. Thus, the intact hippocampus preparation is an ideal tool to study theta activity and its modulation.

Taking advantage of this model we will test whether stimulation of cholinergic fibers (in the presence of muscarinic antagonists) can modify theta oscillations. nAChR antagonists or the use of transgenic mice (in which α7 or β2 genes have been suppressed) would allow dissecting out the nAChR subtypes involved. The possibility that nicotine may alter the theta rhythm independently of nAChRs can be also explored (see Figure 11).

Figure 11

Intact hippocampus could be a useful tool to investigate nicotine effect on theta rhythm *in vitro*



Goutagny et al., 2009

Bibliography

Acsády L, Kamondi A, Sík A, Freund T, Buzsáki G (1998). GABAergic cells are the major postsynaptic targets of mossy fibers in the rat hippocampus. J Neurosci 18: 3386-3403.

Albuquerque EX, Pereira EF, Alkondon M, Rogers SW (2009). Mammalian nicotinic acetylcholine receptors: from structure to function. Physiol Rev 89: 73-120.

Ali AB, Thomson AM (1998). Facilitating pyramid to horizontal oriens-alveus interneurone inputs: dual intracellular recordings in slices of rat hippocampus. J Physiol 507: 185-199.

Alkondon M, Albuquerque EX (1993). Diversity of nicotinic acetylcholine receptors in rat hippocampal neurons. I. Pharmacological and functional evidence for distinct structural subtypes. J Pharmacol Exp Ther 265: 1455-1473.

Alkondon M, Albuquerque EX (2001). Nicotinic acetylcholine receptor alpha7 and alpha4beta2 subtypes differentially control GABAergic input to CA1 neurons in rat hippocampus. J Neurophysiol 86: 3043-3055.

Alkondon M, Albuquerque EX (2004). The nicotinic acetylcholine receptor subtypes and their function in the hippocampus and cerebral cortex. Prog Brain Res 145:109-120.

Andersen P, Eccles JC, Loyning Y (1964). Location of postsynaptic inhibitory synapses on hippocampal pyramids. J Neurophysiol 27: 592-607.

Ascoli GA, Alonso-Nanclares L, Anderson SA, Barrionuevo G, Benavides-Piccione R, Burkhalter A, Buzsáki G, Cauli B, Defelipe J, Fairén A, Feldmeyer D, Fishell G, Fregnac Y, Freund TF, Gardner D, Gardner EP, Goldberg JH,

Helmstaedter M, Hestrin S, Karube F, Kisvárday ZF, Lambolez B, Lewis DA, Marin O, Markram H, Muñoz A, Packer A, Petersen CC, Rockland KS, Rossier J, Rudy B, Somogyi P, Staiger JF, Tamas G, Thomson AM, Toledo-Rodriguez M, Wang Y, West DC, Yuste R. (2008). Petilla terminology: nomenclature of features of GABAergic interneurons of the cerebral cortex. Nat Rev Neurosci 9: 557-568.

Atzori M, Lau D, Tansey EP, Chow A, Ozaita A, Rudy B, McBain CJ (2000). H2 histamine receptor-phosphorylation of Kv3.2 modulates interneuron fast spiking. Nat Neurosci 3: 791-798.

Avossa D, Rosato-Siri MD, Mazzarol F, Ballerini L (2003). Spinal circuits formation: a study of developmentally regulated markers in organotypic cultures of embryonic mouse spinal cord. Neuroscience 122: 391-405.

Bartos M, Vida I, Frotscher M, Geiger JR, Jonas P (2001). Rapid signaling at inhibitory synapses in a dentate gyrus interneuron network. J Neurosci 21: 2687-2698.

Bartus RT, Dean RL 3rd, Beer B, Lippa AS (1982). The cholinergic hypothesis of geriatric memory dysfunction. Science Jul 217: 408-414.

Baude A, Nusser Z, Molnár E, McIlhinney RA, Somogyi P (1995). High-resolution immunogold localization of AMPA type glutamate receptor subunits at synaptic and non-synaptic sites in rat hippocampus. Neuroscience 69: 1031-1055.

Ben Ari Y & Cossart R (2000). Kainate, a double agent that generates seizures: two decades of progress. Trends Neurosci 23: 580-587.

Blasco-Ibáñez JM, Freund TF (1995). Synaptic input of horizontal interneurons in stratum oriens of the hippocampal CA1 subfield: structural basis of feed-back activation. Eur J Neurosci 7: 2170-2180.

Bochet P, Audinat E, Lambolez B, Crépel F, Rossier J, Iino M, Tsuzuki K, Ozawa S (1994). Subunit composition at the single-cell level explains functional properties of a glutamate-gated channel. Neuron 12: 383-388.

Bragin A, Jandó G, Nádasdy Z, Hetke J, Wise K, Buzsáki G (1995). Gamma (40-100 Hz) oscillation in the hippocampus of the behaving rat. J Neurosci 15: 47-60.

Brazhnik ES, Fox SE (1997). Intracellular recordings from medial septal neurons during hippocampal theta rhythm. Exp Brain Res 114: 442-453.

Buhl DL, Harris KD, Hormuzdi SG, Monyer H, Buzsáki G (2003). Selective impairment of hippocampal gamma oscillations in connexin-36 knock-out mouse in vivo. J Neurosci 23: 1013-1018.

Buhl EH, Halasy K, Somogyi P (1994). Diverse sources of hippocampal unitary inhibitory postsynaptic potentials and the number of synaptic release sites. Nature 368: 823-828.

Buisson B, Bertrand D (2001). Chronic exposure to nicotine upregulates the human (alpha)4((beta)2 nicotinic acetylcholine receptor function. J Neurosci 21: 1819-1829.

Bureau I, Bischoff S, Heinemann SF, Mulle C (1999). Kainate receptor-mediated responses in the CA1 field of wild-type and GluR6-deficient mice. J Neurosci 19: 653-663.

Burgess NE, (2002). The human hippocampus and spatial and episodic memory. Neuron 35: 625-641.

Buzsáki G (1984). Feed-forward inhibition in the hippocampal formation. Prog Neurobiol 22: 131-153.

Buzsáki G (1986). Hippocampal sharp waves: their origin and significance. Brain Res 398: 242-252.

Buzsáki G (2002). Theta oscillations in the hippocampus. Neuron 33: 325-340.

Buzsáki G, Chrobak JJ (1995). Temporal structure in spatially organized neuronal ensembles: a role for interneuronal networks. Curr Opin Neurobiol 5: 504-510.

Buzsáki G, Eidelberg E (1983). Phase relations of hippocampal projection cells and interneurons to theta activity in the anesthetized rat. Brain Res 266: 334-339.

Catania MV, Tölle TR, Monyer H (1995). Differential expression of AMPA receptor subunits in NOS-positive neurons of cortex, striatum, and hippocampus. J Neurosci 11: 7046-7061.

Cauli B, Audinat E, Lambolez B, Angulo MC, Ropert N, Tsuzuki K, Hestrin S, Rossier J (1997). Molecular and physiological diversity of cortical nonpyramidal cells. J Neurosci 17: 3894-3906.

Changeux JP (2010). Nicotine addiction and nicotinic receptors: lessons from genetically modified mice. Nat Rev Neurosci 11: 389-401.

Cheng L, Kinard K, Rajamani R, Sanguinetti MC (2007). Molecular mapping of the binding site for a blocker of hyperpolarization-activated, cyclic nucleotide-modulated pacemaker channels. J Pharmacol Exp Ther 322: 931-939.

Cobb SR, Buhl EH, Halasy K, Paulsen O, Somogyi P (1995). Synchronization of neuronal activity in hippocampus by individual GABAergic interneurons. Nature 378: 75-78.

Condorelli DF, Parenti R, Spinella F, Trovato Salinaro A, Belluardo N, Cardile V, Cicirata F (1998). Cloning of a new gap junction gene (Cx36) highly expressed in mammalian brain neurons. Eur J Neurosci 10: 1202-1208.

Contant C, Umbriaco D, Garcia S, Watkins KC, Descarries L (1996). Ultrastructural characterization of the acetylcholine innervation in adult rat neostriatum. Neuroscience 71: 937-947.

Corringer PJ, Le Novère N, Changeux JP (2000). Nicotinic receptors at the amino acid level. Annu Rev Pharmacol Toxicol 40: 431-458.

Cossart R, Esclapez M, Hirsch JC, Bernard C, Ben-Ari Y (1998). GluR5 kainate receptor activation in interneurons increases tonic inhibition of pyramidal cells. Nat Neurosci 1: 470-478.

Cossart R, Petanjek Z, Dumitriu D, Hirsch JC, Ben-Ari Y, Esclapez M, Bernard C (2006). Interneurons targeting similar layers receive synaptic inputs with similar kinetics. Hippocampus 16: 408-420.

DeVries SH, Schwartz EA (1989). Modulation of an electrical synapse between solitary pairs of catfish horizontal cells by dopamine and second messengers. J Physiol 414: 351-375.

Douglas RJ, Martin KA (1998). The Synaptic Organization of the Brain (ed. Shepherd, G. M.; Oxford Univ. Press, Oxford,) 459-511.

Dragoi G, Harris KD, Buzsáki G (2003). Place representation within hippocampal networks is modified by long-term potentiation. Neuron 39: 843-853.

Draguhn A, Traub RD, Schmitz D, Jefferys JG (1998). Electrical coupling underlies high-frequency oscillations in the hippocampus in vitro. Nature 394: 189-192.

Dutar P, Bassant MH, Senut MC, Lamour Y (1995). The septohippocampal pathway: structure and function of a central cholinergic system. Physiol Rev 75: 393-427.

Everitt, BJ & Robbins (1997). Central cholinergic systems and cognition. Annu Rev Psycho 48: 649-684.

Fabian-Fine R, Skehel P, Errington ML, Davies HA, Sher E, Stewart MG, Fine A (2001). Ultrastructural distribution of the alpha7 nicotinic acetylcholine receptor subunit in rat hippocampus. J Neurosci 21: 7993-8003.

Fellous JM, Sejnowski TJ (2000). Cholinergic induction of oscillations in the hippocampal slice in the slow (0.5-2 Hz), theta (5-12 Hz), and gamma (35-70 Hz) bands. Hippocampus 10: 187-197.

Fenster CP, Whitworth TL, Sheffield EB, Quick MW, Lester RA (1999). Upregulation of surface alpha4beta2 nicotinic receptors is initiated by receptor desensitization after chronic exposure to nicotine. J Neurosci 19: 4804-4814.

Fox SE (1989). Membrane potential and impedance changes in hippocampal pyramidal cells during theta rhythm. Exp Brain Res 77: 283-294.

Fox SE, Wolfson S, Ranck JB Jr (1986). Hippocampal theta rhythm and the firing of neurons in walking and urethane anesthetized rats. Exp Brain Res 62: 495-508.

Frazier CJ, Buhler AV, Weiner JL, Dunwiddie TV (1998b). Synaptic potentials mediated via alpha-bungarotoxin-sensitive nicotinic acetylcholine receptors in rat hippocampal interneurons. J Neurosci 18: 8228-8235.

Frazier CJ, Rollins YD, Breese CR, Leonard S, Freedman R, Dunwiddie TV (1998a). Acetylcholine activates an alpha-bungarotoxin-sensitive nicotinic

current in rat hippocampal interneurons, but not pyramidal cells. J Neurosci 18: 1187-1195.

Freund TF (2003). Interneuron diversity series: Rhythm and mood in perisomatic inhibition. Trend Neurosci 26: 489-495.

Freund TF, Buzsáki G (1996). Interneurons of the hippocampus. Hippocampus 6: 347-470.

Frisch C, De Souza-Silva MA, Söhl G, Güldenagel M, Willecke K, Huston JP, Dere E (2005). Stimulus complexity dependent memory impairment and changes in motor performance after deletion of the neuronal gap junction protein connexin36 in mice. Behav Brain Res 157: 177-185.

Fucile S (2004). Ca2+ permeability of nicotinic acetylcholine receptors. Cell Calcium 35: 1-8.

Fujii S, Ji Z, Morita N, Sumikawa K (1999). Acute and chronic nicotine exposure differentially facilitate the induction of LTP. Brain Res 846: 137-143.

Fyhn M, Molden S, Witter MP, Moser EI, Moser MB (2004). Spatial representation in the entorhinal cortex. Science 27 :1258-1264.

Gage FH, Björklund A, Stenevi U (1984). Cells of origin of the ventral cholinergic septohippocampal pathway undergoing compensatory collateral sprouting following fimbria-fornix transection. Neurosci Lett 44: 211-216.

Galarreta M, Hestrin S (1999). A network of fast-spiking cells in the neocortex connected by electrical synapses. Nature 402: 72-75.

Gao B, Fritschy JM (1994). Selective allocation of GABAA receptors containing the alpha 1 subunit to neurochemically distinct subpopulations of rat hippocampal interneurons. Eur J Neurosci 6: 837-853.

Gaykema RP, van der Kuil J, Hersh LB, Luiten PG (1991). Patterns of direct projections from the hippocampus to the medial septum-diagonal band complex: anterograde tracing with Phaseolus vulgaris leucoagglutinin combined with immunohistochemistry of choline acetyltransferase. Neuroscience 43: 349-360.

Geiger JR, Melcher T, Koh DS, Sakmann B, Seeburg PH, Jonas P, Monyer H (1995). Relative abundance of subunit mRNAs determines gating and Ca2+ permeability of AMPA receptors in principal neurons and interneurons in rat CNS. Neuron 15: 193-204.

Gillies MJ, Traub RD, LeBeau FE, Davies CH, Gloveli T, Buhl EH, Whittington MA (2002). A model of atropine-resistant theta oscillations in rat hippocampal area CA1. J Physiol 543: 779-793.

Giniatullin R, Nistri A, Yakel JL (2005). Desensitization of nicotinic ACh receptors: shaping cholinergic signaling. Trends Neurosci 28: 371-378.

Giorgetti A, Carloni P, Mistrik P, Torre V (2005). A homology model of the pore region of HCN channels. Biophys J 89: 932-944.

Gloveli T, Dugladze T, Saha S, Monyer H, Heinemann U, Traub RD, Whittington MA, Buhl EH (2005). Differential involvement of oriens/pyramidale interneurones in hippocampal network oscillations in vitro. J Physiol 562: 131-147.

Goldin M, Epsztein J, Jorquera I, Represa A, Ben-Ari Y, Crépel V, Cossart R (2007). Synaptic kainate receptors tune oriens-lacunosum moleculare interneurons to operate at theta frequency. J Neurosci 27: 9560-9572.

Gorelova N, Seamans JK, Yang CR (2002). Mechanisms of dopamine activation of fast-spiking interneurons that exert inhibition in rat prefrontal cortex. J Neurophysiol 88: 3150-3166.

Goutagny R, Jackson J, Williams S (2009). Self-generated theta oscillations in the hippocampus. Nat Neurosci 12: 1491-1493.

Gray R, Rajan AS, Radcliffe KA, Yakehiro M, Dani JA (1996). Hippocampal synaptic transmission enhanced by low concentrations of nicotine. Nature 383: 713-716.

Gulyas AI, Megias M, Emrci Z, Freund TF (1999). Total number and ratio of excitatory and inhibitory synapses converging onto single interneurons of different types in the CA1 area of the rat hippocampus. J Neurosci 19: 10082-10097.

Gulyás AI, Miles R, Sík A, Tóth K, Tamamaki N, Freund TF (1993). Hippocampal pyramidal cells excite inhibitory neurons through a single release site. Nature 366: 683-687.

Hafting T, Fyhn M, Molden S, Moser MB, Moser EI (2005). Microstructure of a spatial map in the entorhinal cortex. Nature 11: 801-806.

Hájos N, Pálhalmi J, Mann EO, Németh B, Paulsen O, Freund TF (2004). Spike timing of distinct types of GABAergic interneuron during hippocampal gamma oscillations in vitro. J Neurosci 24: 9127-9137.

Halasy K, Buhl EH, Lorinczi Z, Tamas G & Somogyi P (1996). Synaptic target selectivity and input of GABAergic basket and bistratified interneurons in the CA1 area of the rat hippocampus. Hippocampus 6: 306-329.

Han ZS, Buhl EH, Lörinczi Z, Somogyi P (1993). A high degree of spatial selectivity in the axonal and dendritic domains of physiologically identified local-circuit neurons in the dentate gyrus of the rat hippocampus. Eur J Neurosci 5: 395-410.

Haussig S, Schubert A, Mohr FW, Dhein S (2008). Sub-chronic nicotine exposure induces intercellular communication failure and differential down-

regulation of connexins in cultured human endothelial cells. Atherosclerosis 196: 210-218.

Hestrin S & Galarreta M (2005). Synchronous versus asynchronous transmitter release: a tale of two types of inhibitory neurons. Nat Neurosci 8: 1283-1284.

Hestrin S (1993). Different glutamate receptor channels mediate fast excitatory synaptic currents in inhibitory and excitatory cortical neurons. Neuron 11: 1083-1091.

Höhmann CF, Ebner FF (1985). Development of cholinergic markers in mouse forebrain. I. Choline acetyltransferase enzyme activity and acetylcholinesterase histochemistry. Brain Res 355: 225-241.

Hökfelt T, Lundberg JM, Schultzberg M, Johansson O, Skirboll L, Anggård A, Fredholm B, Hamberger B, Pernow B, Rehfeld J, Goldstein M (1980). Cellular localization of peptides in neural structures. Proc R Soc Lond B Biol Sci 210: 63-77.

Hormuzdi SG, Pais I, LeBeau FE, Towers SK, Rozov A, Buhl EH, Whittington MA, Monyer H (2001). Impaired electrical signaling disrupts gamma frequency oscillations in connexin 36-deficient mice. Neuron 31: 487-495.

Houser CR, Olsen RW, Richards JG, Möhler H (1988). Immunohistochemical localization of benzodiazepine/GABAA receptors in the human hippocampal formation. J Neurosci 8: 1370-1383.

Hu M, Liu QS, Chang KT, Berg DK (2002). Nicotinic regulation of CREB activation in hippocampal neurons by glutamatergic and nonglutamatergic pathways. Mol Cell Neurosci 21: 616-625.

Huerta PT, Lisman JE (1995). Bidirectional synaptic plasticity induced by a single burst during cholinergic theta oscillation in CA1 in vitro. Neuron 5: 1053-1063.

Hutcheon B, Yarom Y (2000). Resonance, oscillation and the intrinsic frequency preferences of neurons. Trends Neurosci 23: 216-222.

Janigro D, Martenson ME, BaumannTK (1997). Preferential inhibition of Ih in rat trigeminal ganglion neurons by an organic blocker. J Membr Biol 160: 101-109.

Ji D, Lape R, Dani JA (2001). Timing and location of nicotinic activity enhances or depresses hippocampal synaptic plasticity. Neuron 31:131-141

Jia Y, Yamazaki Y, Nakauchi S, Ito K, Sumikawa K (2010). Nicotine facilitates long-term potentiation induction in oriens-lacunosum moleculare cells via Ca2+ entry through non-alpha7 nicotinic acetylcholine receptors. Eur J Neurosci 31: 463-476.

Jia Y, Yamazaki Y, Nakauchi S, Sumikawa K (2009). Alpha2 nicotine receptors function as a molecular switch to continuously excite a subset of interneurons in rat hippocampal circuits. Eur J Neurosci 29: 1588-1603.

Jiang Y, Lee A, Chen J, Cadene M, Chait BT, MacKinnon R (2002). Crystal structure and mechanism of a calcium-gated potassium channel. Nature 417: 515-522.

Johnston D & Amaral DG (1998). Hippocampus. In “The synaptic organization of the brain” (ed. by G.M Shepherd). Oxford University Press.

Jonas P, Major G, Sakmann B (1993). Quantal components of unitary EPSCs at the mossy fibre synapse on CA3 pyramidal cells of rat hippocampus. J Physiol 472:615-663.

Jonas P, Racca C, Sakmann B, Seeburg PH, Monyer H (1994). Differences in Ca^{2+} permeability of AMPA-type glutamate receptor channels in neocortical neurons caused by differential GluR-B subunit expression. Neuron 12: 1281-1289.

Jones S, Yakel JL (1997). Functional nicotinic ACh receptors on interneurones in the rat hippocampus. J Physiol 504: 603-610.

Jouvet M (1969). Biogenic amines and the states of sleep. Science 862: 32-41.

Kamiya H, Shinozaki H & Yamamoto C (1996). Activation of metabotropic glutamate receptor type 2/3 suppresses transmission at rat hippocampal mossy fibre synapses. J Physiol 493: 447-455.

Kamondi A, Acsády L, Buzsáki G (1998). Dendritic spikes are enhanced by cooperative network activity in the intact hippocampus. J Neurosci 18: 3919-3928.

Kandel ER (2001). The molecular biology of memory storage: a dialogue between genes and synapses. Science 294:1030-1038.

Karlin A, Cox RN, Dipaola M, Holtzman E, Kao PN, Lobel P, Wang L, Yodh N (1986). Functional domains of the nicotinic acetylcholine receptor. Ann N Y Acad Sci 463: 53-69

Katona I, Acsády L, Freund TF (1999). Postsynaptic targets of somatostatin-immunoreactive interneurons in the rat hippocampus. Neuroscience 88: 37-55.

Katz B, Thesleff S (1957). A study of the 'desensitization' produced by acetylcholine at the motor end-plate. J Physiol (I957) I38: 63-80.

Khiroug L, Giniatullin R, Klein RC, Fayuk D, Yakel JL (2003). Functional mapping and Ca2+ regulation of nicotinic acetylcholine receptor channels in rat hippocampal CA1 neurons. J Neurosci 23: 9024-9031.

Kim JJ and Baxter MG (2001). Multiple brain-memory systems: the whole does not equal the sum of its parts. Trends Neurosci 24: 324-330.

Klausberger T & Somogyi P (2008). Neuronal diversity and Temporal Dynamics: The Unity of Hippocampal Circuit Operations. Science 321: 53-57.

Klausberger T, Magill PJ, Márton LF, Roberts JD, Cobden PM, Buzsáki G, Somogyi P (2003). Brain-state- and cell-type-specific firing of hippocampal interneurons in vivo. Nature 421: 844-848.

Klausberger T, Marton LF, Baude A, Roberts JD, Magill PJ & Somogyi P (2004). Spike timing of dendrite-targeting bistratified cells during hippocampal network oscillations in vivo. Nat Neurosci 7: 41-47.

Kosaka T, Katsumaru H, Hama K, Wu JY, Heizmann CW (1987). GABAergic neurons containing the Ca^{2+}-binding protein parvalbumin in the rat hippocampus and dentate gyrus. Brain Res 419: 119-130.

Kullmann DM, Perkel DJ, Manabe T, Nicoll RA (1992). Ca^{2+} entry via postsynaptic voltage-sensitive Ca^{2+} channels can transiently potentiate excitatory synaptic transmission in the hippocampus. Neuron 9: 1175-1183.

Lacaille JC, Mueller AL, Kunkel DD, Schwartzkroin PA (1987). Local circuit interactions between oriens/alveus interneurons and CA1 pyramidal cells in hippocampal slices: electrophysiology and morphology. J Neurosci 7: 1979-1993.

Lamsa K, Heeroma JH, Kullmann DM (2005). Hebbian LTP in feed-forward inhibitory interneurons and the temporal fidelity of input discrimination. Nat Neurosci 8: 916-924.

Lamsa K, Irvine EE, Giese KP, Kullmann DM (2007b). NMDA receptor-dependent long-term potentiation in mouse hippocampal interneurons shows a unique dependence on Ca(2+)/calmodulin-dependent kinases. J Physiol 584: 885-894.

Lamsa KP, Heeroma JH, Somogyi P, Rusakov DA, Kullmann DM (2007). Anti-Hebbian long-term potentiation in the hippocampal feedback inhibitory circuit. Science 315: 1262-1266.

Larson J, Lynch G (1986). Induction of synaptic potentiation in hippocampus by patterned stimulation two events. Science 232: 985-988.

Lawrence JJ, Grinspan ZM, Statland JM, McBain CJ (2006). Muscarinic receptor activation tunes mouse stratum oriens interneurones to amplify spike reliability. J Physiol 571: 555-562.

Lawrence JJ, Saraga F, Churchill JF, Statland JM, Travis KE, Skinner FK, McBain CJ (2006). Somatodendritic Kv7/KCNQ/M channels control interspike interval in hippocampal interneurons. J Neurosci 26: 12325-12338.

Le Magueresse C, Cherubini E (2007). Presynaptic calcium stores contribute to nicotine-elicited potentiation of evoked synaptic transmission at CA3-CA1 connections in the neonatal rat hippocampus. Hippocampus 17: 316-325.

Le Magueresse C, Safiulina V, Changeux JP, Cherubini E (2006). Nicotinic modulation of network and synaptic transmission in the immature hippocampus investigated with genetically modified mice. J Physiol 576: 533-546.

Lee MG, Chrobak JJ, Sik A, Wiley RG, Buzsáki G (1994). Hippocampal theta activity following selective lesion of the septal cholinergic system. Neuroscience 62: 1033-1047.

Leranth C, Szeidemann Z, Hsu M, Buzsáki G (1996). AMPA receptors in the rat and primate hippocampus: a possible absence of GluR2/3 subunits in most interneurons. Neuroscience 70: 631-652.

Leung LS, Yim CY (1986). Intracellular records of theta rhythm in hippocampal CA1 cells of the rat. Brain Res 367: 323-327.

Leung LW (1984). Model of gradual phase shift of theta rhythm in the rat. J Neurophysiol 52: 1051-65.

Lien CC, Jonas P (2003). Kv3 potassium conductance is necessary and kinetically optimized for high-frequency action potential generation in hippocampal interneurons. J Neurosci 23: 2058-2068.

Lien CC, Martina M, Schultz JH, Ehmke H, Jonas P (2002). Gating, modulation and subunit composition of voltage-gated K(+) channels in dendritic inhibitory interneurones of rat hippocampus. J Physiol 538: 405-419.

Lisman JE, Idiart MA (1995). Storage of 7 +/- 2 short-term memories in oscillatory subcycles. Science 267: 1512-1515.

Lorente de No R (1934). Studies on the structure of the cerebral cortex – II. Continuation of the study of the ammonic system. J Psychol 46: 113-177.

Losonczy A, Zhang L, Shigemoto R, Somogyi P, Nusser Z (2002). Cell type dependence and variability in the short-term plasticity of EPSCs in identified mouse hippocampal interneurones. J Physiol 542: 193-210.

Lu CB, Henderson Z (2010). Nicotine induction of theta frequency oscillations in rodent hippocampus in vitro. Neuroscience 166: 84-93.

Lukas RJ, Changeux JP, Le Novère N, Albuquerque EX, Balfour DJ, Berg DK, Bertrand D, Chiappinelli VA, Clarke PB, Collins AC, Dani JA, Grady SR, Kellar KJ, Lindstrom JM, Marks MJ, Quik M, Taylor PW, Wonnacott S (1999). International Union of Pharmacology. XX. Current status of the nomenclature for nicotinic acetylcholine receptors and their subunits. Pharmacol Rev 51: 397-401.

Lupica CR, Bell JA, Hoffman AF, Watson PL (2001). Contribution of the hyperpolarization-activated current (I(h)) to membrane potential and GABA release in hippocampal interneurons. J Neurophysiol 86: 261-268.

Maccaferri G (2005). Stratum oriens horizontal interneurone diversity and hippocampal network dynamics. J Physiol 562: 73-80.

Maccaferri G and Lacaille GC (2003). Interneuron Diversity series: Hippocampal interneuron classifications – making things as simple as possible, not simpler. Trends in Neurosci 26: 564-571.

Maccaferri G, McBain CJ (1995). Passive propagation of LTD to stratum oriens-alveus inhibitory neurons modulates the temporoammonic input to the hippocampal CA1 region. Neuron 15: 137-145.

Maccaferri G, McBain CJ (1996). Long-term potentiation in distinct subtypes of hippocampal nonpyramidal neurons. J Neurosci 16: 5334-5343.

Maccaferri G, McBain CJ (1996). The hyperpolarization-activated current (Ih) and its contribution to pacemaker activity in rat CA1 hippocampal stratum oriens-alveus interneurones. J Physiol 497: 119-130.

Maccaferri G, Roberts JD, Szucs P, Cottingham CA, Somogyi P (2000). Cell surface domain specific postsynaptic currents evoked by identified GABAergic neurones in rat hippocampus in vitro. J Physiol 524: 91-116.

MacVicar BA, Dudek FE (1981). Electrotonic coupling between pyramidal cells: a direct demonstration in rat hippocampal slices. Science 213: 782-785.

Magee JC, Christofi G, Miyakawa H, Christie B, Lasser-Ross N, Johnston D (1995). Subthreshold synaptic activation of voltage-gated Ca2+ channels mediates a localized Ca2+ influx into the dendrites of hippocampal pyramidal neurons. J Neurophysiol 74: 1335-1342.

Maggi L, Le Magueresse C, Changeux JP, Cherubini E (2003). Nicotine activates immature "silent" connections in the developing hippocampus. Proc Natl Acad Sci U S A 100: 2059-2064.

Maggi L, Sher E, Cherubini E (2001). Regulation of GABA release by nicotinic acetylcholine receptors in the neonatal rat hippocampus. J Physiol 536: 89-100.

Maggi L, Sola E, Minneci F, Le Magueresse C, Changeux JP, Cherubini E (2004) Persistent decrease in synaptic efficacy induced by nicotine at Schaffer collateral-CA1 synapses in the immature rat hippocampus. J Physiol 559: 863-874.

Mann EO, Greenfield SA (2003). Novel modulatory mechanisms revealed by the sustained application of nicotine in the guinea-pig hippocampus in vitro. J Physiol 551: 539-50.

Martin LJ, Blackstone CD, Huganir RL, Price DL (1992). Cellular localization of a metabotropic glutamate receptor in rat brain. Neuron 9: 259-270.

Martina M, Vida I, Jonas P (2000). Distal initiation and active propagation of action potentials in interneuron dendrites. Science 287: 295-300.

McBain CJ, Fisahn A (2001) Interneurons unbound. Nat Rev Neurosci 2: 11-23.

McBain CJ, DiChiara TJ, Kauer JA (1994). Activation of metabotropic glutamate receptors differentially affects two classes of hippocampal interneurons and potentiates excitatory synaptic transmission J Neurosci 14: 4433-4445.

McQuiston AR, Madison DV (1999). Nicotinic receptor activation excites distinct subtypes of interneurons in the rat hippocampus. J Neurosci 19: 2887-2896.

Miles R & Wong RK (1986). Excitatory synaptic interactions between CA3 neurones in the guinea-pig hippocampus. J Physiol 373: 397-418.

Miles R, Tóth K, Gulyás AI, Hájos N, Freund TF (1996). Differences between somatic and dendritic inhibition in the hippocampus. Neuron 16: 815-823.

Milner B et al. (1998). Cognitive neuroscience and the study of memory. Neuron 20:445-468.

Milner B, Squire LR, Kandel ER (1998). Cognitive neuroscience and the study of memory. Neuron 20:445-468.

Milner TA, Amaral DG (1984). Evidence for a ventral septal projection to the hippocampal formation of the rat. Exp Brain Res 55: 579-585.

Minneci F, Janahmadi M, Migliore M, Dragicevic N, Avossa D, Cherubini E (2007). Signaling properties of stratum oriens interneurons in the hippocampus of transgenic mice expressing EGFP in a subset of somatostatin-containing cells. Hippocampus 17: 538-553.

Mizuno K, Giese KP (2005). Hippocampus-dependent memory formation: do memory type-specific mechanisms exist? J Pharmacol Sci 98: 191-197.

Morin F, Beaulieu C, Lacaille JC (1996). Membrane properties and synaptic currents evoked in CA1 interneuron subtypes in rat hippocampal slices. J Neurophysiol 76: 1-16.

Mulle C, Sailer A, Swanson GT, Brana C, O'Gorman S, Bettler B, Heinemann SF (2000). Subunit composition of kainate receptors in hippocampal interneurons. Neuron 28: 475-484.

Murthy VN, Fetz EE (1992). Coherent 25- to 35-Hz oscillations in the sensorimotor cortex of awake behaving monkeys. Proc Natl Acad Sci U S A 89: 5670-5674.

Narayanan R, Johnston D (2007). Long-term potentiation in rat hippocampal neurons is accompanied by spatially widespread changes in intrinsic oscillatory dynamics and excitability. Neuron 56: 1061-1075.

Nelson ME, Kuryatov A, Choi CH, Zhou Y, Lindstrom J (2003). Alternate stoichiometries of alpha4beta2 nicotinic acetylcholine receptors. Mol Pharmacol 63: 332-341.

Newhouse PA, Potter A, Singh A (2004). Effects of nicotinic stimulation on cognitive performance. Curr Opin Pharmacol 4: 36-46.

Nguyen PV, Woo NH (2003). Regulation of hippocampal synaptic plasticity by cyclic AMP-dependent protein kinases. Prog Neurobiol 71: 401-437.

Nusser Z, Roberts JD, Baude A, Richards JG, Sieghart W, Somogyi P (1995). Immunocytochemical localization of the alpha 1 and beta 2/3 subunits of the GABAA receptor in relation to specific GABAergic synapses in the dentate gyrus. Eur J Neurosci 7: 630-646.

Nyakas C, Luiten PG, Spencer DG, Traber J (1987). Detailed projection patterns of septal and diagonal band efferents to the hippocampus in the rat with

emphasis on innervation of CA1 and dentate gyrus. Brain Res Bull 18: 533-545.

O'Keefe J (1983). Two spatial systems in the rat brain-implications for the neural basis of learning and memory. Prog Brain Res 58:453-464.

O'Keefe J, Recce ML (1993). Phase relationship between hippocampal place units and the EEG theta rhythm. Hippocampus 3: 317-330.

Oliva AA Jr, Jiang M, Lam T, Smith KL, Swann JW (2000). Novel hippocampal interneuronal subtypes identified using transgenic mice that express green fluorescent protein in GABAergic interneurons. J Neurosci 20: 3354-3368.

Oren I, Mann EO, Paulsen O, Hájos N (2006). Synaptic currents in anatomically identified CA3 neurons during hippocampal gamma oscillations in vitro. J Neurosci 26: 9923-9934.

Oren I, Nissen W, Kullmann DM, Somogyi P, Lamsa KP (2009). Role of ionotropic glutamate receptors in long-term potentiation in rat hippocampal CA1 oriens-lacunosum moleculare interneurons. J Neurosci 29: 939-950.

Ouardouz M, Lacaille JC (1995). Mechanisms of selective long-term potentiation of excitatory synapses in stratum oriens/alveus interneurons of rat hippocampal slices. J Neurophysiol 73: 810-819.

Paradiso KG, Steinbach JH (2003). Nicotine is highly effective at producing desensitization of rat alpha4beta2 neuronal nicotinic receptors. J Physiol 553: 857-871.

Paterson D, Nordberg A (2000). Neuronal nicotinic receptors in the human brain Prog Neurobiol 61: 75-111.

Peracchia C (1978). Calcium effects on gap junction structure and cell coupling. Nature 271: 669-671.

Peracchia C, Wang XG, Peracchia LL (2000). Slow gating of gap junction channels and calmodulin. J Membr Biol 178: 55-70.

Perez Y, Morin F, Lacaille JC (2001). A hebbian form of long-term potentiation dependent on mGluR1a in hippocampal inhibitory interneurons. Proc Natl Acad Sci U S A 98: 9401-9406.

Perry E, Martin-Ruiz C, Lee M, Griffiths M, Johnson M, Piggott M, Haroutunian V, Buxbaum JD, Nãsland J, Davis K, Gotti C, Clementi F, Tzartos S, Cohen O, Soreq H, Jaros E, Perry R, Ballard C, McKeith I, Court J (2000). Nicotinic receptor subtypes in human brain ageing, Alzheimer and Lewy body diseases. Eur J Pharmacol 393: 215-222.

Pike FG, Goddard RS, Suckling JM, Ganter P, Kasthuri N, Paulsen O (2000). Distinct frequency preferences of different types of rat hippocampal neurones in response to oscillatory input currents. J Physiol 529: 205-213.

Pouille F, Scanziani M (2001). Enforcement of temporal fidelity in pyramidal cells by somatic feed-forward inhibition. Science 293: 1159-1163.

Pouille F, Scanziani M (2004). Routing of spike series by dynamic circuits in the hippocampus. Nature 429: 717-723.

Puil E, Gimbarzevsky B, Miura RM (1986). Quantification of membrane properties of trigeminal root ganglion neurons in guinea pigs. J Neurophysiol 55: 995-1016.

Ramon y Cajal S (1893). *Estructura del asta de Ammon y fascia dentate*. Anat. de la Socied. Espan. de Historia natural t. XXII (Ann Soc Esp Hist Nat 22).

Ramón y Cajal S (1911). *Histologie de systeme nerveux de l'Homme et des vertebras*. tome II. Maloine, Paris.

Ribak CE, Vaughn JE, Saito K. (1978). Immunocytochemical localization of glutamic acid decarboxylase in neuronal somata following colchicine inhibition of axonal transport. Brain Res 140: 315-332.

Richards JG, Schoch P, Häring P, Takacs B, Möhler H (1987). Resolving GABAA/benzodiazepine receptors: cellular and subcellular localization in the CNS with monoclonal antibodies. J Neurosci 7: 1866-1886.

Richards KS, Bommert K, Szabo G, Miles R (2007). Differential expression of Na+/K+-ATPase alpha-subunits in mouse hippocampal interneurones and pyramidal cells. J Physiol 585: 491-505.

Role LW, Berg DK (1996). Nicotinic receptors in the development and modulation of CNS synapses. Neuron 16: 1077-1085.

Rose B, Simpson I, Loewenstein WR (1977). Calcium ion produces graded changes in permeability of membrane channels in cell junction. Nature 267: 625-627.

Sah P (1996). Ca(2+)-activated K+ currents in neurones: types, physiological roles and modulation. Trends Neurosci 19: 150-154.

Savić N, Pedarzani P, Sciancalepore M (2001). Medium afterhyperpolarization and firing pattern modulation in interneurons of stratum radiatum in the CA3 hippocampal region. J Neurophysiol 85: 1986-1997.

Schreiber S, Fellous JM, Tiesinga P, Sejnowski TJ (2004). Influence of ionic conductances on spike timing reliability of cortical neurons for suprathreshold rhythmic inputs. J Neurophysiol 91: 194-205.

Séguéla P, Wadiche J, Dineley-Miller K, Dani JA, Patrick JW (1993). Molecular cloning, functional properties, and distribution of rat brain alpha 7: a nicotinic cation channel highly permeable to calcium. J Neurosci 13: 596-604.

Seress L, Ribak CE (1983). GABAergic cells in the dentate gyrus appear to be local circuit and projection neurons. Exp Brain Res 50: 173-182.

Shacka JJ, Robinson SE (1998). Postnatal developmental regulation of neuronal nicotinic receptor subunit alpha 7 and multiple alpha 4 and beta 2 mRNA species in the rat. Brain Res Dev Brain Res 109: 67-75.

Siok CJ, Rogers JA, Kocsis B, Hajós M (2006). Activation of alpha7 acetylcholine receptors augments stimulation-induced hippocampal theta oscillation. Eur J Neurosci 23: 570-574.

Söhl G, Degen J, Teubner B, Willecke K (1998). The murine gap junction gene connexin36 is highly expressed in mouse retina and regulated during brain development. FEBS Lett 428: 27-31.

Soltesz I, Deschênes M (1993). Low- and high-frequency membrane potential oscillations during theta activity in CA1 and CA3 pyramidal neurons of the rat hippocampus under ketamine-xylazine anesthesia. J Neurophysiol 70: 97-116.

Somogyi P & Klausberger T (2005). Defined types of cortical interneurone structure space and spike timing in the hippocampus. J Physiol 562: 9-26.

Somogyi P, Tamás G, Lujan R, Buhl EH (1998). Salient features of synaptic organisation in the cerebral cortex. Brain Res Brain Res Rev 26: 113-135.

Son JH, Winzer-Serhan UH (2008). Expression of neuronal nicotinic acetylcholine receptor subunit mRNAs in rat hippocampal GABAergic interneurons. J Comp Neurol 511: 286-299.

Spray DC, Harris AL, Bennett MV (1981). Equilibrium properties of a voltage-dependent junctional conductance. J Gen Physiol 77: 77-93.

Srinivas M, Rozental R, Kojima T, Dermietzel R, Mehler M, Condorelli DF, Kessler JA, Spray DC (1999). Functional properties of channels formed by the neuronal gap junction protein connexin36. J Neurosci 19: 9848-9855.

Steriade M, McCormick DA, Sejnowski TJ (1993). Thalamocortical oscillations in the sleeping and aroused brain. Science 262: 679-685.

Stewart M, Fox SE (1990). Firing relations of lateral septal neurons to the hippocampal theta rhythm in urethane anesthetized rats. Exp Brain Res 79: 92-96.

Storm-Mathisen J, Leknes AK, Bore AT, Vaaland JL, Edminson P, Haug FM, Ottersen OP (1983). First visualization of glutamate and GABA in neurones by immunocytochemistry. Nature 301: 517-520.

Sudweeks SN, Yakel JL (2000). Functional and molecular characterization of neuronal nicotinic ACh receptors in rat CA1 hippocampal neurons. J Physiol 527: 515-528.

Svoboda KR, Lupica CR (1998). Opioid inhibition of hippocampal interneurons via modulation of potassium and hyperpolarization-activated cation (Ih) currents. J Neurosci 18: 7084-7098.

Tan Y, Hori N & Carpenter DO (2006). Electrophysiological effects of three groups of glutamate metabotropic receptors in rat piriform cortex. Cell Mol Neurobiol 26: 915-924.

Taverna S, Tkatch T, Metz AE, Martina M (2005). Differential expression of TASK channels between horizontal interneurons and pyramidal cells of rat hippocampus. J Neurosci 25: 9162-9170.

Topolnik L, Congar P, Lacaille JC (2005). Differential regulation of metabotropic glutamate receptor- and AMPA receptor-mediated dendritic Ca2+ signals by presynaptic and postsynaptic activity in hippocampal interneurons. J Neurosci 25: 990-1001.

Tóth K & Freund TF (1992). Calbindin D28k-containing nonpyramidal cells in the rat hippocampus: their immunoreactivity for GABA and projection to the medial septum. Neuroscience 49: 793-805.

Tóth K, Borhegyi Z, Freund TF (1993). Postsynaptic targets of GABAergic hippocampal neurons in the medial septum-diagonal band of broca complex. J Neurosci 13: 712-724.

Tóth K, Freund TF, Miles R (1997). Disinhibition of rat hippocampal pyramidal cells by GABAergic afferents from the septum. J Physiol 500: 463-474.

Tóth K, McBain CJ (1998). Afferent-specific innervation of two distinct AMPA receptor subtypes on single hippocampal interneurons. Nat Neurosci 7: 572-578.

Traub RD, Miles R (1991). Multiple modes of neuronal population activity emerge after modifying specific synapses in a model of the CA3 region of the hippocampus. Ann N Y Acad Sci 627: 277-290.

Traub RD, Bibbig A, Fisahn A, LeBeau FE, Whittington MA, Buhl EH (2000). A model of gamma-frequency network oscillations induced in the rat CA3 region by carbachol in vitro. Eur J Neurosci 12: 4093-4106.

Tribollet E, Bertrand D, Marguerat A, Raggenbass M (2004). Comparative distribution of nicotinic receptor subtypes during development, adulthood and aging: an autoradiographic study in the rat brain. Neuroscience 124: 405-420.

Tsubokawa H, Ross WN (1996). IPSPs modulate spike backpropagation and associated $[Ca2+]_i$ changes in the dendrites of hippocampal CA1 pyramidal neurons. J Neurophysiol 76: 2896-28906.

Umbriaco D, Garcia S, Beaulieu C, Descarries L (1995). Relational features of acetylcholine, noradrenaline, serotonin and GABA axon terminals in the stratum radiatum of adult rat hippocampus (CA1). Hippocampus 5: 605-620.

Umbriaco D, Watkins KC, Descarries L, Cozzari C, Hartman BK (1994). Ultrastructural and morphometric features of the acetylcholine innervation in adult rat parietal cortex: an electron microscopic study in serial sections. J Comp Neurol 348: 351-373.

Vanderwolf CH (1969). Hippocampal electrical activity and voluntary movement in the rat. Electroencephalogr Clin Neurophysiol. 26: 407-418.

Vizi ES, Lendvai B (1999). Modulatory role of presynaptic nicotinic receptors in synaptic and non-synaptic chemical communication in the central nervous system. Brain Res Brain Res Rev 30: 219-235.

Vreugdenhil M, Jefferys JG, Celio MR, Schwaller B (2003). Parvalbumin-deficiency facilitates repetitive IPSCs and gamma oscillations in the hippocampus. J Neurophysiol 89: 1414-1422.

Wada E, Wada K, Boulter J, Deneris E, Heinemann S, Patrick J, Swanson LW (1989). Distribution of alpha 2, alpha 3, alpha 4, and beta 2 neuronal nicotinic receptor subunit mRNAs in the central nervous system: a hybridization histochemical study in the rat. J Comp Neurol 284: 314-335.

Wanaverbecq N, Semyanov A, Pavlov I, Walker MC, Kullmann DM (2007). Cholinergic axons modulate GABAergic signaling among hippocampal interneurons via postsynaptic alpha 7 nicotinic receptors. J Neurosci 27: 5683-5693.

White TW, Paul DL (1999). Genetic diseases and gene knockouts reveal diverse connexin functions. Annu Rev Physiol 61:283-310.

Whittington MA & Traub RD (2003). Interneuron diversity series: inhibitory interneurons and network oscillations in vitro. Trends Neurosci 26: 676-682.

Wigström H, Gustafsson B (1983). Facilitated induction of hippocampal long-lasting potentiation during blockade of inhibition. Nature 301: 603-604.

Williams JH, Kauer JA (1997). Properties of carbachol-induced oscillatory activity in rat hippocampus. J Neurophysiol 78: 2631-2640.

Ylinen A, Bragin A, Nádasdy Z, Jandó G, Szabó I, Sik A, Buzsáki G (1995). Sharp wave-associated high-frequency oscillation (200 Hz) in the intact hippocampus: network and intracellular mechanisms. J Neurosci 15: 30-46.

Zhang J, Berg DK (2007). Reversible inhibition of GABAA receptors by alpha7-containing nicotinic receptors on the vertebrate postsynaptic neurons. J Physiol 579: 753-763.

Zhang L, McBain CJ (1995). Potassium conductances underlying repolarization and after-hyperpolarization in rat CA1 hippocampal interneurones. J Physiol 488: 661-672 (a).

Zhang L, McBain CJ (1995). Voltage-gated potassium currents in stratum oriens-alveus inhibitory neurones of the rat CA1 hippocampus. J Physiol 488: 647-660 (b).

Zhang XL, Zhang L, Carlen PL (2004). Electrotonic coupling between stratum oriens interneurones in the intact in vitro mouse juvenile hippocampus. J Physiol 558: 825-839.

Zhou Y, Nelson ME, Kuryatov A, Choi C, Cooper J, Lindstrom J (2003). Human alpha4beta2 acetylcholine receptors formed from linked subunits. J Neurosci 23: 9004-9015.

Zimprich F, Zezula J, Sieghart W, Lassmann H (1991). Immunohistochemical localization of the alpha 1, alpha 2 and alpha 3 subunit of the GABAA receptor in the rat brain. Neurosci Lett 127: 125-128.

Zoli M, Léna C, Picciotto MR, Changeux JP (1998). Identification of four classes of brain nicotinic receptors using beta2 mutant mice. J Neurosci 18: 4461-4472.

Acknowledgements

I am deeply grateful to my supervisor Prof. Enrico Cherubini for his continuous teaching, guiding and encouragement. Special thanks to Dr Laura Lagostena and Dr Marcelo Rosato-Siri for their friendship, for their help and for their precious advices. I am also very grateful to Michele and Rocco for the useful discussions and for their contribution to the working funny atmosphere.

I thank my friends Claudia and Assunta for the amazing time that we have spent in Trieste over the last 4 years.

I thank my family and Beniamino, whose love, support and encouragement have made this incredible experience possible.